NASA TECHNICAL MEMORANDUM

NASA TM X-62,079

NASA TM X-62,079

LARGE–SCALE WIND–TUNNEL INVESTIGATION OF A SEMISPAN WING EQUIPPED WITH AN EXTERNALLY–BLOWN JET FLAP

Michael D. Falarski and Thomas N. Aiken

Ames Research Center
and
U. S. Army Air Mobility Research & Development Laboratory
Moffett Field, Calif. 94035

July 1971

LARGE-SCALE WIND-TUNNEL INVESTIGATION OF A SEMISPAN WING EQUIPPED WITH AN EXTERNALLY-BLOWN JET FLAP

Michael D. Falarski and Thomas N. Aiken

Ames Research Center
and
U.S. Army Air Mobility R. & D. Laboratory

1

SUMMARY

A wind tunnel investigation was made of the aerodynamic characteristics of a 4.42 m (14.5 foot) semispan, externally-blown jet flap model. The model was equipped with a single 76.2 cm (30 inch) diameter, ducted fan with a 1.03 pressure ratio. The effects of flap size, fan vertical location, and wing sweep on the longitudinal aerodynamic characteristics were studied. This report presents the data from this investigation.

INTRODUCTION

The externally-blown flap (EBF) is one of several configurations being investigated for use as a STOL transport. The EBF consits of a wing with a large-chord, multiple element, slotted flap system and pod mounted high by-pass ratio fans. The mass flow of the fans is blown against the deflected flap, thereby augmenting the lift by inducing circulation around the airfoil. Extensive small scale studies have been completed and several are reported in ref. 1 to 4. Several large scale configurations have also been investigated and are reported in ref. 5 and 6.

This paper presents the data of an investigation undertaken to study the effects of flap size, fan vertical location, and wing sweep on the longitudinal aerodynamic characteristics of the EBF. The model was a 4.42 m (14.5 foot) semispan wing powered by a 76.2 cm (30 inch) ducted fan with a pressure ratio of 1.03. The tests were performed in the Ames 40- by 80-Foot Wind Tunnel.

NOTATION

b	wing semispan measured from end plate, m(ft)
c_f	flap chord, streamwise, m(ft)
c_w	wing chord, streamwise m(ft)
C_D	drag coefficient, $\frac{\text{drag}}{qS}$
C_L	lift coefficient, $\frac{\text{lift}}{qS}$
C_m	pitching moment coefficient, $\frac{\text{pitching moment}}{qSc_w}$
C_μ	gross thrust coefficient, $\frac{\text{gross thrust}}{qS}$
D_S	ducted fan exit diameter, m(ft)
L	lift, n(lb)
q	free-stream dynamic pressure, n/sq m (lb/sq ft)
R	resultant force, $\sqrt{L^2 + X^2}$, n(lb)
S	wing area, $m^2(ft^2)$
T	ducted fan gross thrust, n(lb)
X	longitudinal force parallel to thrust axis, n(lb)
Z	distance from wing chord to centerline of nacelle, m(ft)
α	angle of attack referenced to wing chordline, deg
δ_f	flap deflection, deg
Λ	sweep angle, deg
θ	angle of static resultant force vector from chordline, deg

MODEL DESCRIPTION

Basic Model

Photographs of the model installed in the wind tunnel are shown in figure 1. The basic geometry of the model is presented in figure 2 and Table I. The end plate was attached to the wing while the fairing was isolated from the model.

The geometry of the ducted fan is presented in figure 3(a) and Table I. The blade plan-form curves for the 8 bladed, 1.03 pressure ratio fan are presented in figure 3(b). The static thrust as a function of fan speed is presented in figure 6(a). Shown in figure 6(b) is the fan gross thrust coefficient versus free-stream dynamic pressure.

Flap System

The three flap systems tested are shown in figure 4(a). The reference dimension for the systems is given in Table I.

Flap I is a large chord, triple slotted flap. The geometric details are shown in figure 4(b). This system was made by attaching a modification to the aft flap of flap III.

Flap II is a large chord, double slotted flap. For this system the first element of flap I was set at 0°, the first slot sealed and the remaining two elements deflected.

Flap III is a smaller chord, double slotted flap. Its basic geometry is shown in figure 4(c) and its coordinates are given in Table II. This system is very similar to the flap used on the propellor driven, deflected-slipstream STOL model reported in ref. 7.

Ducted Fan Pylons

The model was tested with the ducted fan mounted at three vertical distances below the wing. The duct positions are described in figure 5. Mounted on the long pylon, the fan was 1.25 diameters below the wing chord line. The medium pylon positioned the fan .79 diameters below the wing. The cross section of the pylon is also shown in figure 5. With the pylon removed the fan was mounted .33 diameters below the wing, allowing a portion of the fan efflux to flow over the top of the wing.

Wing Sweep

The model was tested at $\Lambda = 0$ and $30°$. For $\Lambda = 30°$ the wing and flaps were extended to maintain semispan = 4.42 m (14.5 ft). The ducted fan was located at midspan for both sweep angles.

TESTS

The tests were performed by varying angle of attack at a constant C_μ. Gross thrust coefficient was varied by changing free-stream dynamic pressure with the fan rotational speed set at 5000 RPM. The gross thrust was determined from a calibration of fan exit total pressure versus static ducted fan thrust. C_μ was varied from 0 to 6.

The other test variable was flap deflection. Data was recorded for each flap system at flap deflections of 0°, 30°, 60°, and 90°. This was done for each fan vertical position and wing sweep angles of 0° and 30°.

The static (q = 0 psf) aerodynamic characteristics were determined at $\alpha = 0°$ and a fan gross thrust of approximately 1424 n (320 lb).

DATA PRESENTATION

An index of data figures is presented in Table III. The longitudinal characteristics with the wing sweep at 0° are presented in figures 9 to 15. Figures 16 to 25 present the data for the model at 30° sweep. The forces and moments are referred to the wind axes. The moment reference center was located at 25 percent of the mean aerodynamic chord. The data has not been corrected for wind tunnel wall effects because they were within the accuracy of the measuring device.

REFERENCES

1. Parlett, Lysle P.; Fink, Marvin P.; and Freeman, Delma C., Jr.: Wind-Tunnel Investigation of a Large Jet Transport Model Equipped With and External Flow Jet Flap. NASA TND-4928, 1968.

2. Newsom, William A.: Wind-Tunnel Investigation oa a Deflected- Slipstream Cruise-Fan V/STOL Aircraft Wing. NASA TND-4262, 1969.

3. Parlett, Lysle P.; and Shivers, James P.: Wind-Tunnel Investigation of an STOL Aircraft Configuration Equipped With an External-Flow Jet Flap. NASA TND-5364, 1969.

4. Freeman, Delma C., Jr.; and Grafton, Sue B.; and D'Amato, Richard: Static and Dynamic Stability Derivatives of a Model of a Jet Transport Equipped With External-Flow Jet-Augmented Flaps. NASA TND-5408, 1969.

5. Kirk, Jerry V.; Hickey, David H.; and Aoyagi, Kiyoshi: Larg-Scale Wind Tunnel Investigation of a Model With an External Jet-Augmented Flap. NASA TND-4278, 1967.

6. Aoyagi, Kiyoshi; and Dickinson, Stanley O.: Investigation of a 0.3-Scale Jet Transport Model Having a Jet-Augmented Boundary-Layer-Control Flap With Direct-Lift Control Capability. NASA TND-5129, 1969.

7. Page, V. Robert; Dickinson, Stanley O.; and Deckert, Wallace H.: Large-Scale Wind-Tunnel Tests of a Deflected Slipstream STOL Model With Wings of Various Aspect Ratios. NASA TND-4448, 19

TABLE I. - REFERENCE DIMENSIONS

	$\Lambda = 0°$	$\Lambda = 30°$
Flap I:		
Wing area, S, $m^2(ft^2)$	11.0(118.4)	12.69(136.8)
Wing chord, c_w, m(ft)	2.49(8.17)	2.88(9.43)
Flap chord, c_f, m(ft)	1.62(5.30)	1.87(6.12)
c_f/c_w	0.65	0.65
c_f/D_S	2.12	2.45
Flap II:		
Wing area, S, $m^2(ft^2)$	11.0(118.4)	12.69(136.8)
Wing chord, c_w, m(ft)	2.49(8.17)	2.88(9.43)
Flap chord, c_f, m(ft)	1.28(4.19)	1.48(4.85)
c_f/c_w	0.514	0.514
c_f/D_S	1.68	1.94
Flap III:		
Wing area, S, $m^2(ft^2)$	7.40(79.8)	8.55(92.1)
Wing chord, c_w, m(ft)	1.68(5.5)	1.94(6.35)
Flap chord, c_f, m(ft)	0.71(2.31)	0.81(2.67)
c_f/c_w	0.42	0.42
c_f/D_S	0.93	1.07
Semispan, b, m(ft)	4.42(14.5)	

TABLE I. - Continued

Pylons	Z, m(ft)	Z/D_S
Long Pylon	0.96(3.13)	1.24
Medium Pylon	0.604(1.98)	0.79
No Pylon	0.253(0.83)	0.33

Ducted Fan	
Duct	
Inside Diameter, m(ft)	.0.762(2.5)
Exit Diameter, m(ft)	0.762(2.5)
Chord, m(ft)	0.655(2.146)
Fan Station, percent of duct chord	35.13
Fan	
Planform curves	see figure 3(b)
Number of Blades	8
Hub-to-Tip Diameter Ratio	0.533
Blade Angle at Tip, deg	30
Approx. Blade Tip Clearance, cm(in)	0.81(0.032)
Pressure Ratio	1.03

TABLE II. - COORDINATES FOR FLAP III

FORE FLAP

CHORDWISE STATION	UPPER ORDINATE	LOWER ORDINATE
0	0	0
0.75	4.50	- 6.25
1.50	6.60	- 8.10
2.50	8.64	-10.00
3.75	10.75	-11.74
5.00	12.50	-13.02
10.00	17.20	-15.75
15.00	20.70	-16.65
20.00	23.10	-16.44
25.00	24.85	-15.90
30.00	26.15	-15.45
35.00	26.90	-15.00
40.00	27.41	-14.55
45.00	27.72	-14.09
50.00	27.63	-13.63
62.10	26.65	-12.88
63.70	26.50	0
75.00	24.61	12.50
87.50	22.10	17.65
100.00	19.24	19.00

L.E. RADIUS = 15.00

CHORD = 33.52 cm (13.2 inches)

AFT FLAP

CHORDWISE STATION	UPPER ORDINATE	LOWER ORDINATE
0	0	0
1.16	5.21	-4.18
2.32	7.36	-5.77
3.49	8.95	-6.76
4.65	10.03	-7.54
6.90	11.61	-8.28
9.30	12.91	-8.53
11.61	13.72	-8.39
13.95	14.37	-8.17
18.60	14.92	-7.71
23.22	15.14	-7.29
34.85	13.24	-6.19
46.50	10.91	-5.04
58.10	8.59	-3.94
69.70	6.19	-2.89
81.40	3.87	-1.72
93.00	1.48	-0.69
100.00	-0.09	-0.14

L.E. RADIUS = 8.39

CHORD = 36.06 cm (14.2 inches)

ALL DIMENSIONS IN PERCENT CHORD

TABLE II. - Continued

Basic Wing Coordinates

UPPER SURFACE		LOWER SURFACE	
CHORDWISE STATION	ORDINATE	CHORDWISE STATION	ORDINATE
0	0	0	0
0.42	1.93	0.985	-1.63
0.74	2.38	1.37	-1.96
1.39	3.11	2.12	-2.47
3.10	4.45	3.94	-3.33
6.57	6.40	7.52	-4.50
10.05	7.90	11.05	-5.35
13.57	9.13	14.57	-6.01
20.61	11.01	21.55	-6.98
27.75	12.41	28.55	-7.65
34.80	13.41	35.30	-8.05
42.00	14.05	42.47	-8.22
49.00	14.35	49.45	-8.16
57.40	14.30	56.40	-7.87
63.25	13.95	63.35	-7.37
70.25	13.33	70.30	-6.73
77.50	12.49	77.30	-5.88
84.60	11.40	78.70	-5.74
93.80	10.19	84.30	3.94
100.00	8.52	91.30	8.19
		100.00	8.40

Leading Edge Radius - 1.171

CHORD = 1.194 m (47.0 inches)

All Dimensions in Percent Chord

TABLE III. - INDEX OF DATA FIGURES

FIGURE	SWEEP ANGLE, deg	PYLON	FLAP	δ_f, deg	
7a	0	MED. & LONG	I-III	∿	q = 0
b	↓	NO	↓	↓	↓
8a	30	LONG			
b	↓	MEDIUM			
c		NO			
9a	0	LONG	III	90	
b	↓	↓	↓	60	
c				30	
d				0	
10a		MEDIUM	I	90	
b		↓	↓	60	
c				30	
d				0	
11a			II	90	
b			↓	60	
c				30	
d				0	
12a			III	90	
b			↓	60	
c				30	
d				0	
13a		NO	I	90	
b		↓	↓	60	
c				30	
d				0	
14a			II	60	
b			↓	30	
c				0	
15a			III	90	
b			↓	60	
c				30	
d				0	
e	↓	↓	↓	0	nacelle removed

TABLE III. - Concluded.

FIGURE	SWEEP ANGLE, deg	PYLON	FLAP	δ_f, deg	
16a	30	LONG	I	90	
b				60	
c				30	
d				0	
17a			II	90	
b				60	
c				30	
d				0	
18a			III	90	
b				60	
c				30	
d				0	
19a		MEDIUM	I	90	
b				60	
c				30	
d				0	
20a			II	90	
b				60	
c				0	
21a			III	90	
b				60	
c				30	
d				0	
22a		NO	I	90	
b				60	
c				30	
23a			II	90	
b				60	
c				30	
d				0	
24a			III	90	
b				60	
c				30	
d				0	
25		-	I-III	~	nacelle removed

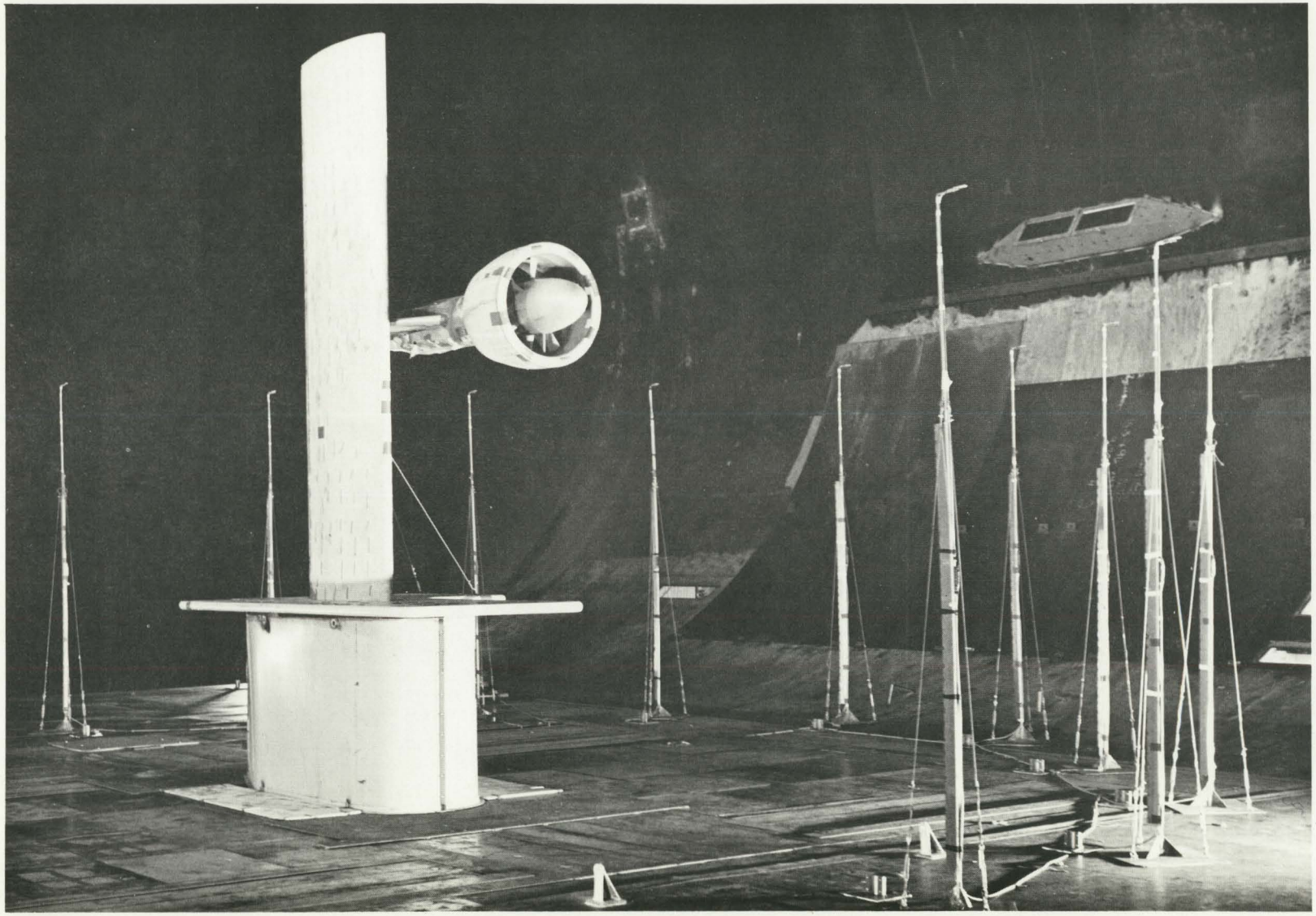

(a) Three-quarter front view; $\Lambda = 0^{\circ}$, flap III, med. pylon

Figure 1.- Installation of model in wind tunnel.

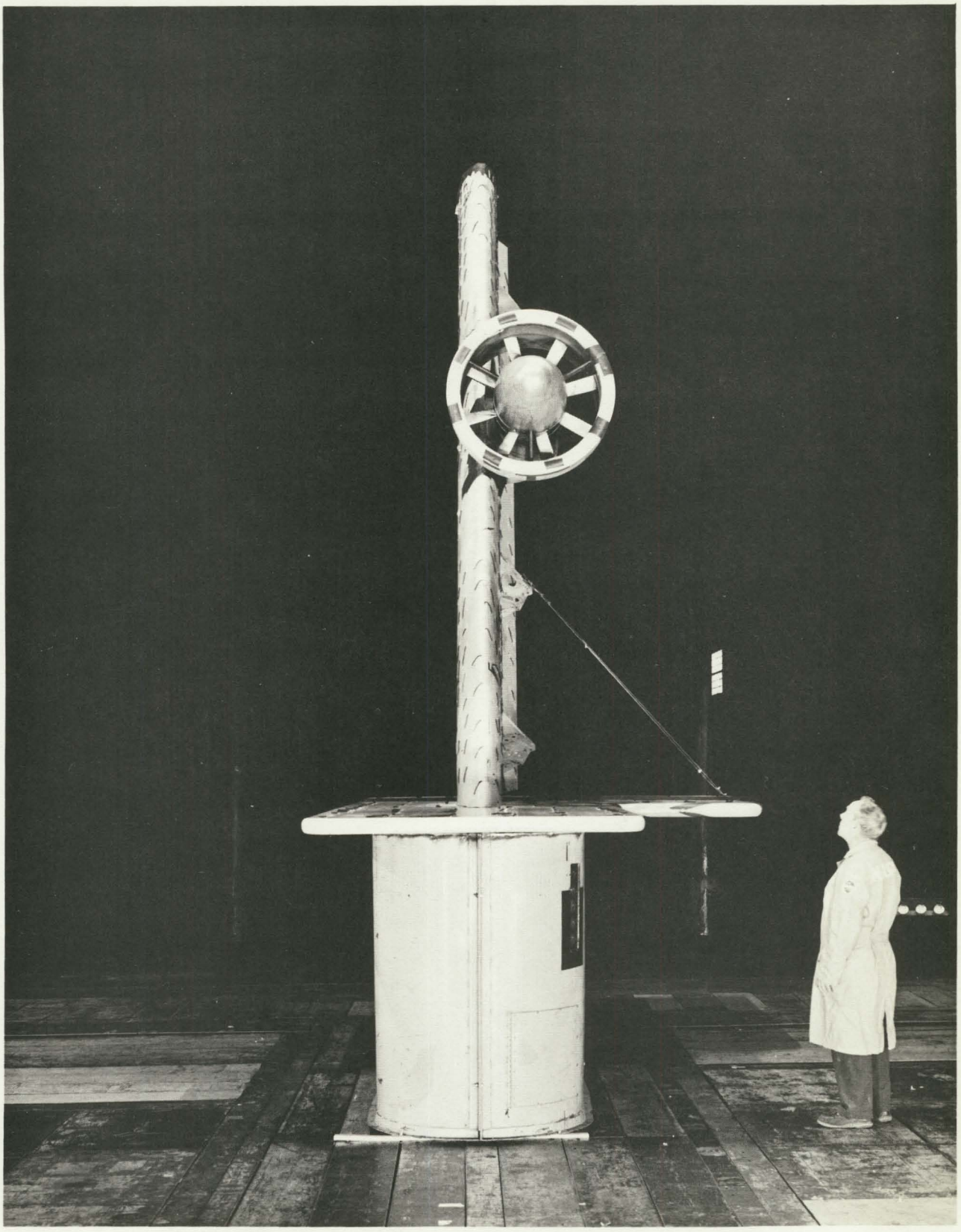

A70-1026

(b) Front view; $\Lambda = 30^{\circ}$, flap III, no pylon

Figure 1.- Continued.

(c) Three-quarter rear view; $\Lambda = 30^\circ$, flap I, long pylon

Figure 1.- Concluded.

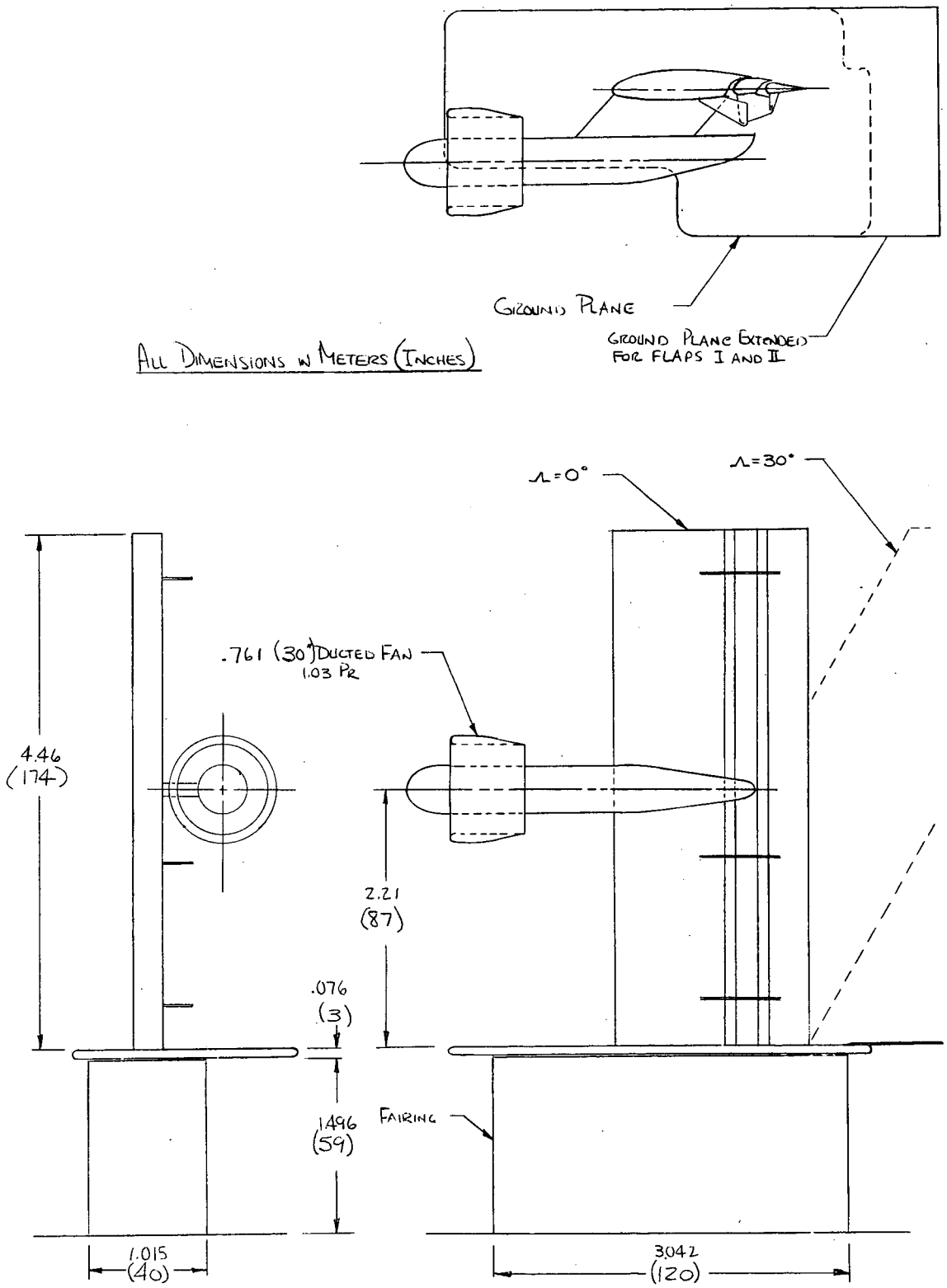

Figure 2.- Geometric details of semispan model; flap III, med. pylon.

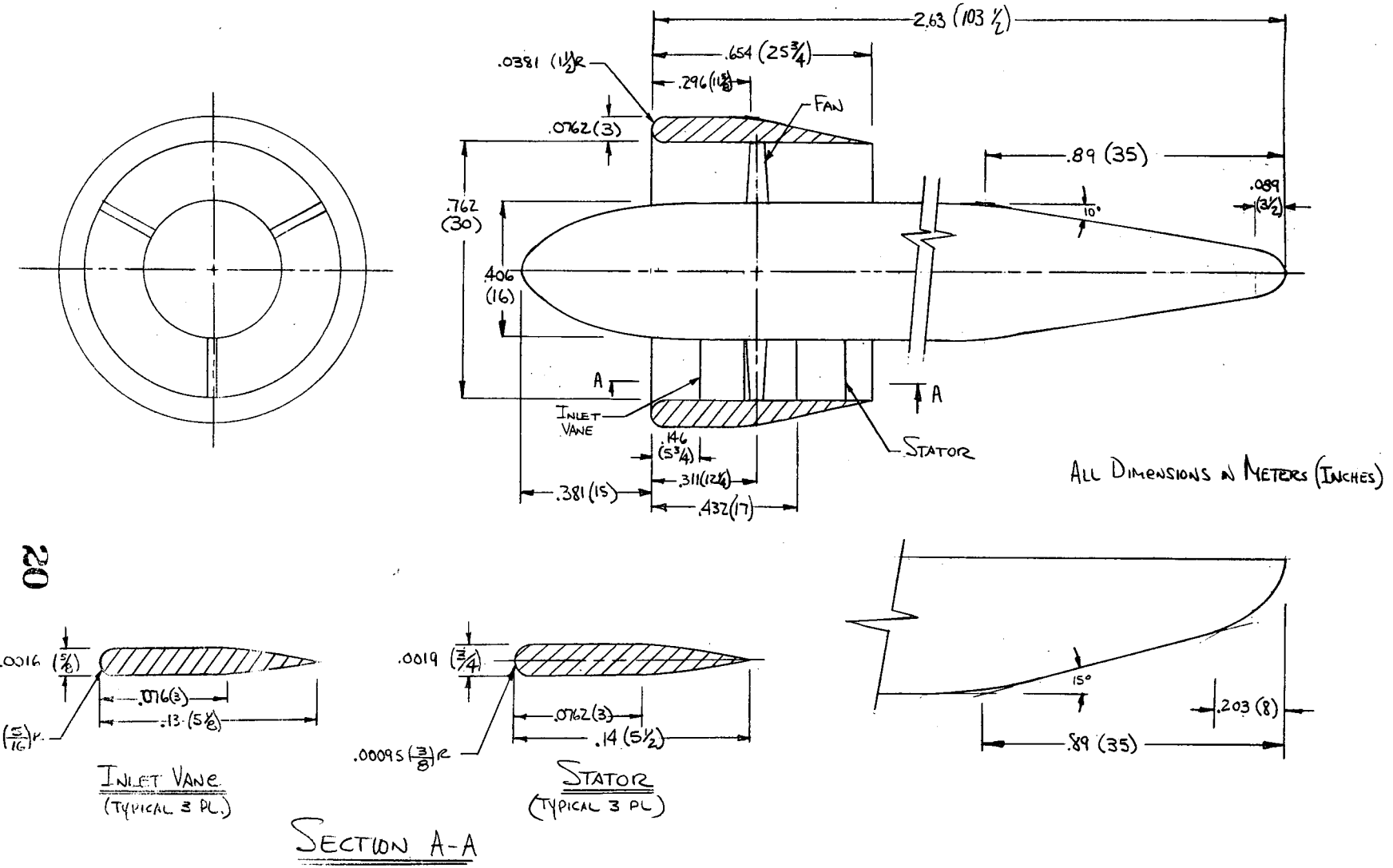

(a) General arrangement

Figure 3.- Geometric details of 30 in. ducted fan.

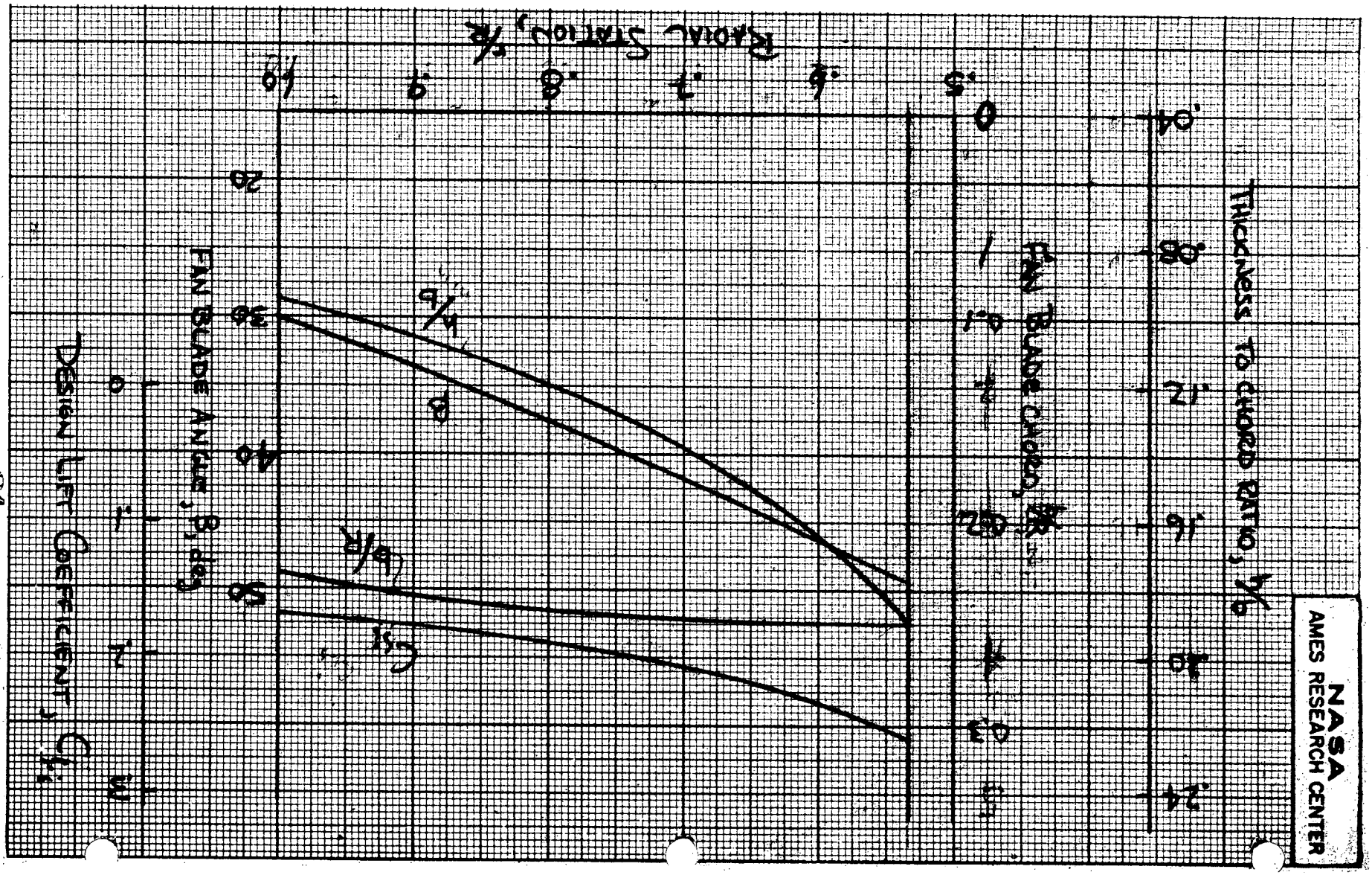

(b) Fan blade planform curves

Figure 3.- Concluded.

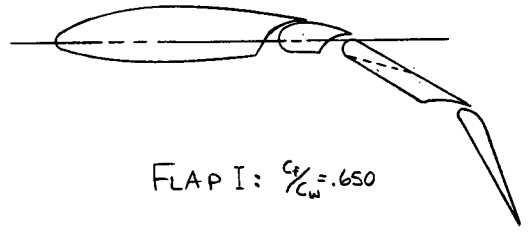

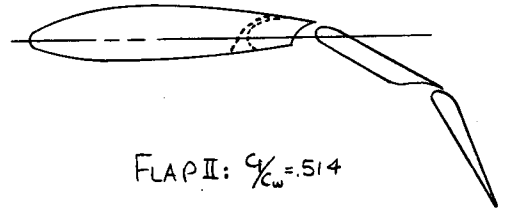

(a) Comparison of flap systems; $\Lambda = 30°$

Figure 4.- Geometric details of flap systems.

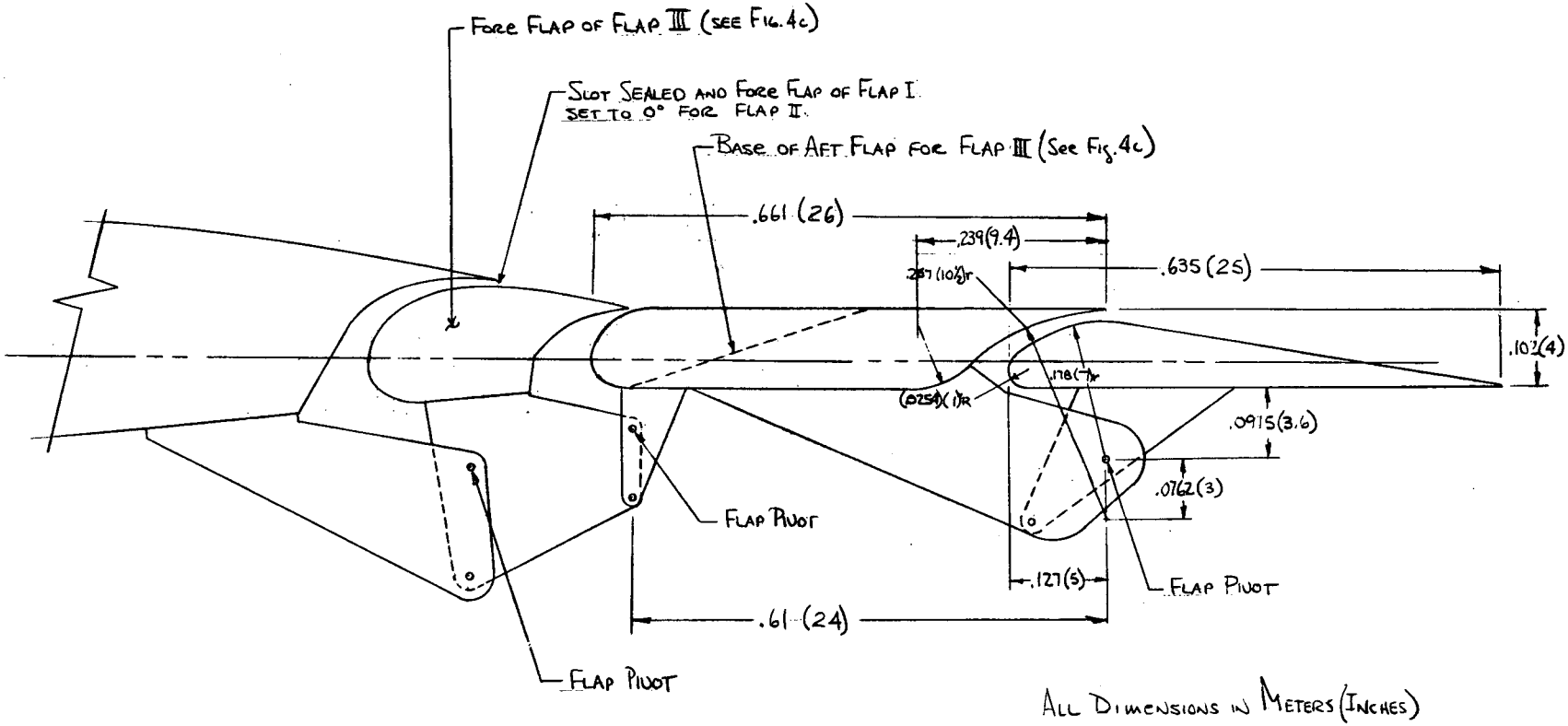

(b) Details of flaps I and II; $\Lambda = 0°$

Figure 4.- Continued.

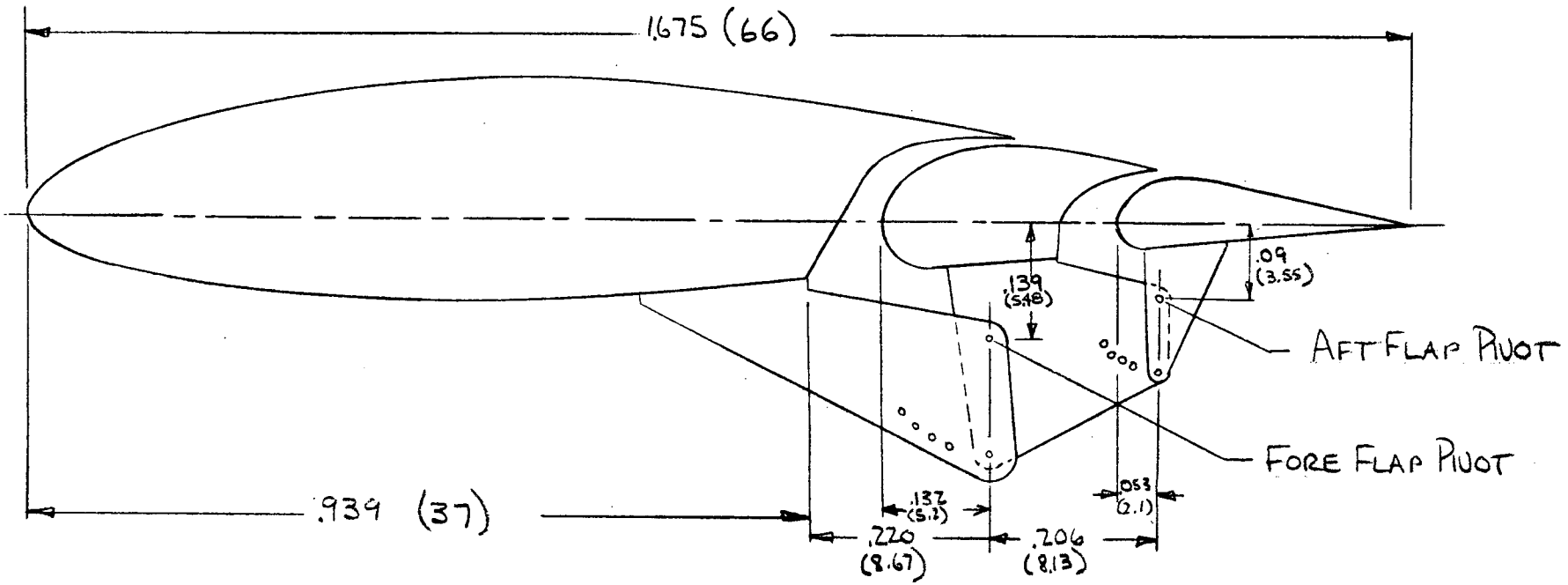

(c) Details of flap III; $\Lambda = 0°$

Figure 4.- Concluded.

ALL DIMENSIONS IN METERS (INCHES)
SEE TABLE II

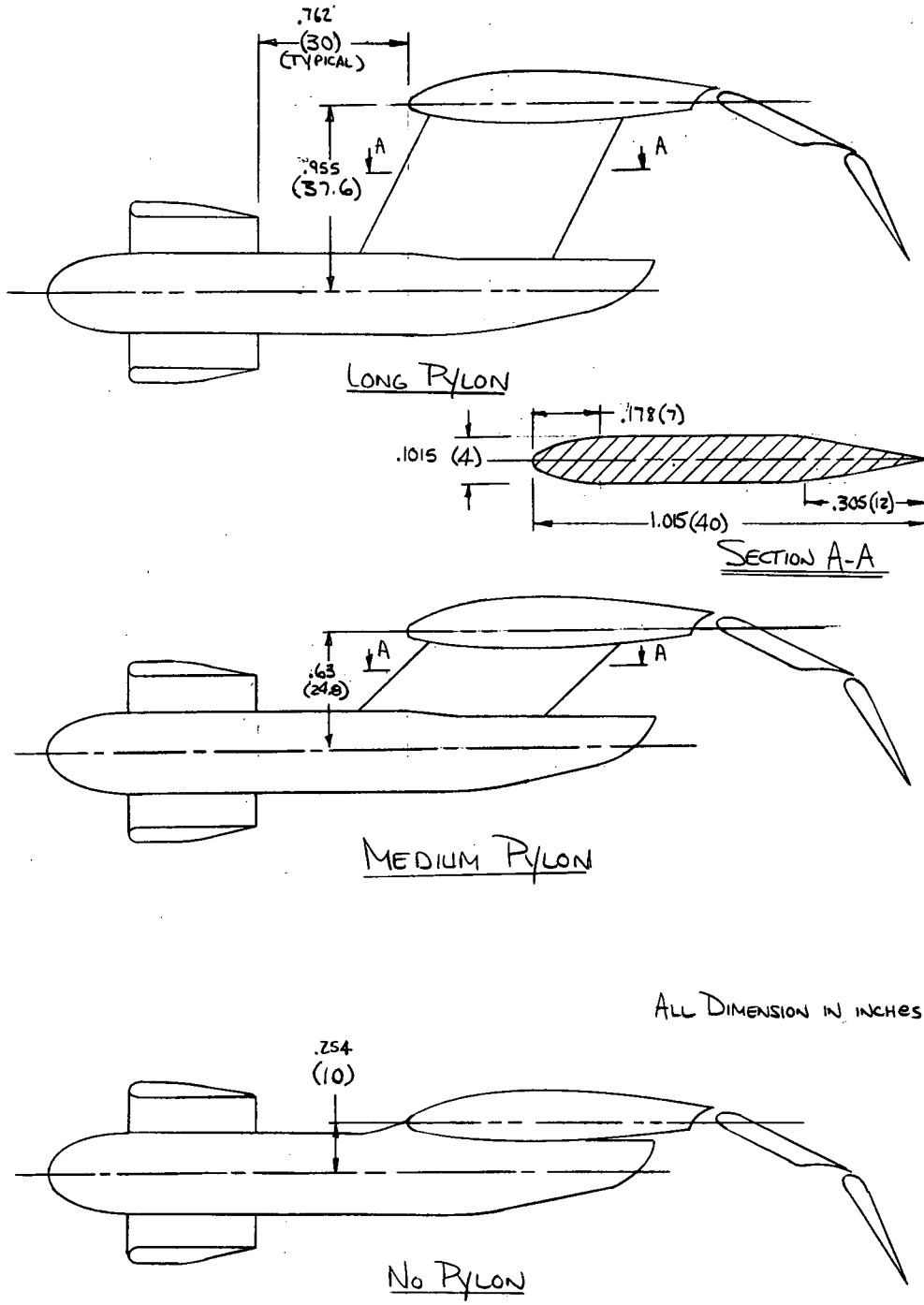

Figure 5.- Geometric details of ducted fan pylons; $\Lambda = 30^{\circ}$, flap II.

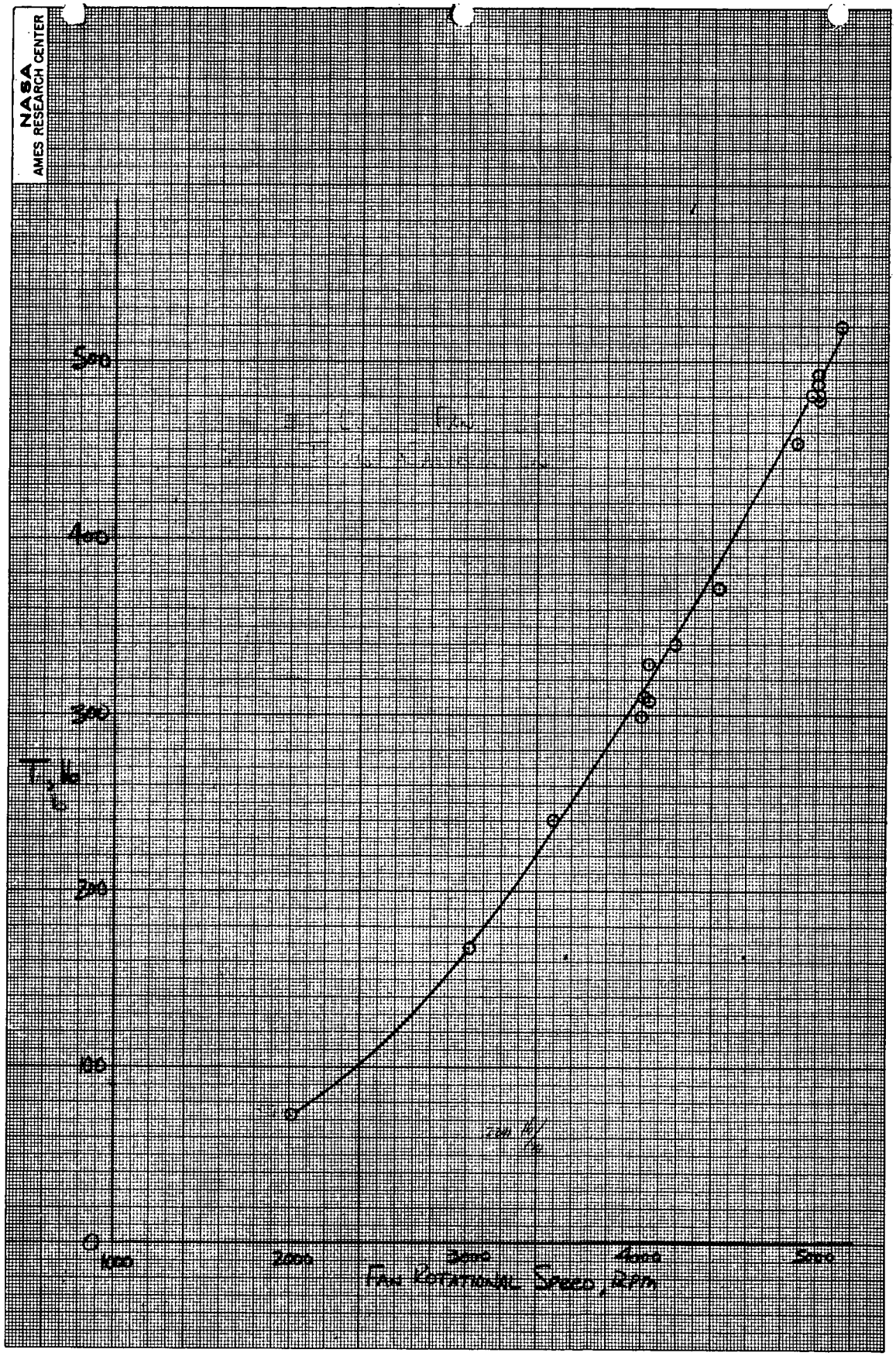

(a) Static thrust versus fan rotational speed

Figure 6.- Ducted fan performance characteristics.

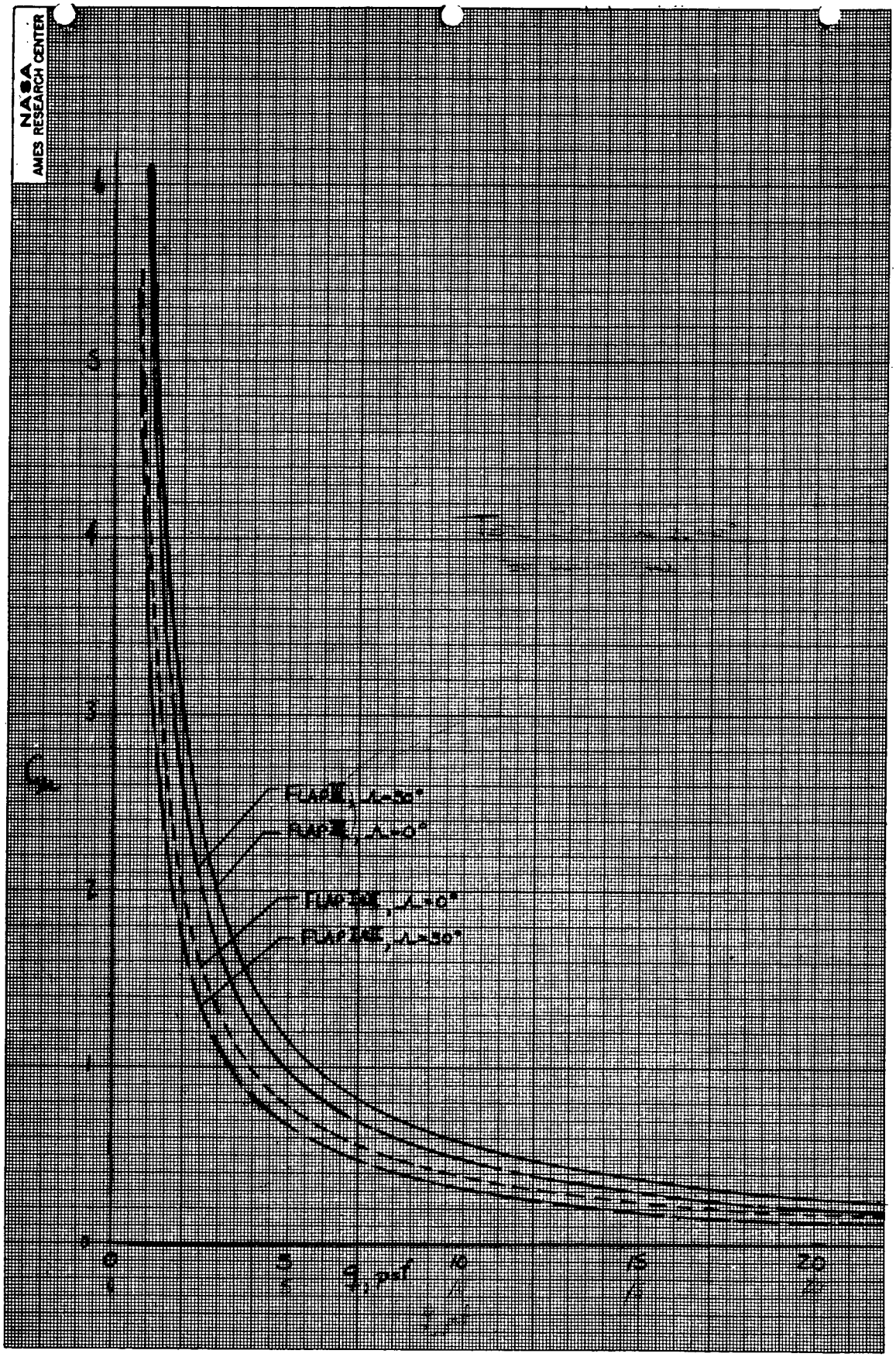

(b) Gross thrust coefficient as a function of free-stream dynamic pressure; RPM 5000

Figure 6.- Concluded.

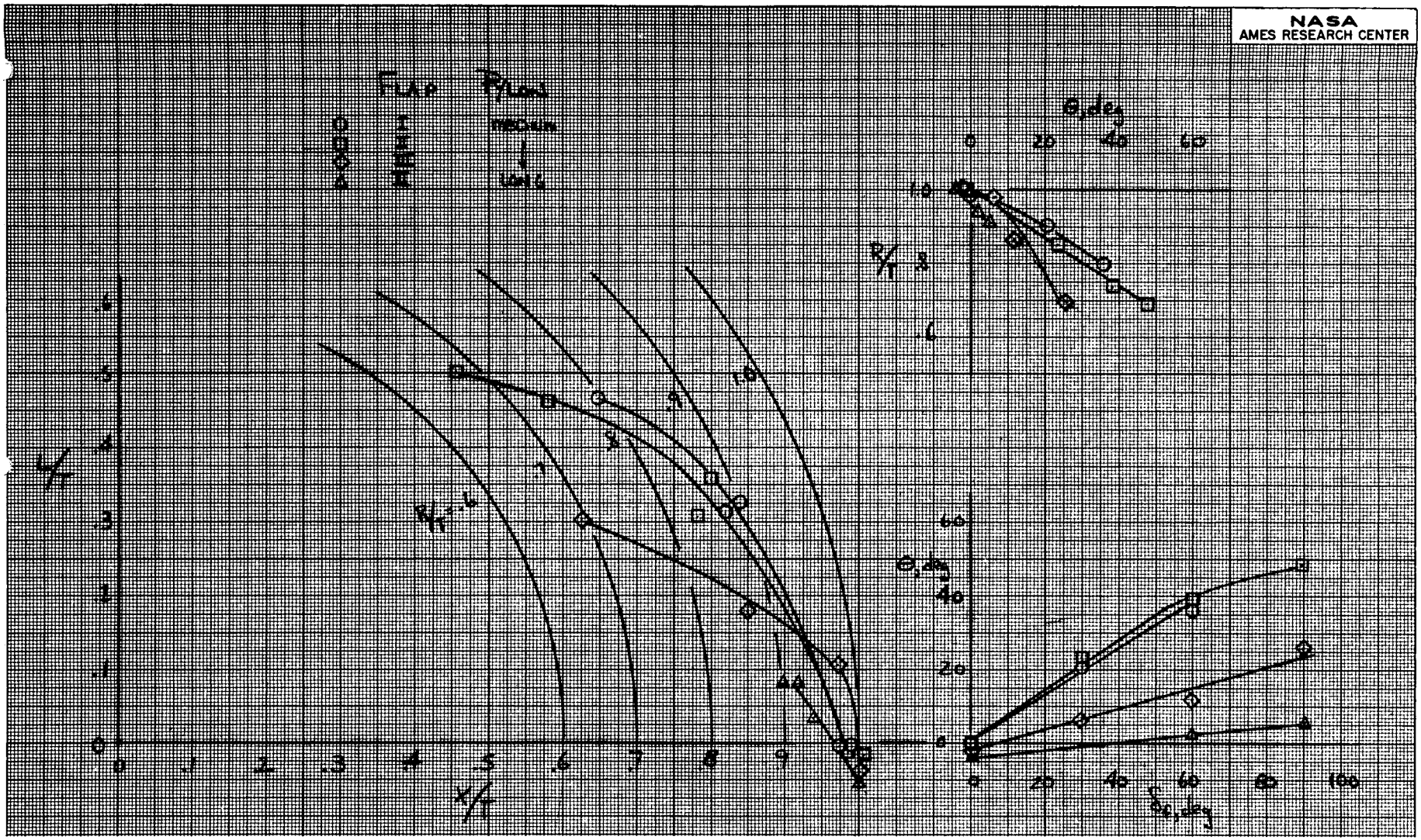

(a) Medium and long pylons

Figure 7.- Static longitudinal aerodynamic characteristics of the flap systems; $\Lambda = 0°$, q = 0psf.

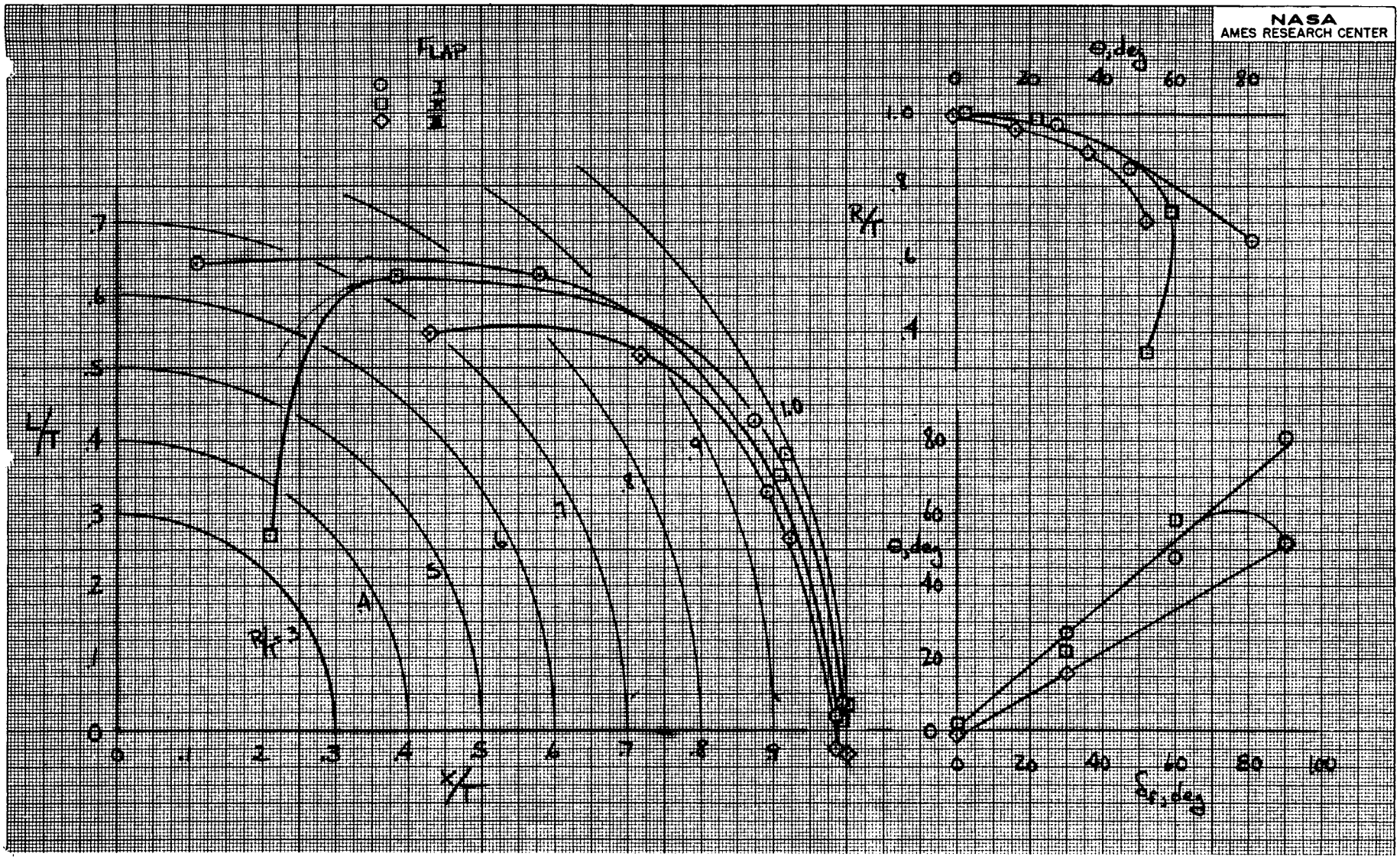

(b) No pylon

Figure 7.- Concluded.

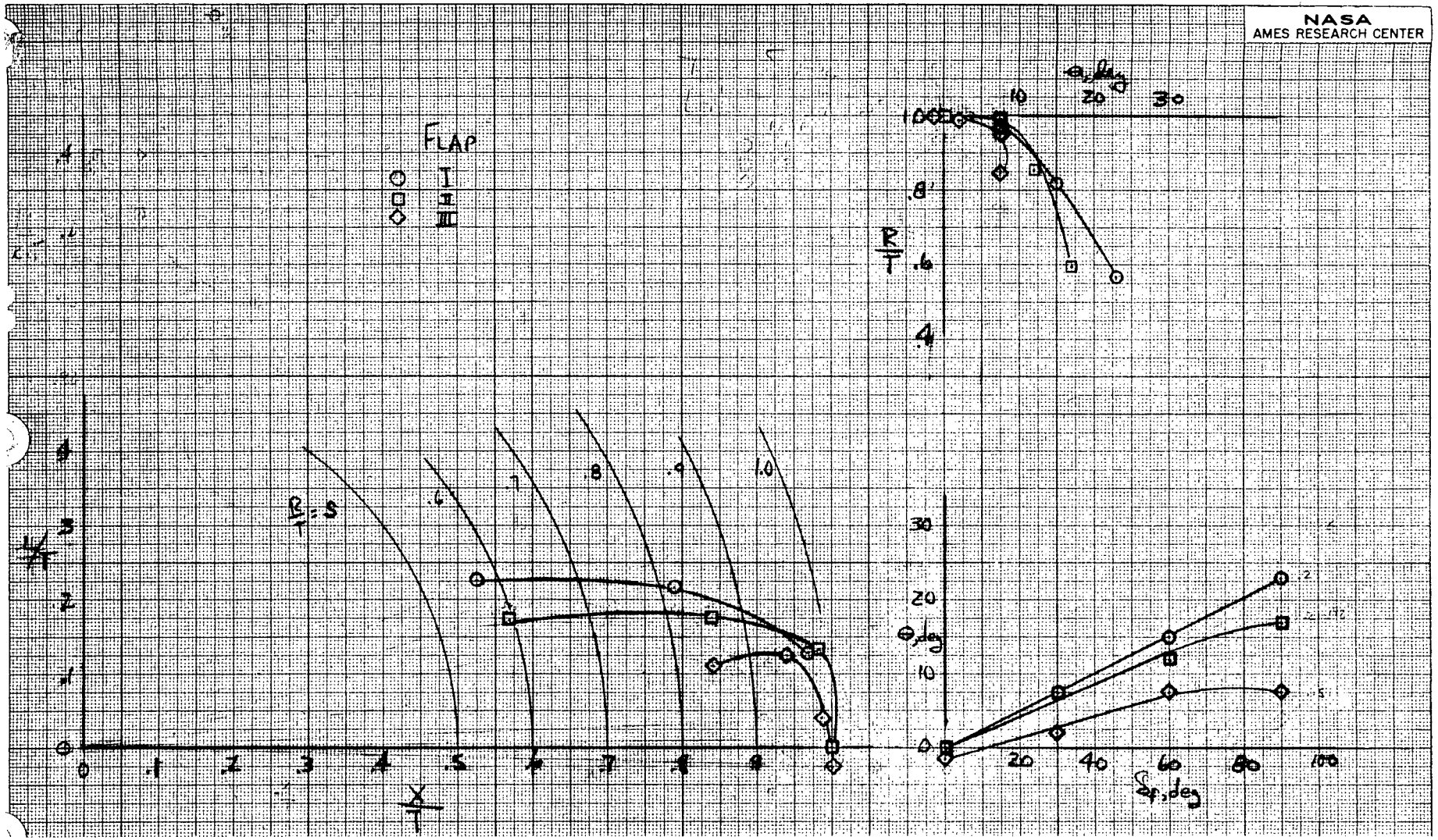

(a) Long pylon

Figure 8.- Static longitudinal aero dynamic characteristics of the flap systems; $\Lambda = 30^\circ$, q=0psf.

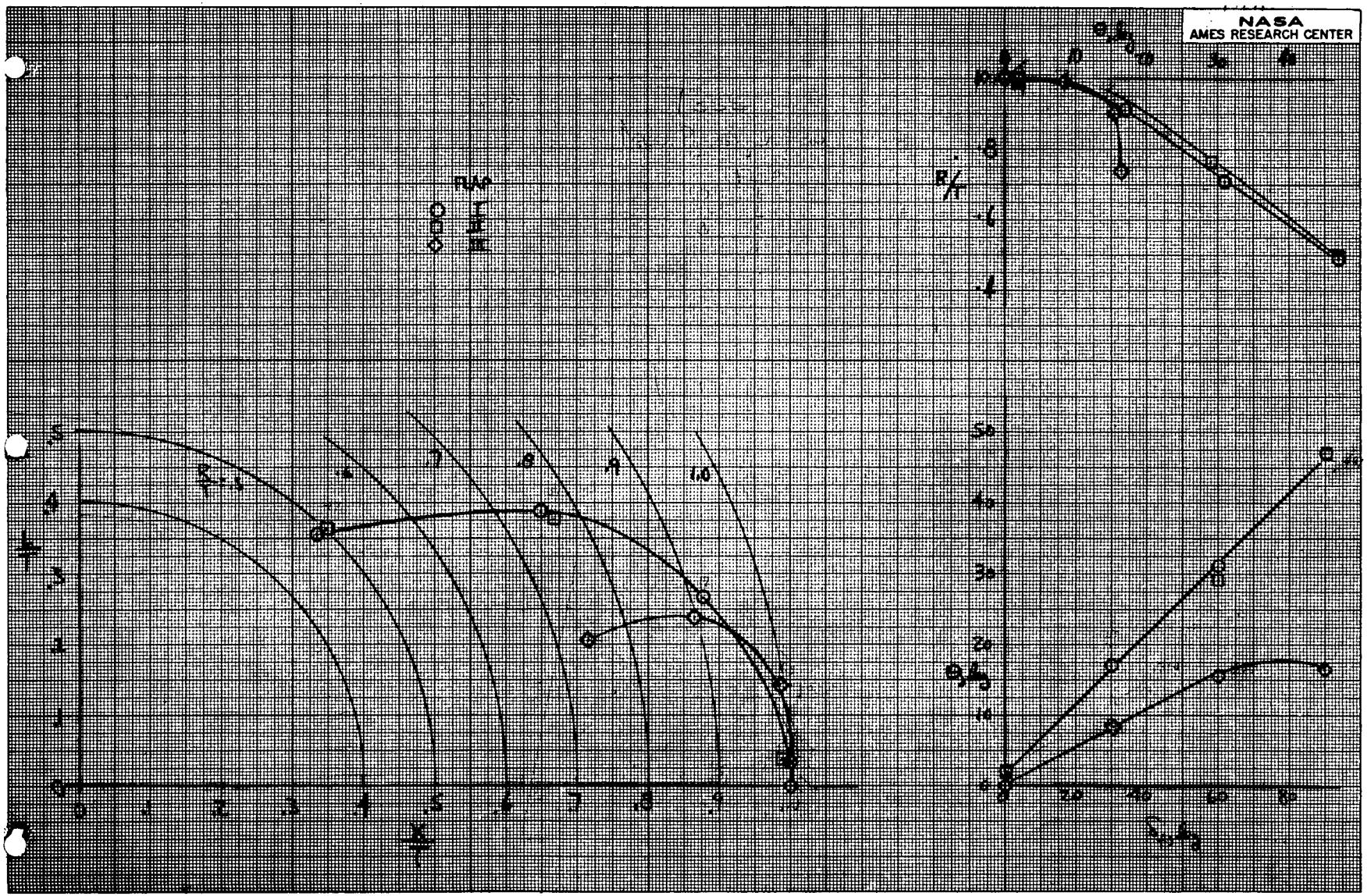

(b) Medium pylon

Figure 8.- Continued.

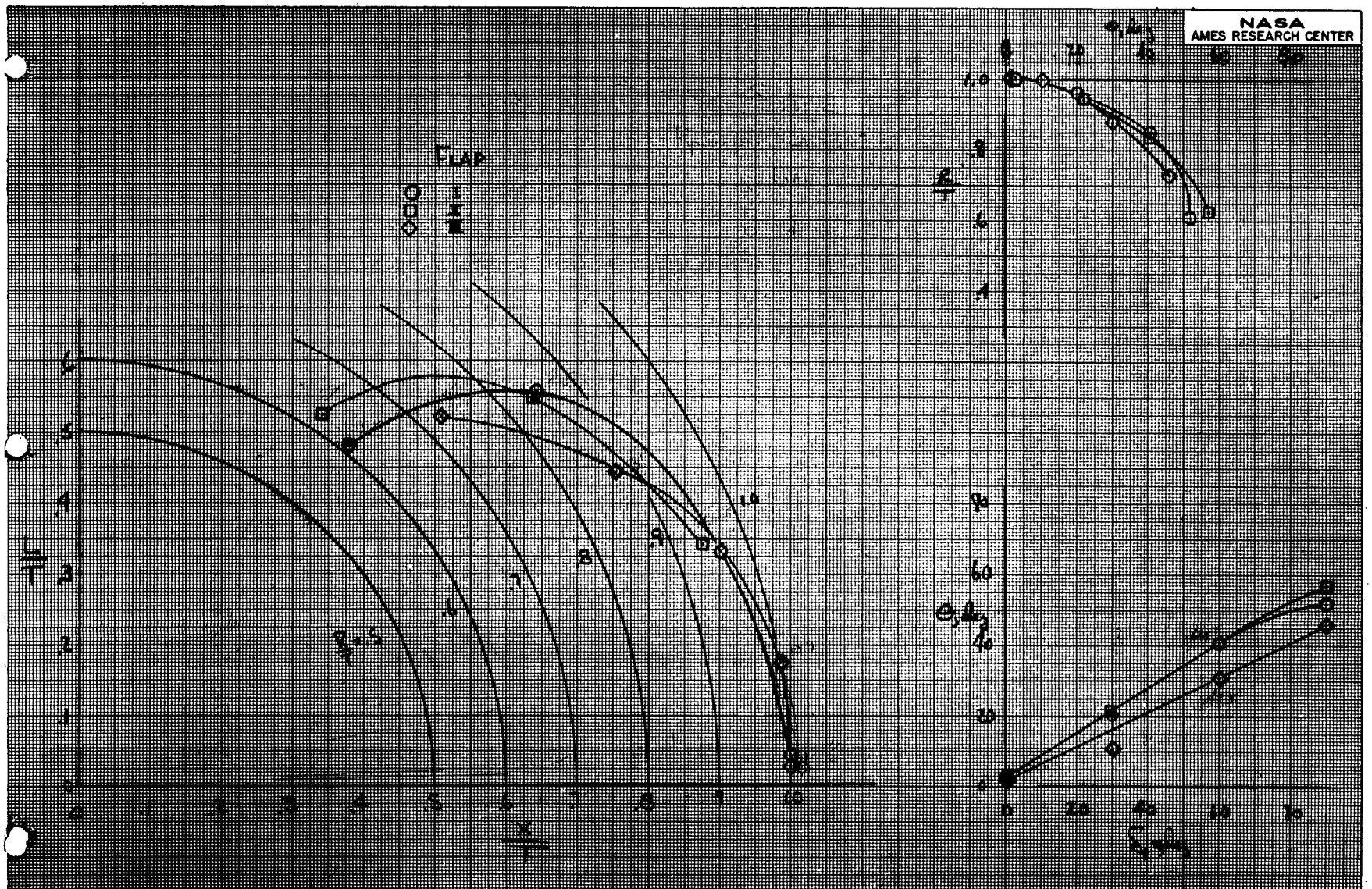

(c) No pylon

Figure 8.- Concluded.

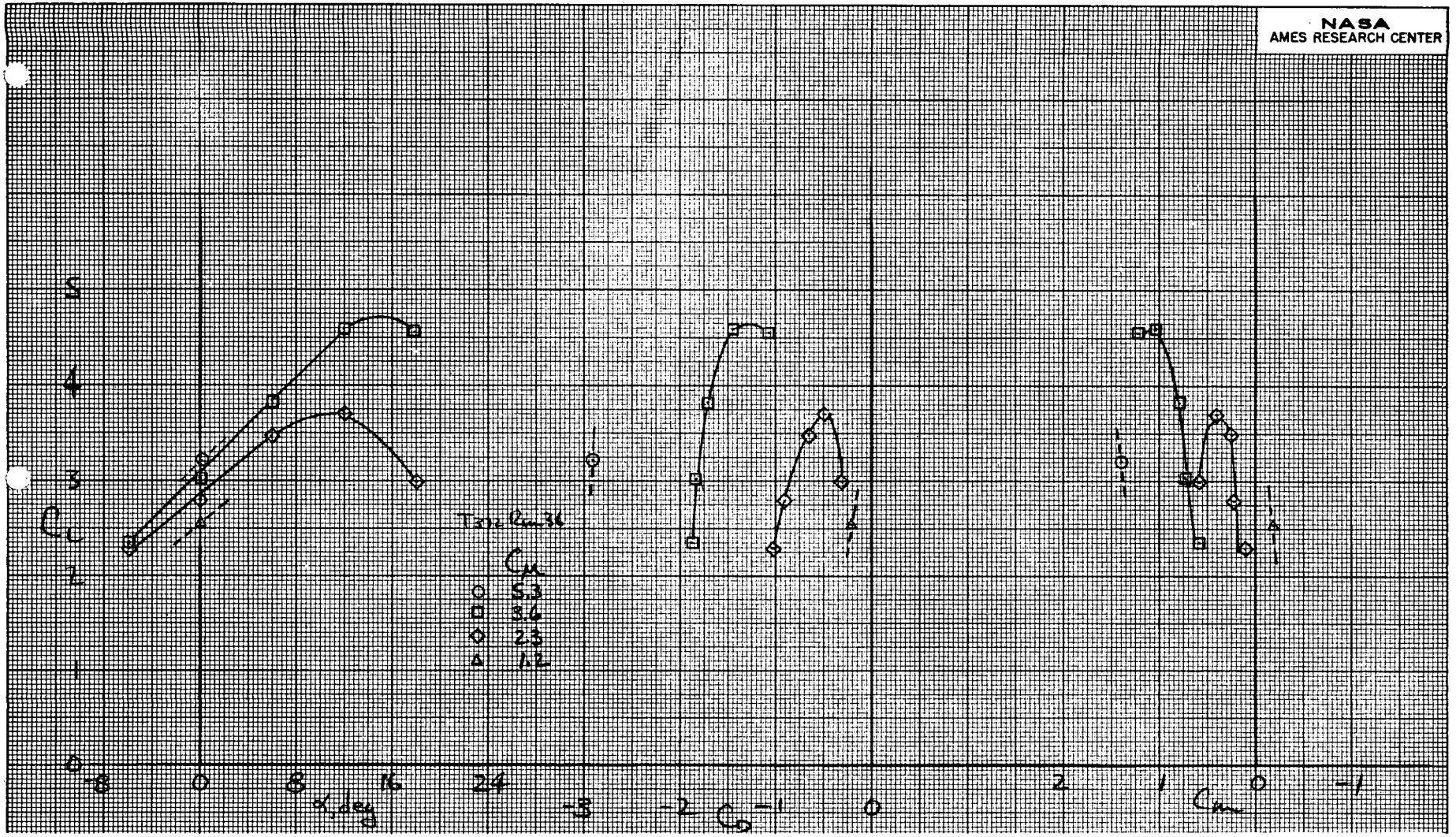

(a) $\delta_f = 90^\circ$

Figure 9.- Longitudinal aerodynamic characteristics;

$\Lambda = 0^\circ$, long pylon, flap III.

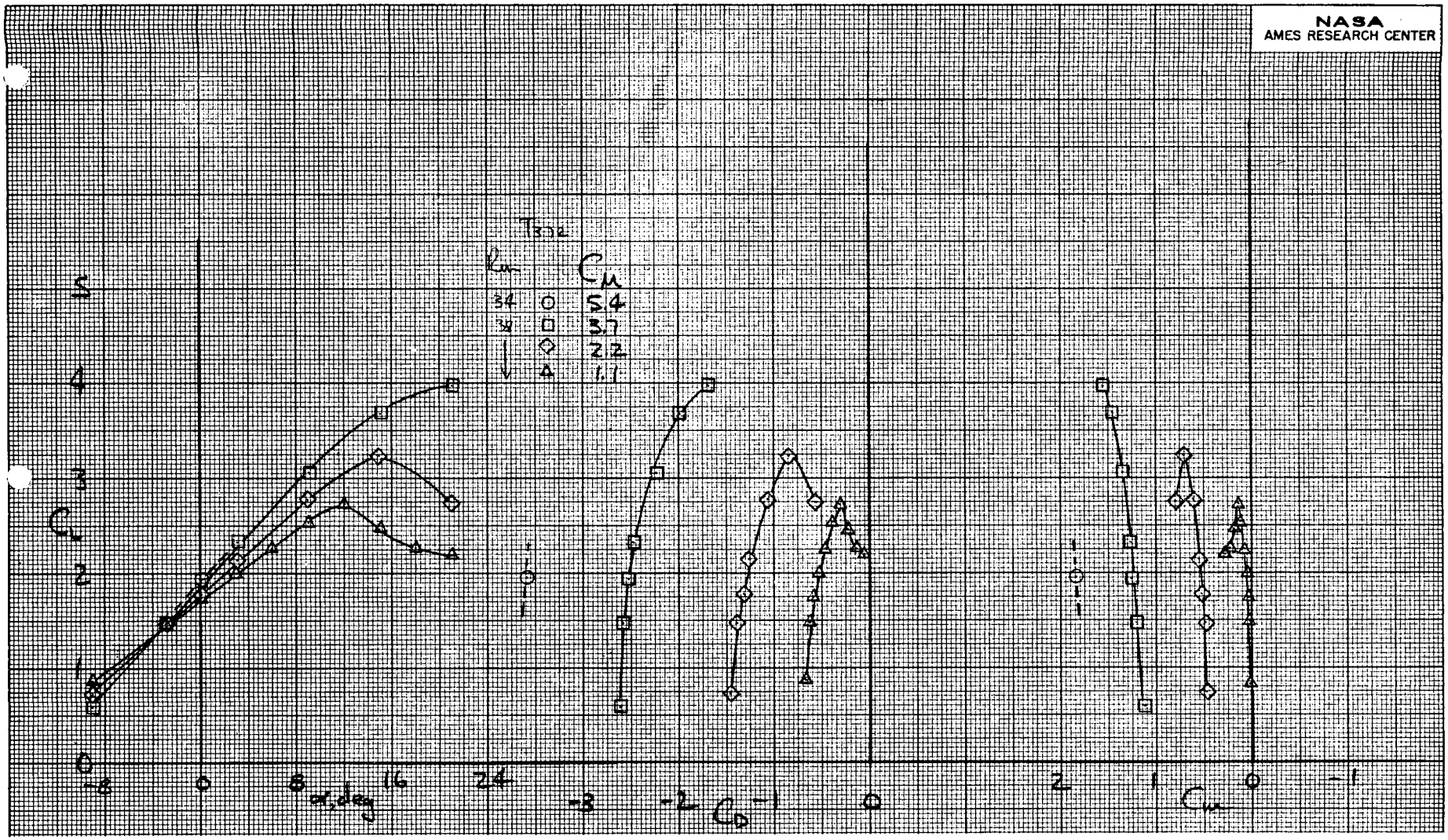

(b) $\delta_f = 60°$

Figure 9.- Continued.

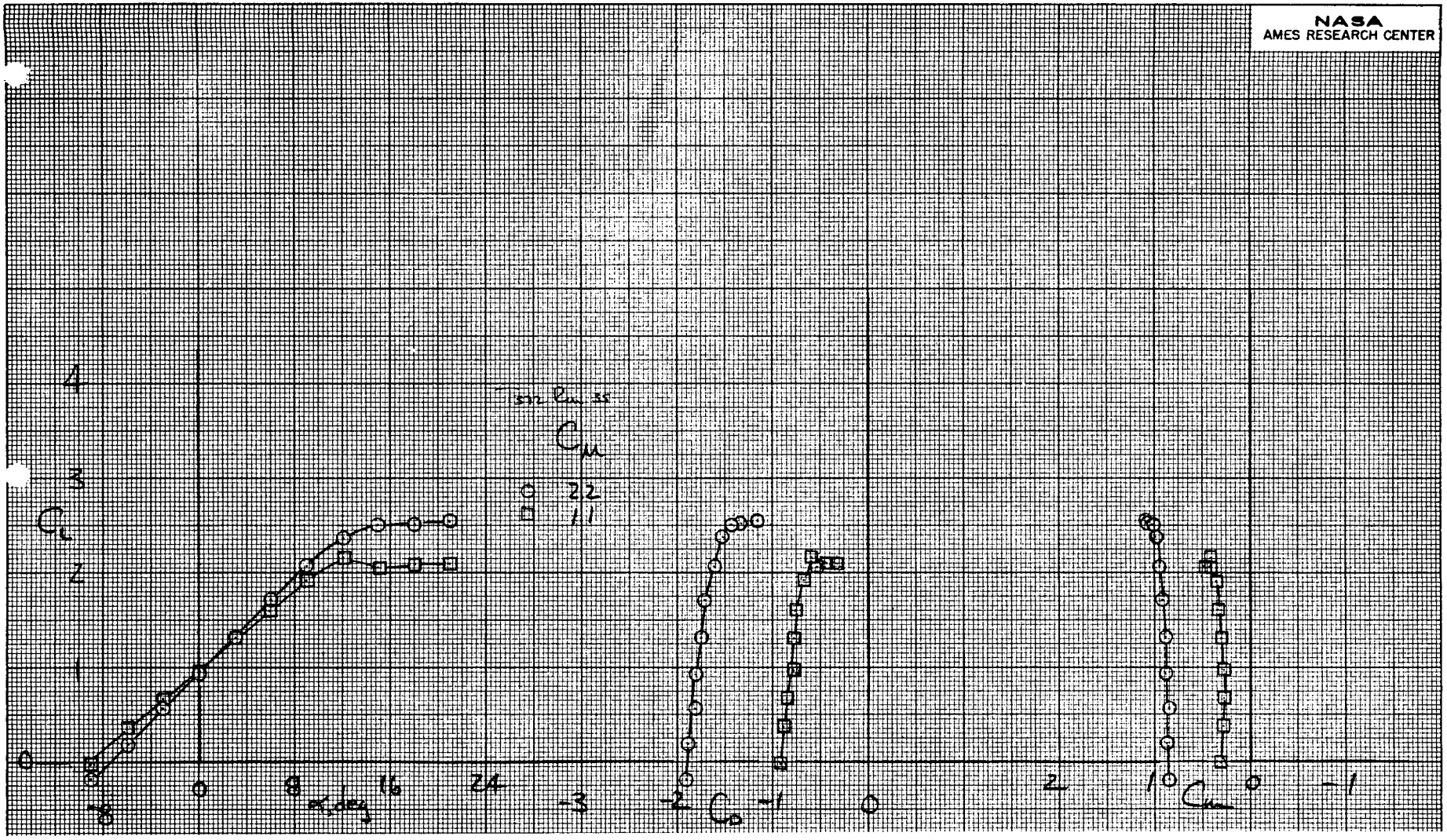

(c) $\delta_f = 30°$

Figure 9.- Continued.

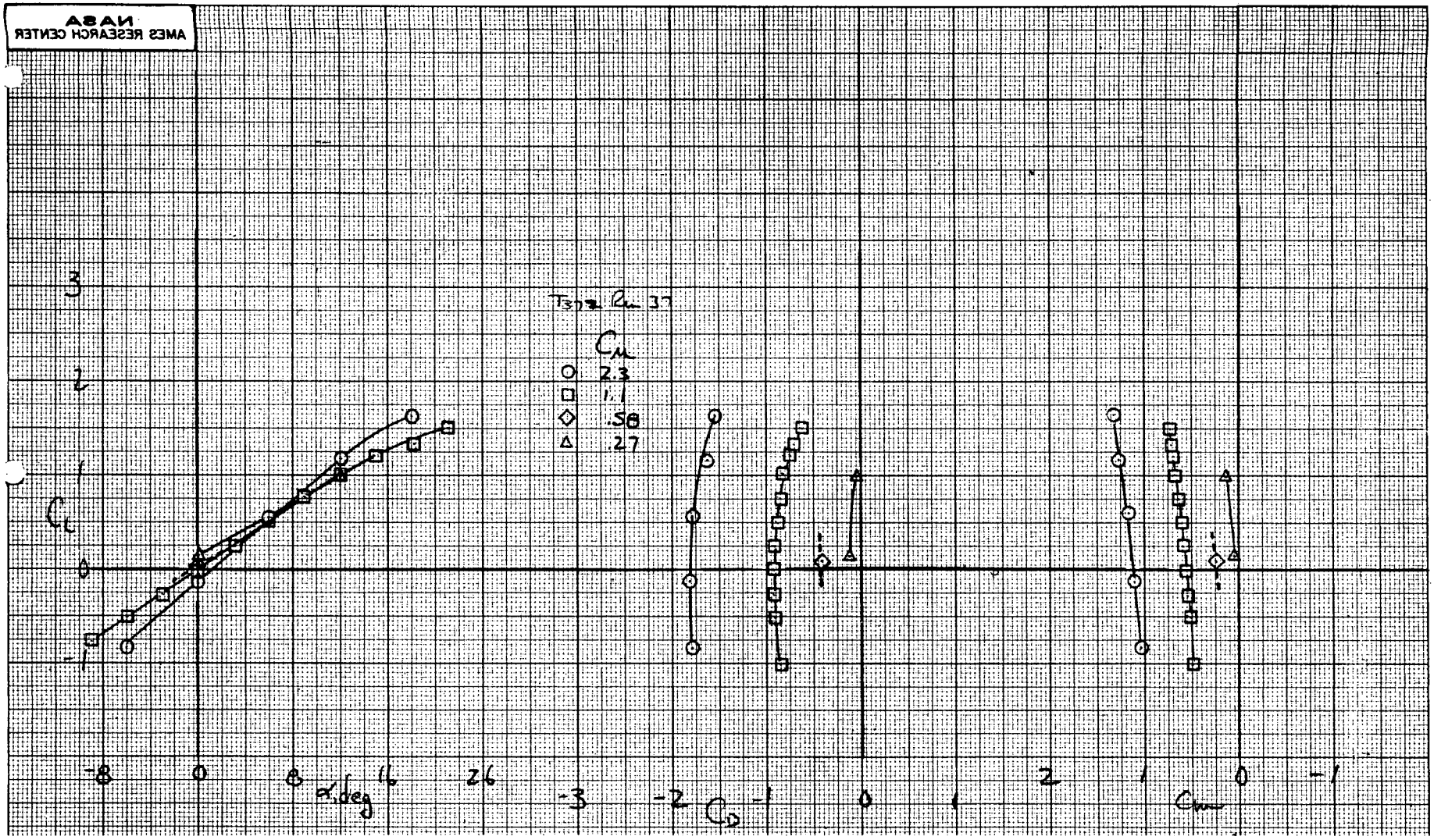

(d) $\delta_f = 0°$

Figure 9.- Concluded.

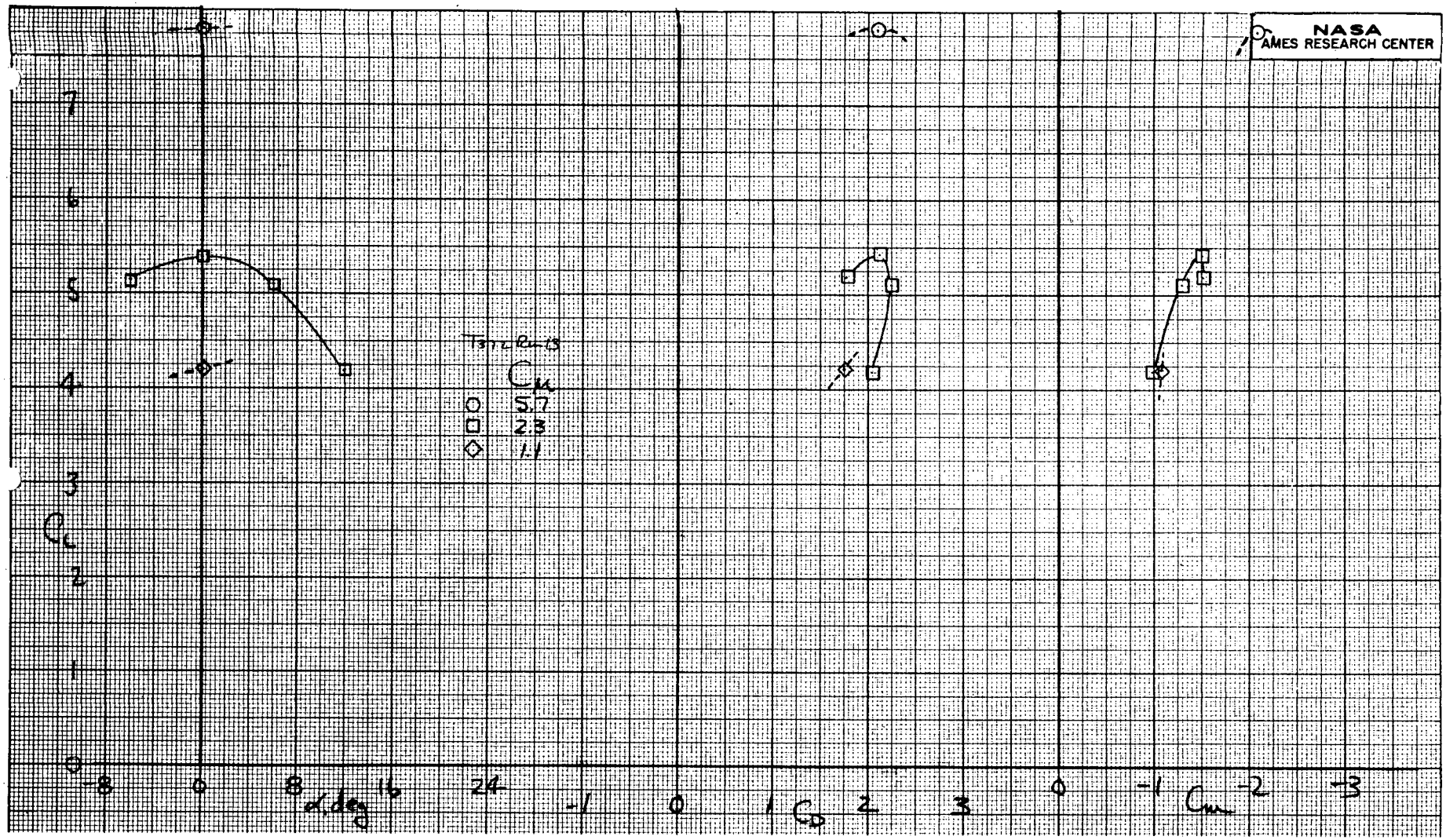

(a) $\delta_f = 90^\circ$

Figure 10.- Longitudinal aerodynamic characteristics; $\Lambda = 0^\circ$, medium pylon, flap I.

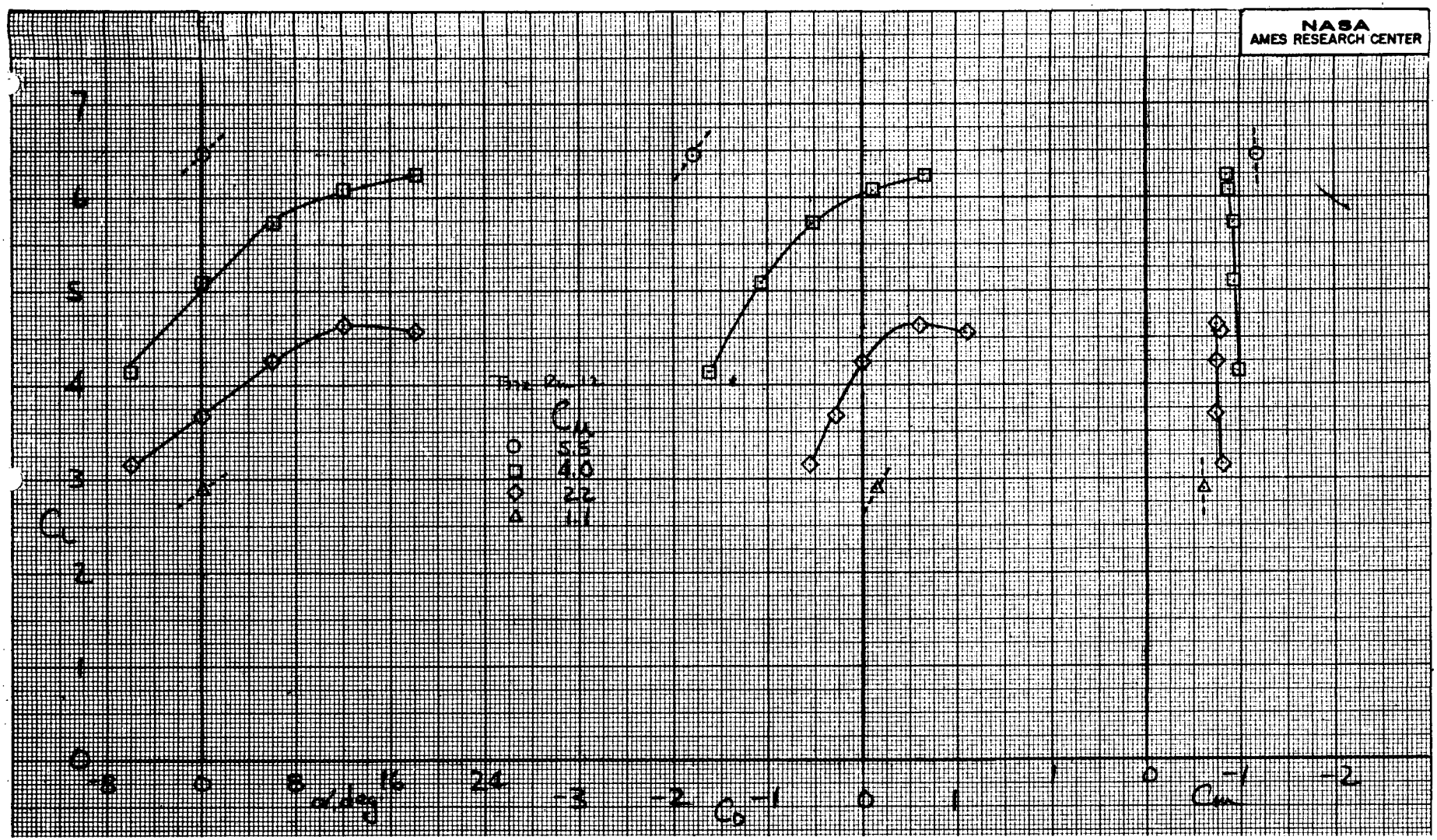

(b) $\delta_f = 60°$

Figure 10.- Continued.

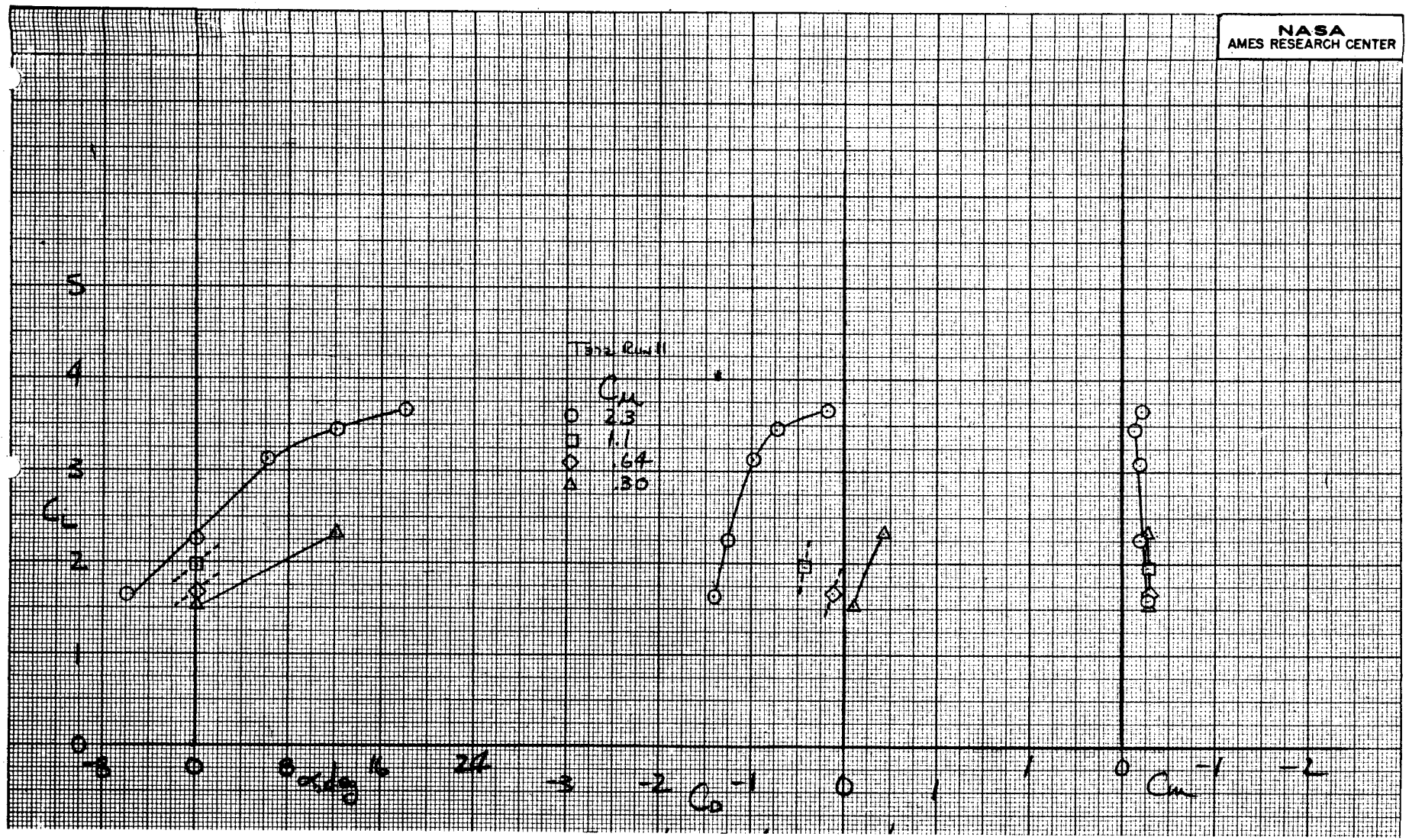

(c) $\delta_f = 30°$

Figure 10.- Continued.

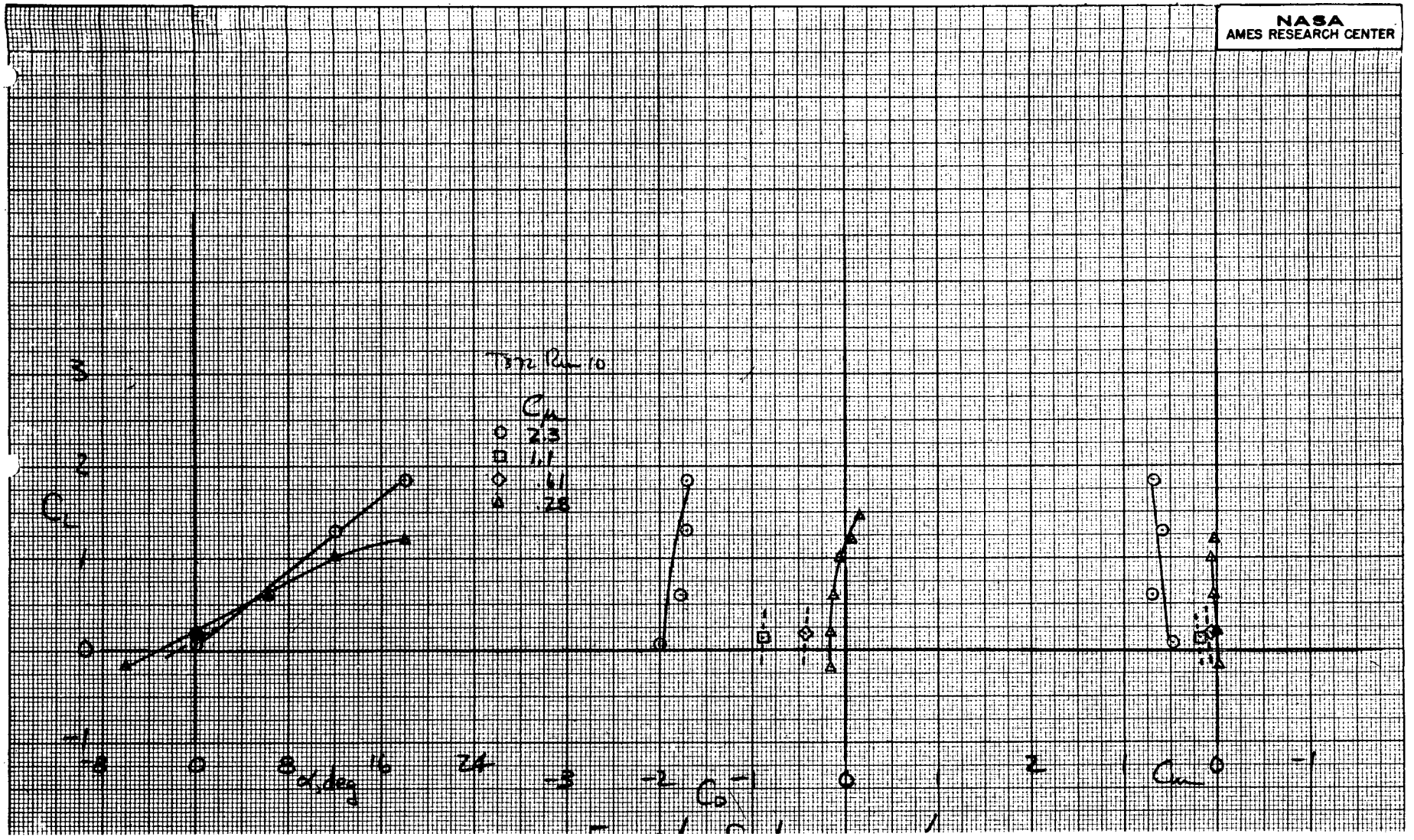

(d) $\delta_f = 0°$

Figure 10.- Concluded.

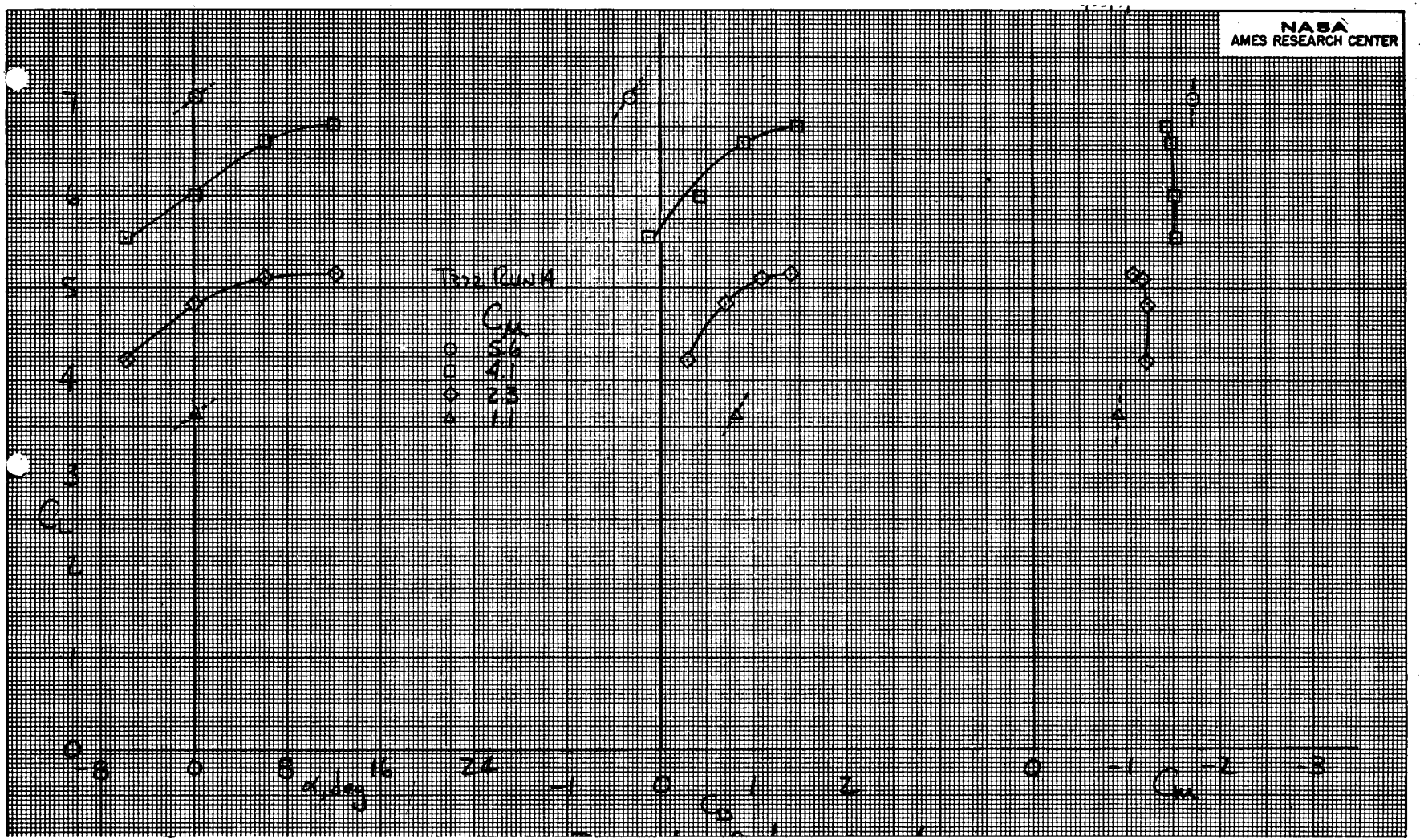

(a) $\delta_f = 90°$

Figure 11.- Longitudinal aerodynamic characteristics; $\Lambda = 0°$, medium pylon, flap II.

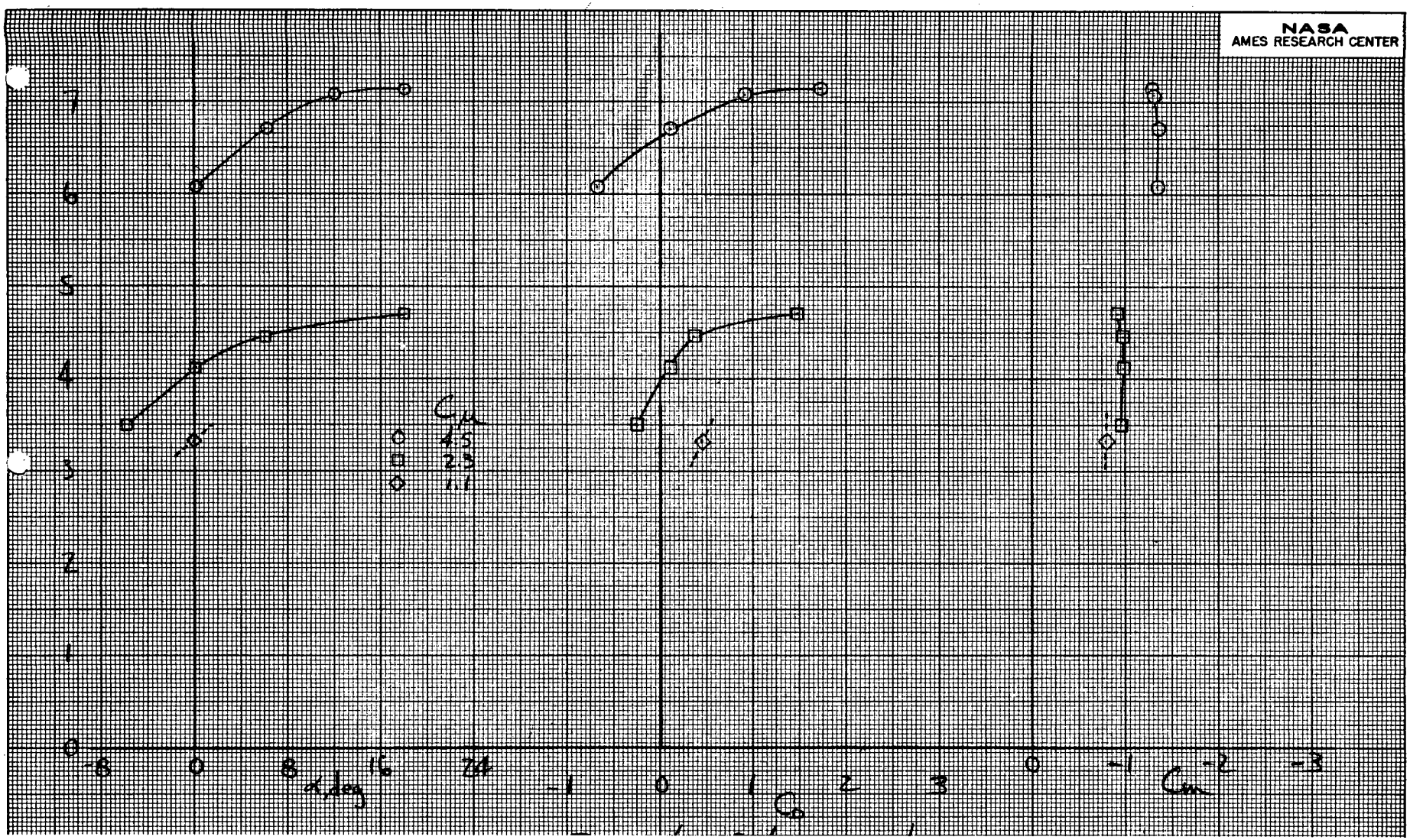

(b) $\delta_f = 60°$

Figure 11.- Continued.

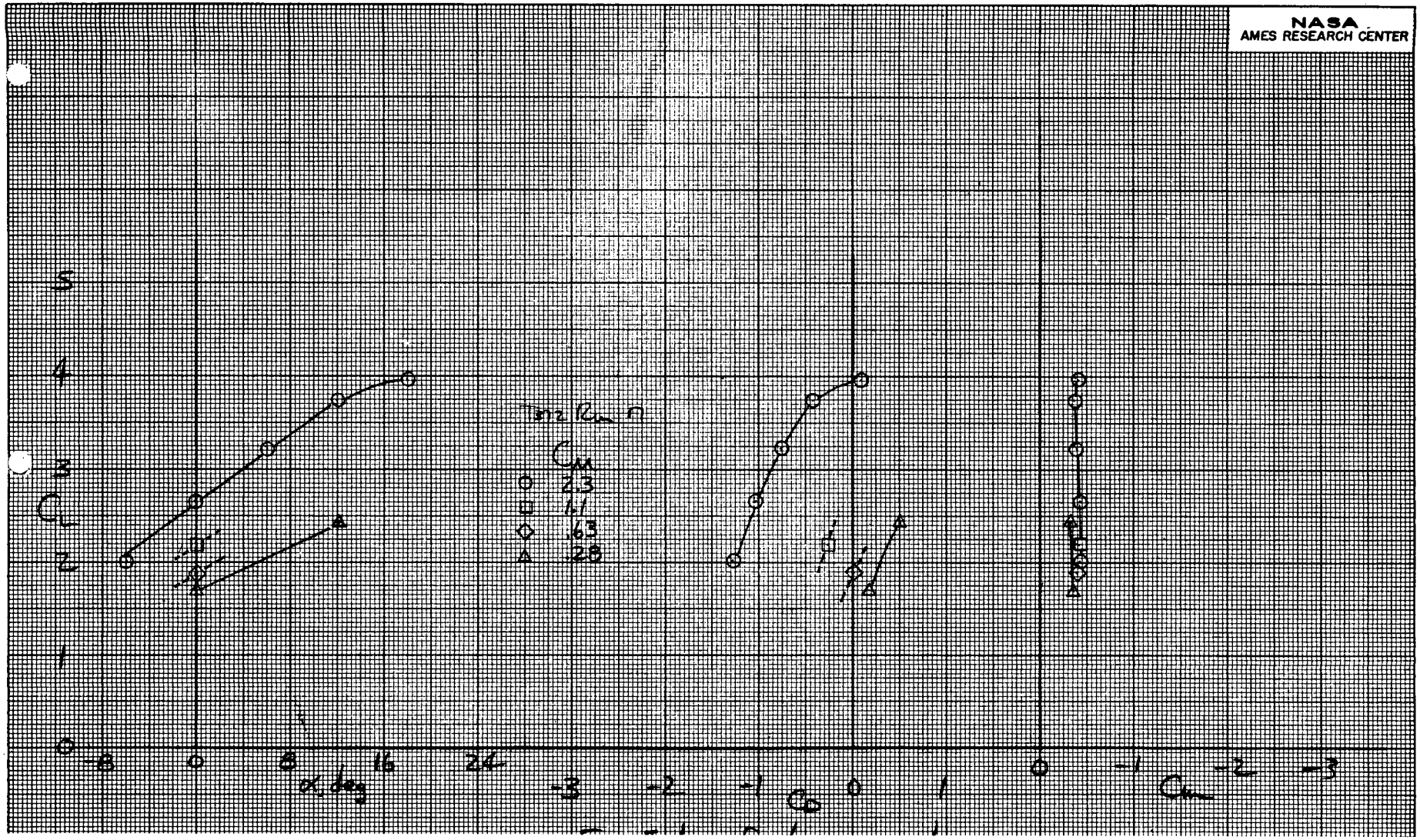

(c) $\delta_f = 30°$

Figurell.- Continued.

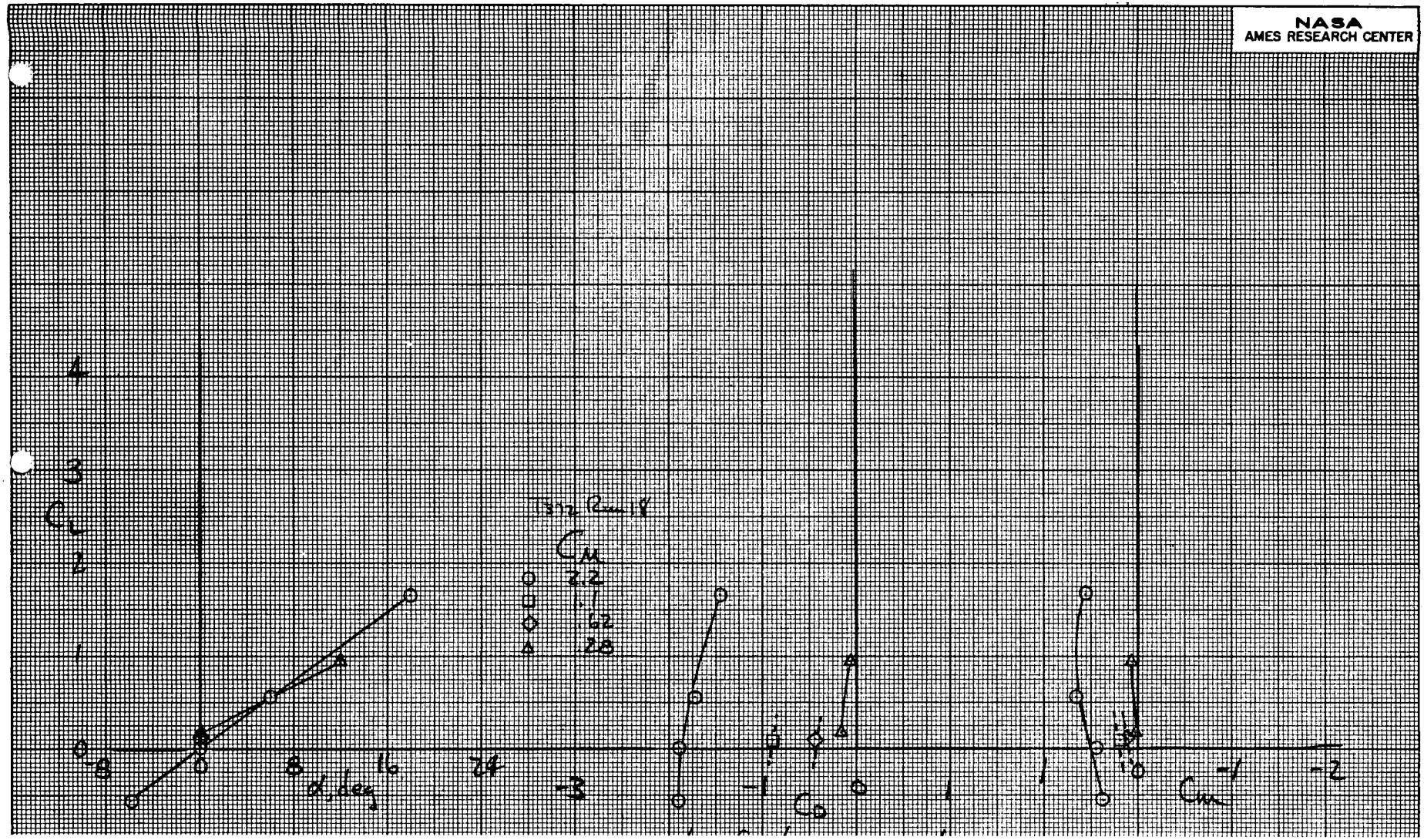

(d) $\delta_f = 0°$

Figure 11.- Concluded.

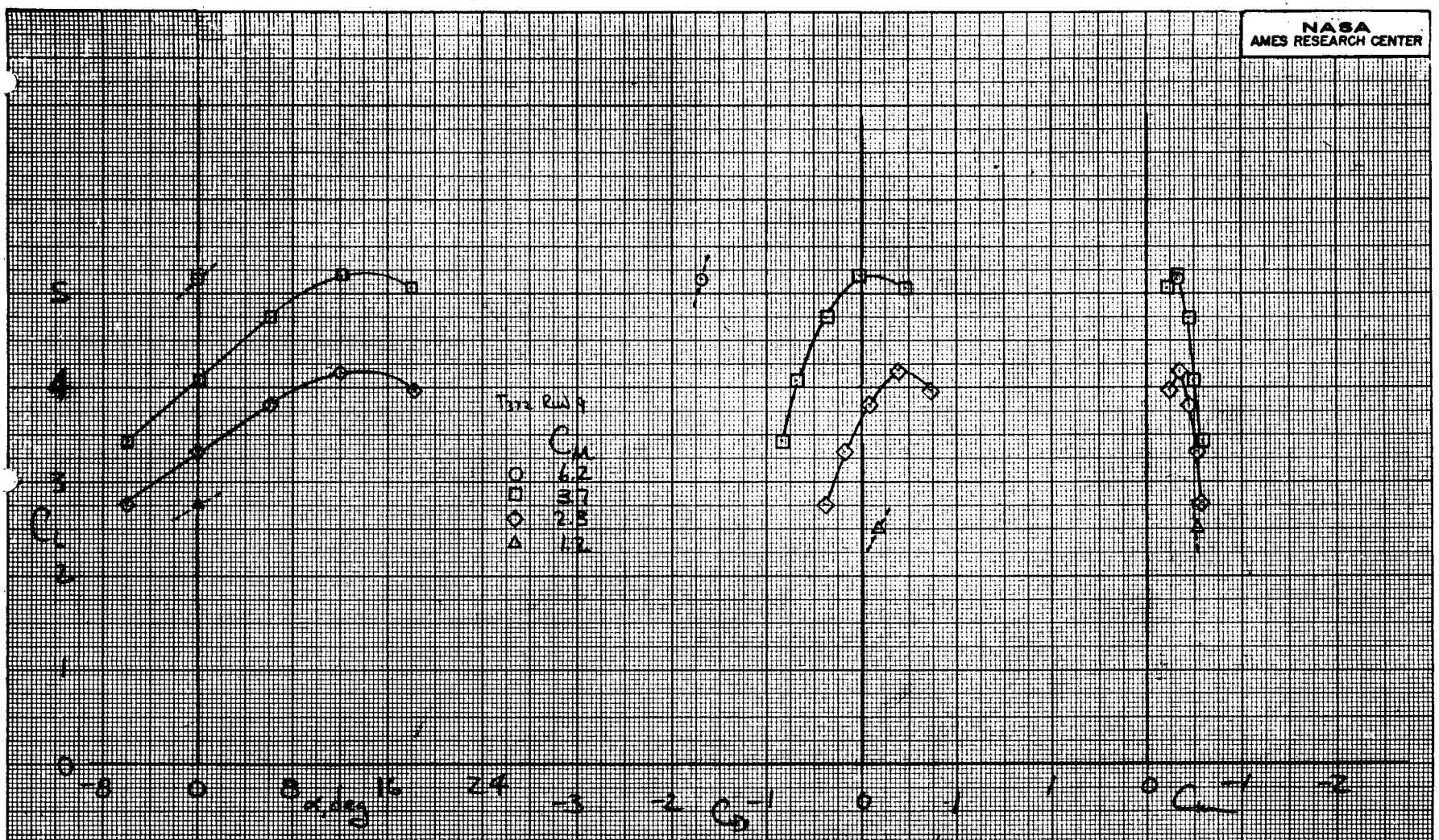

(a) $\delta_f = 90^\circ$

Figure 12.- Longitudinal aerodynamic characteristics; $\Lambda = 0^\circ$, medium pylon, flap III.

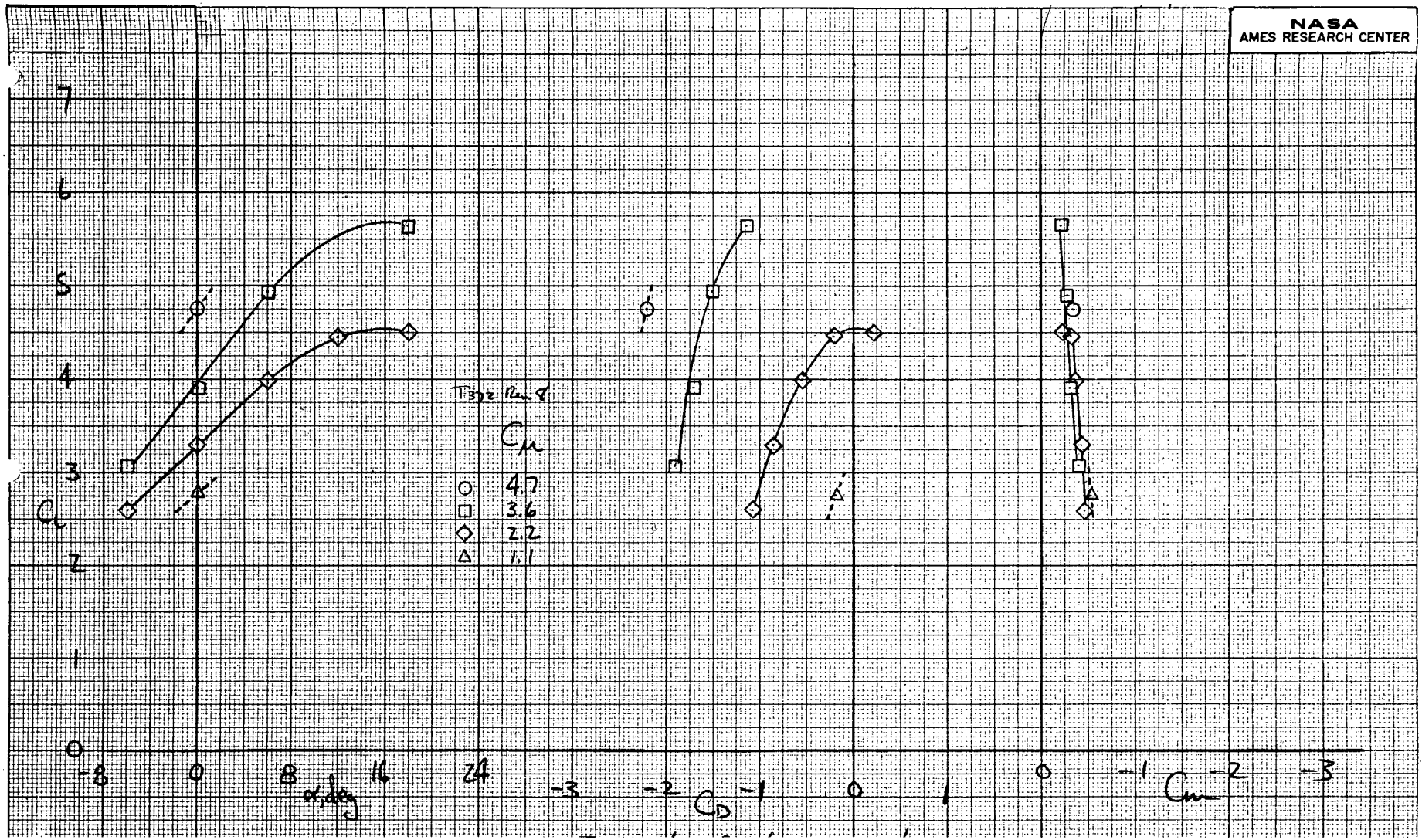

(b) $\delta_f = 60°$

Figure 12.- Continued.

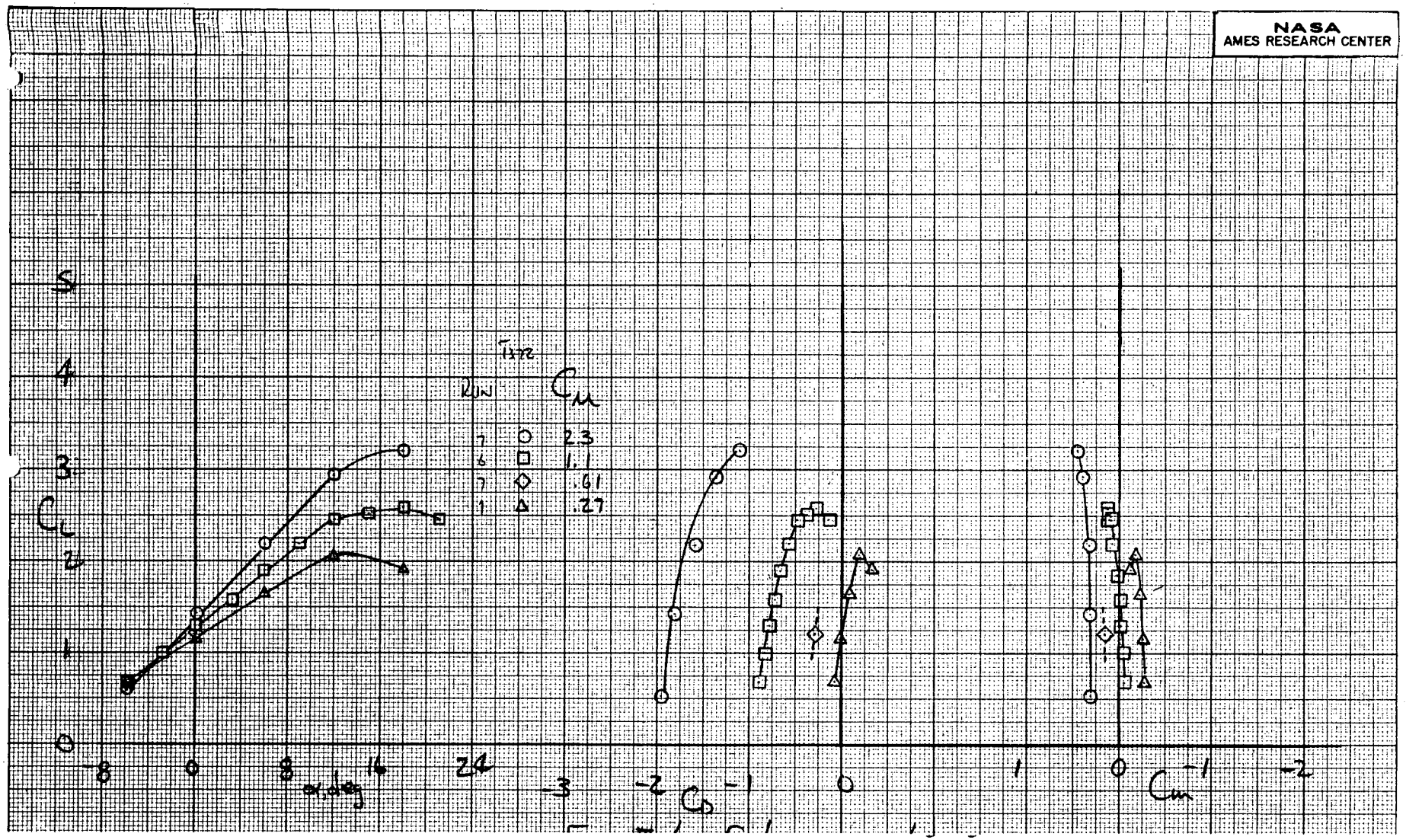

(c) $\delta_f = 30°$

Figure 12.- Continued.

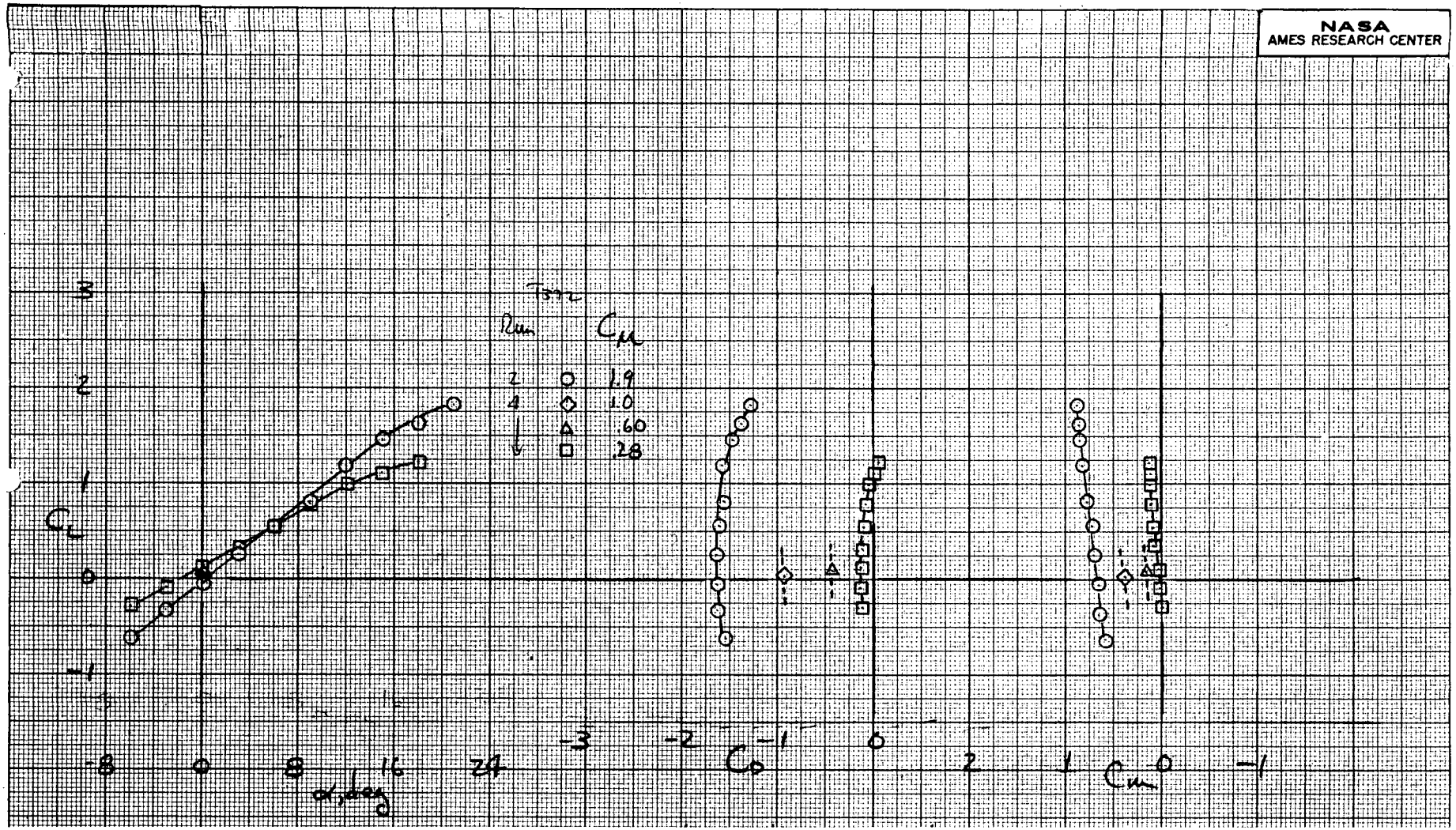

(d) $\delta_f = 0°$

Figure 12.- Concluded.

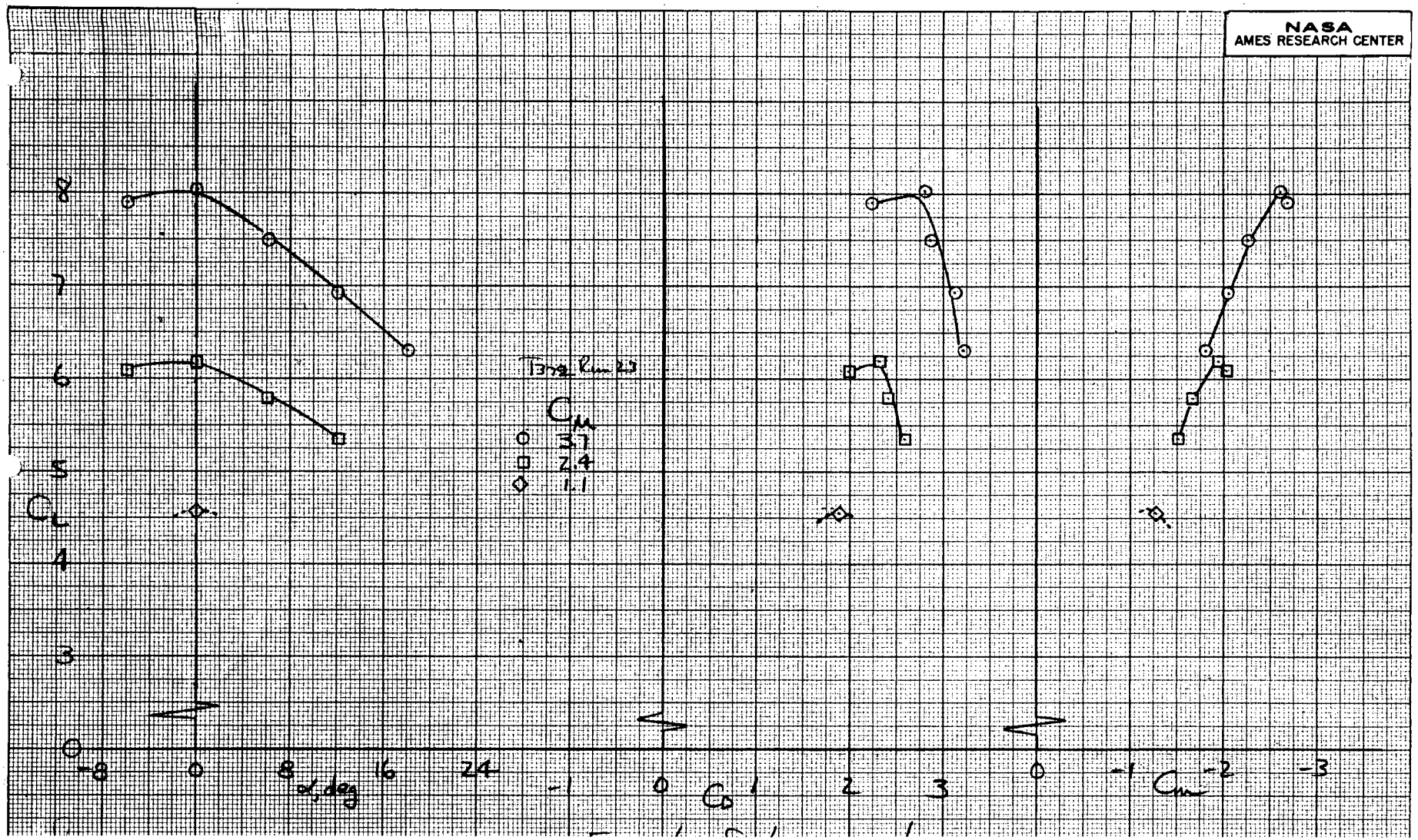

(a) $\delta_f = 90°$

Figure 13.- Longitudinal aerodynamic characteristics; $\Lambda = 0°$, no pylon, flap I.

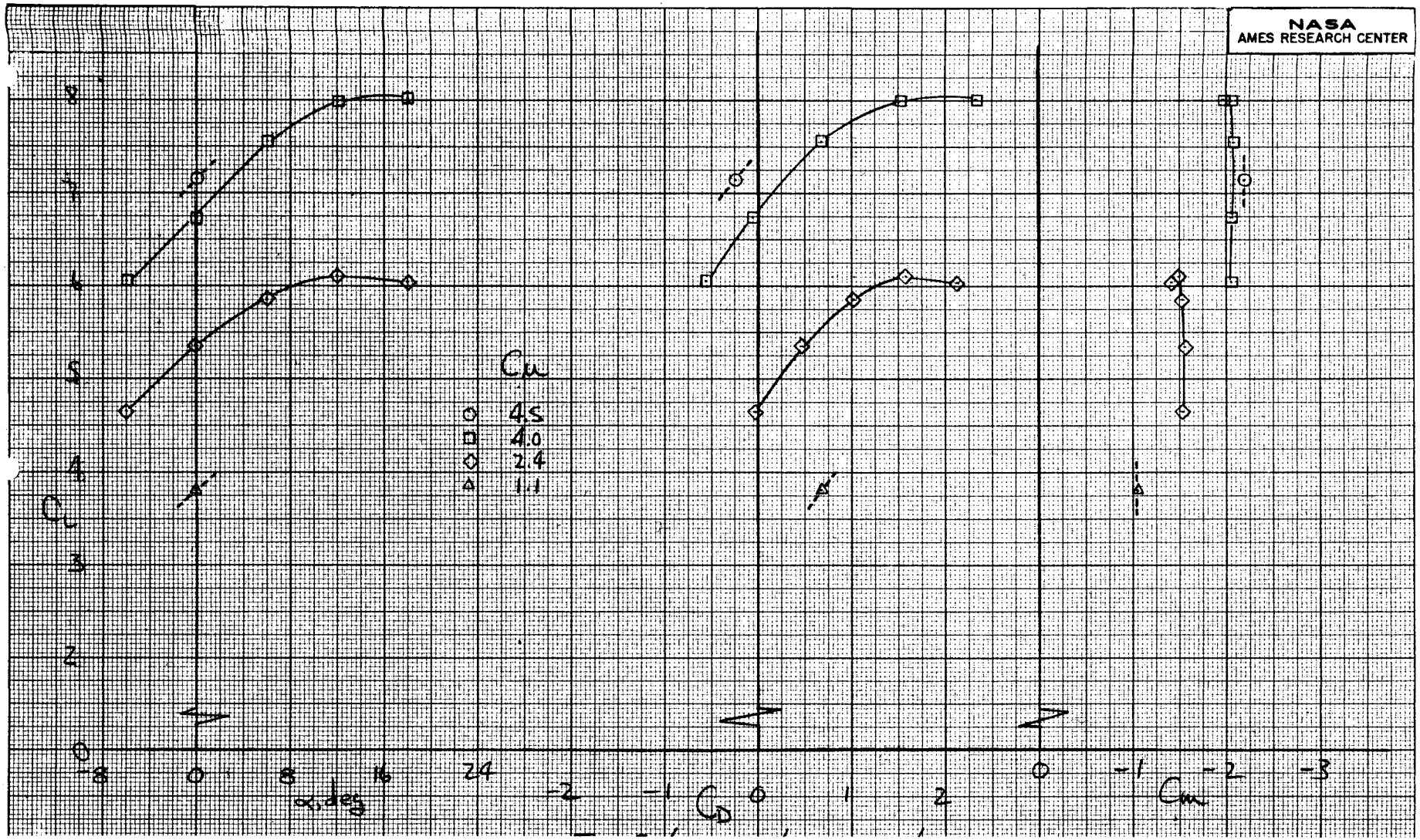

(b) $\delta_f = 60°$

Figure 13.- Continued.

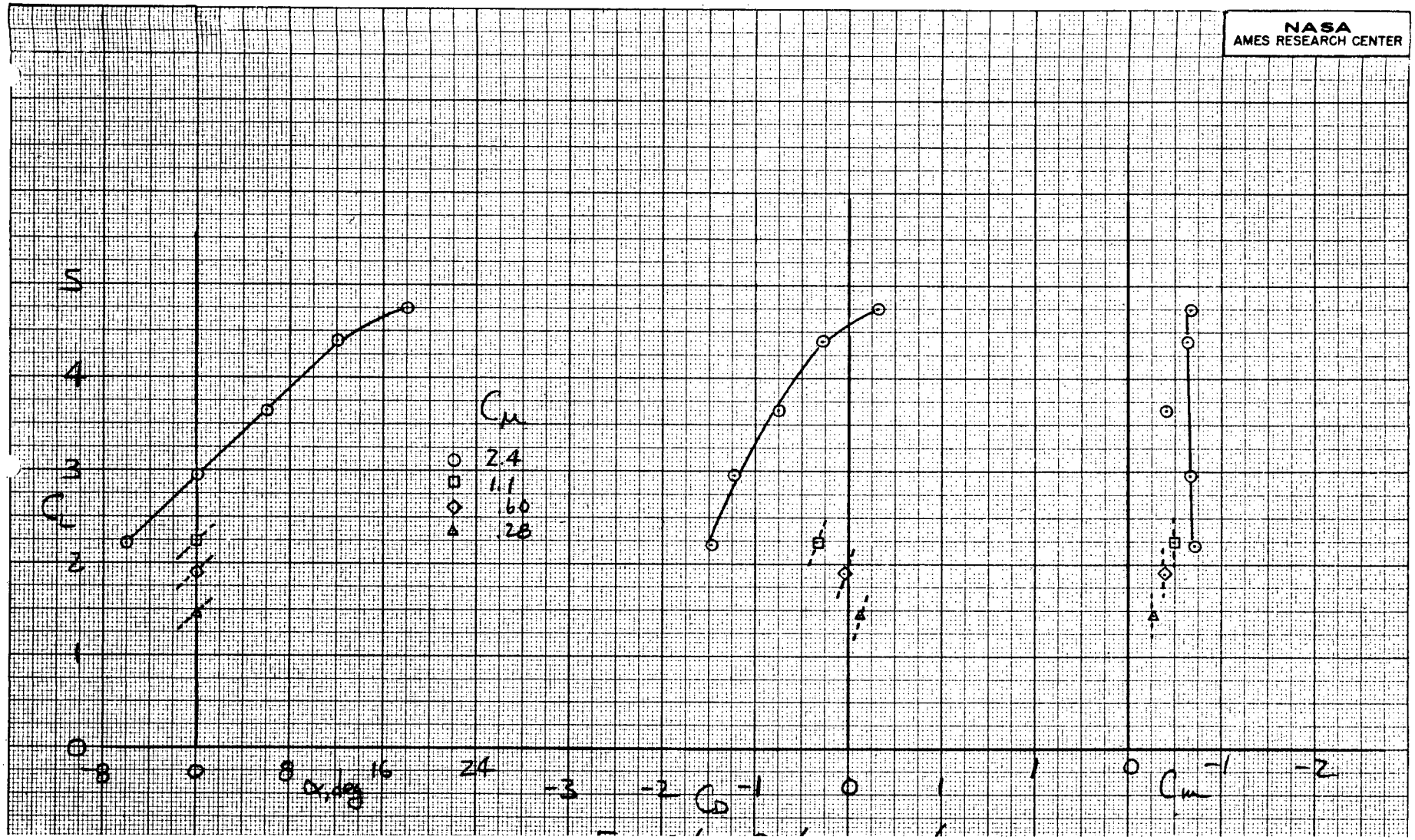

(c) $\delta_f = 30°$

Figure 13.- Continued.

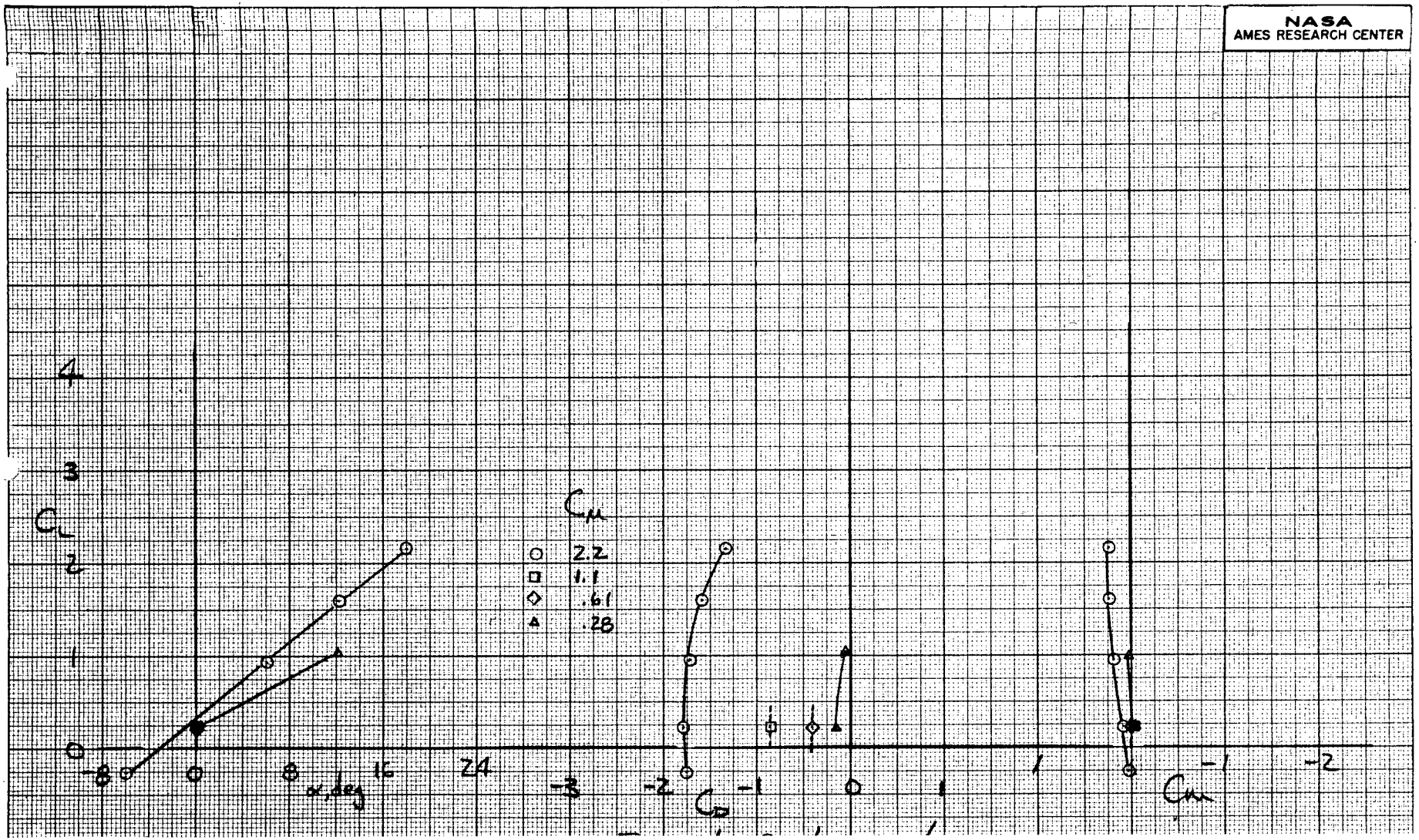

(d) $\delta_f = 0°$

Figure 13.- Concluded.

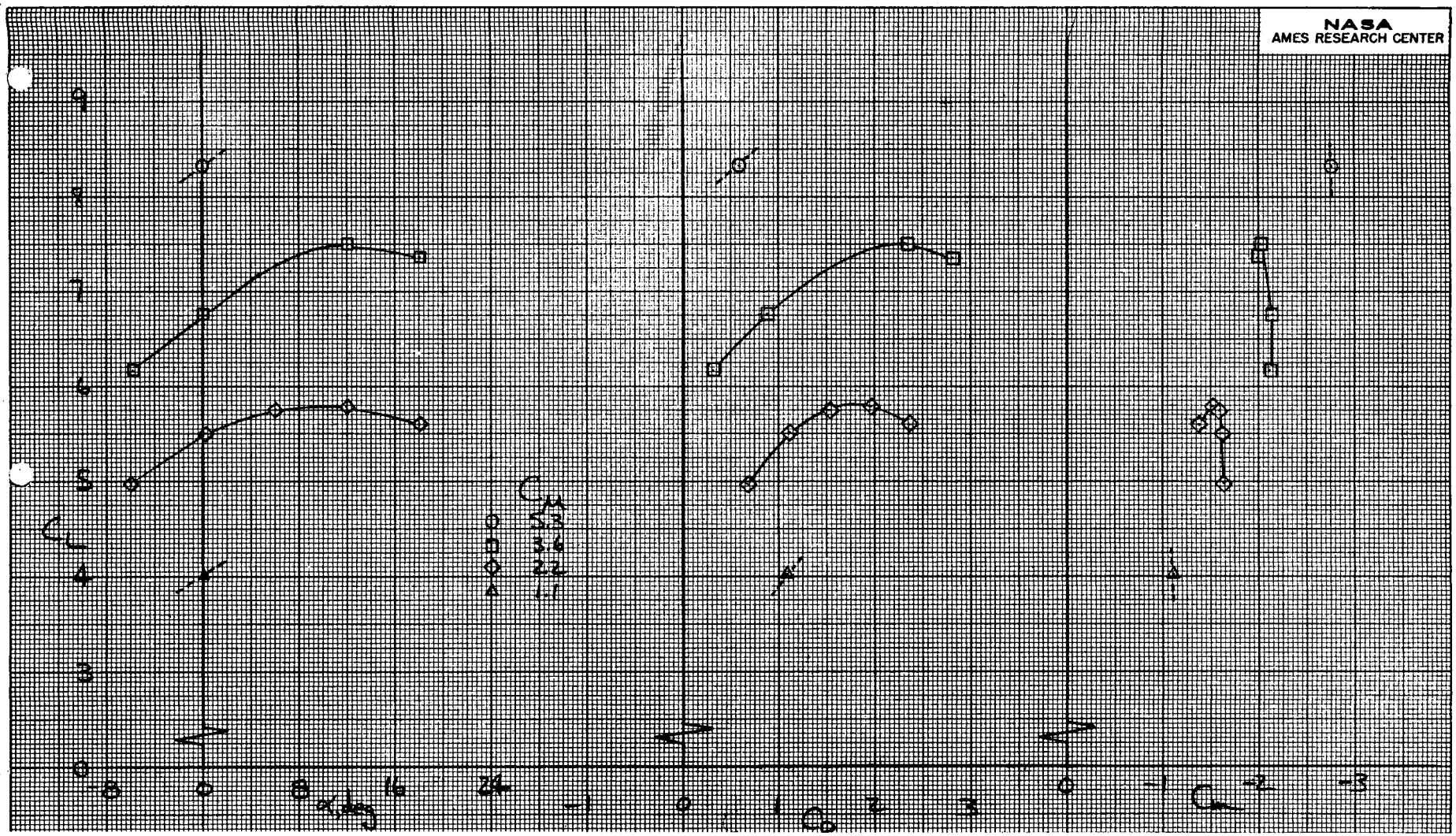

(a) $\delta_f = 60°$

Figure 14.- Longitudinal aerodynamic characteristics; $\Lambda = 0°$, no pylon, flap II.

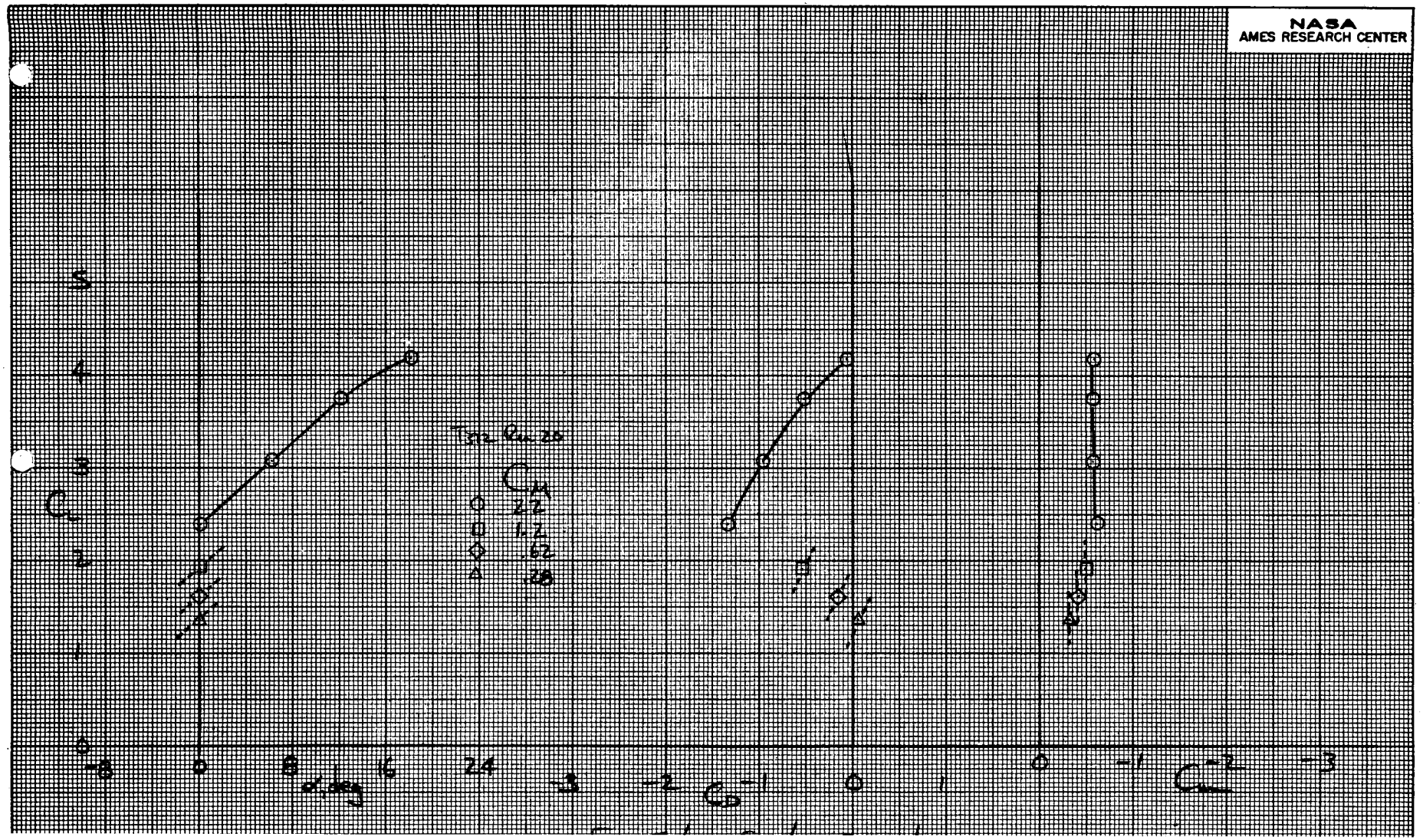

(b) $\delta_f = 30°$

Figure 14.- Continued.

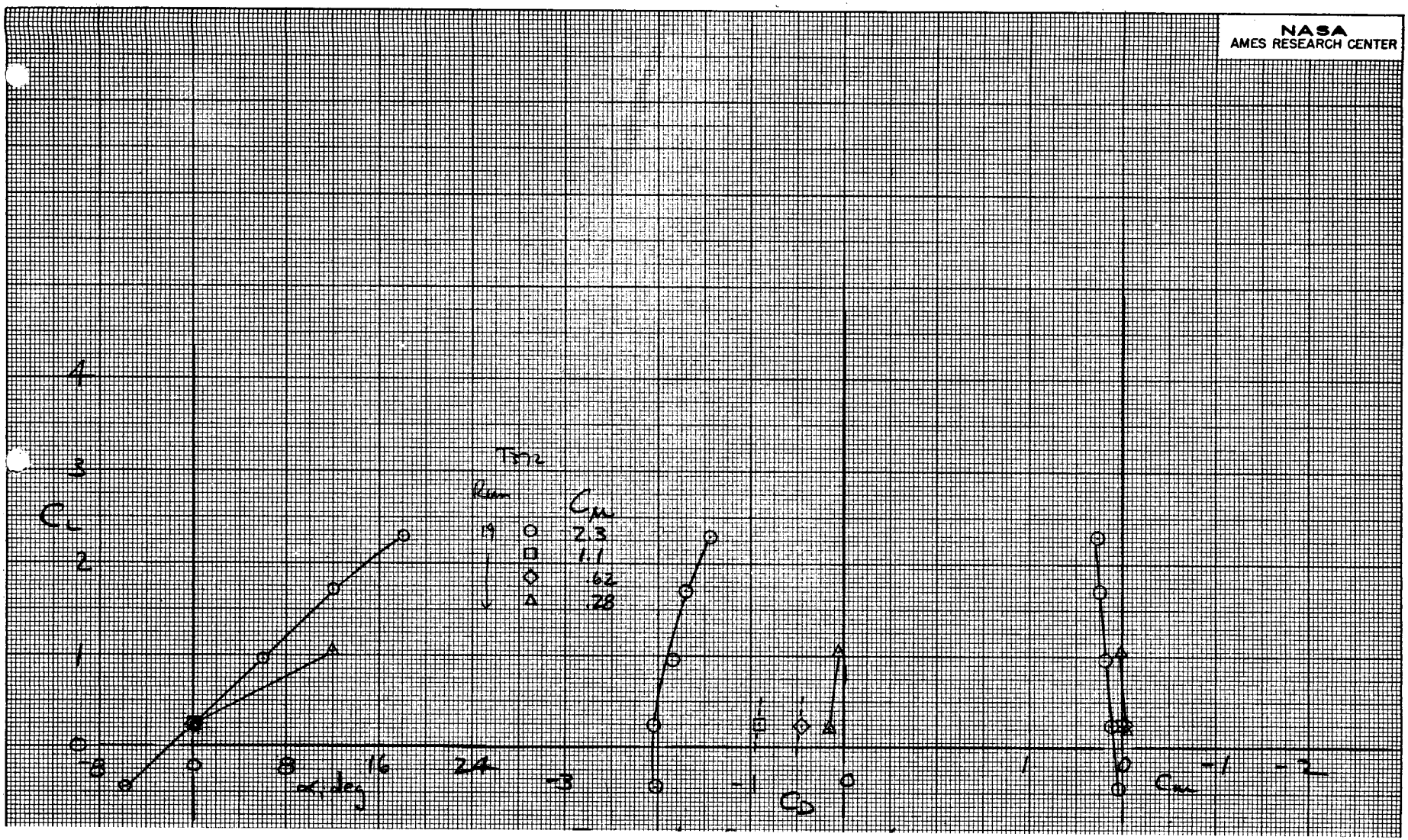

(c) $\delta_f = 0°$

Figure 14.- Concluded

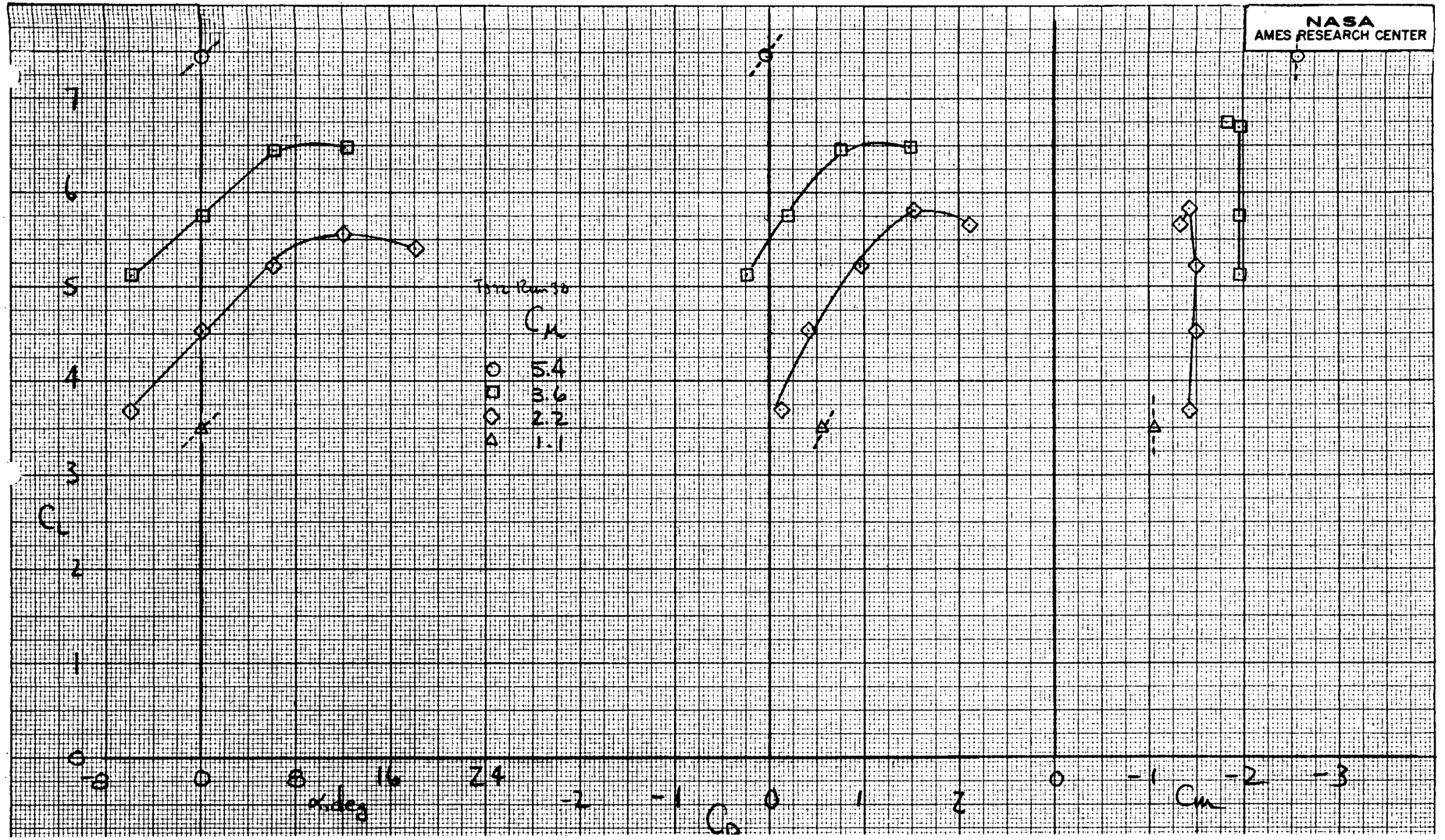

(a) $\delta_f = 90°$

Figure 15.- Longitudinal aerodynamic characteristics; $\Lambda = 0°$, no pylon, flap III.

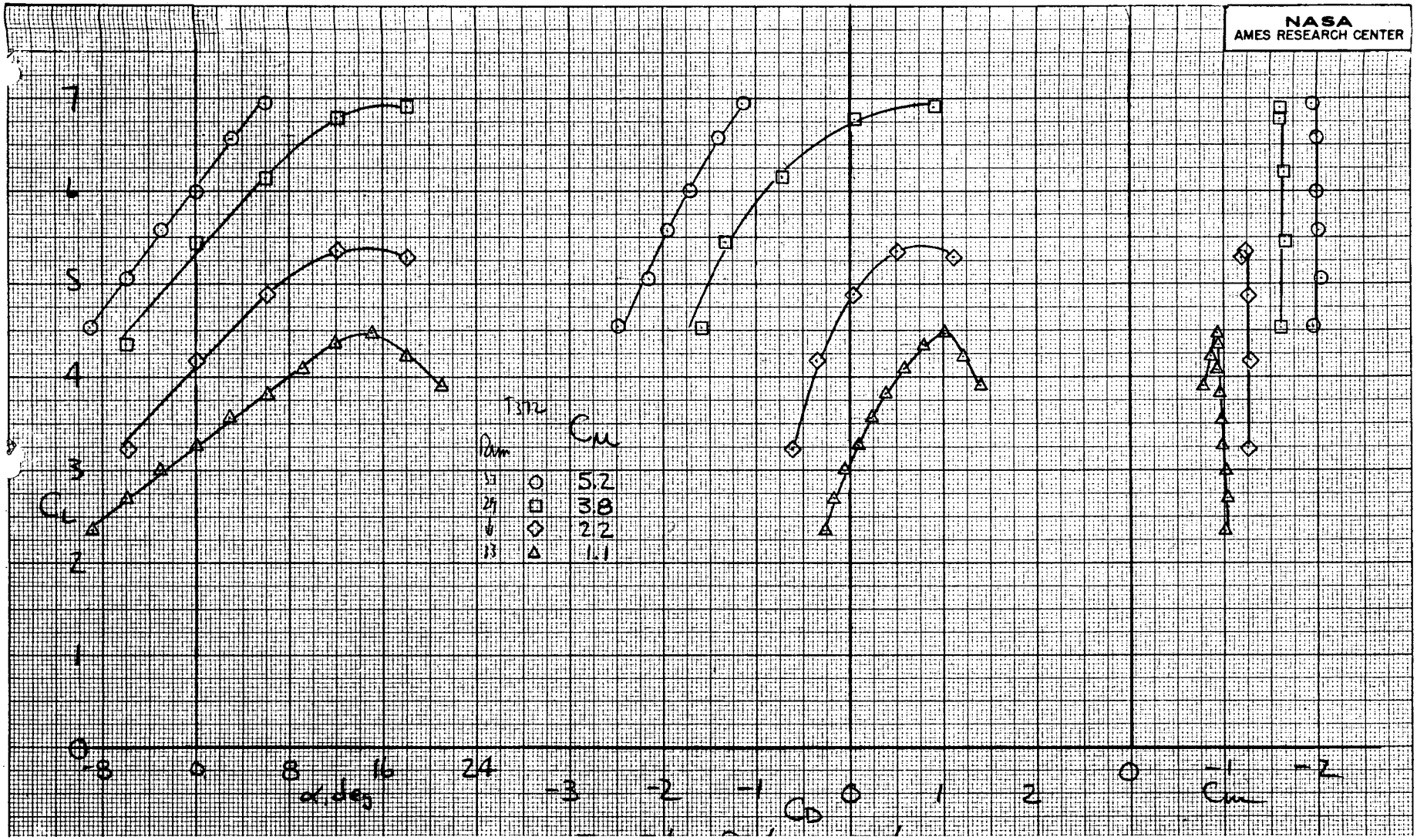

(b) $\delta_f = 60°$

Figure 15.- Continued.

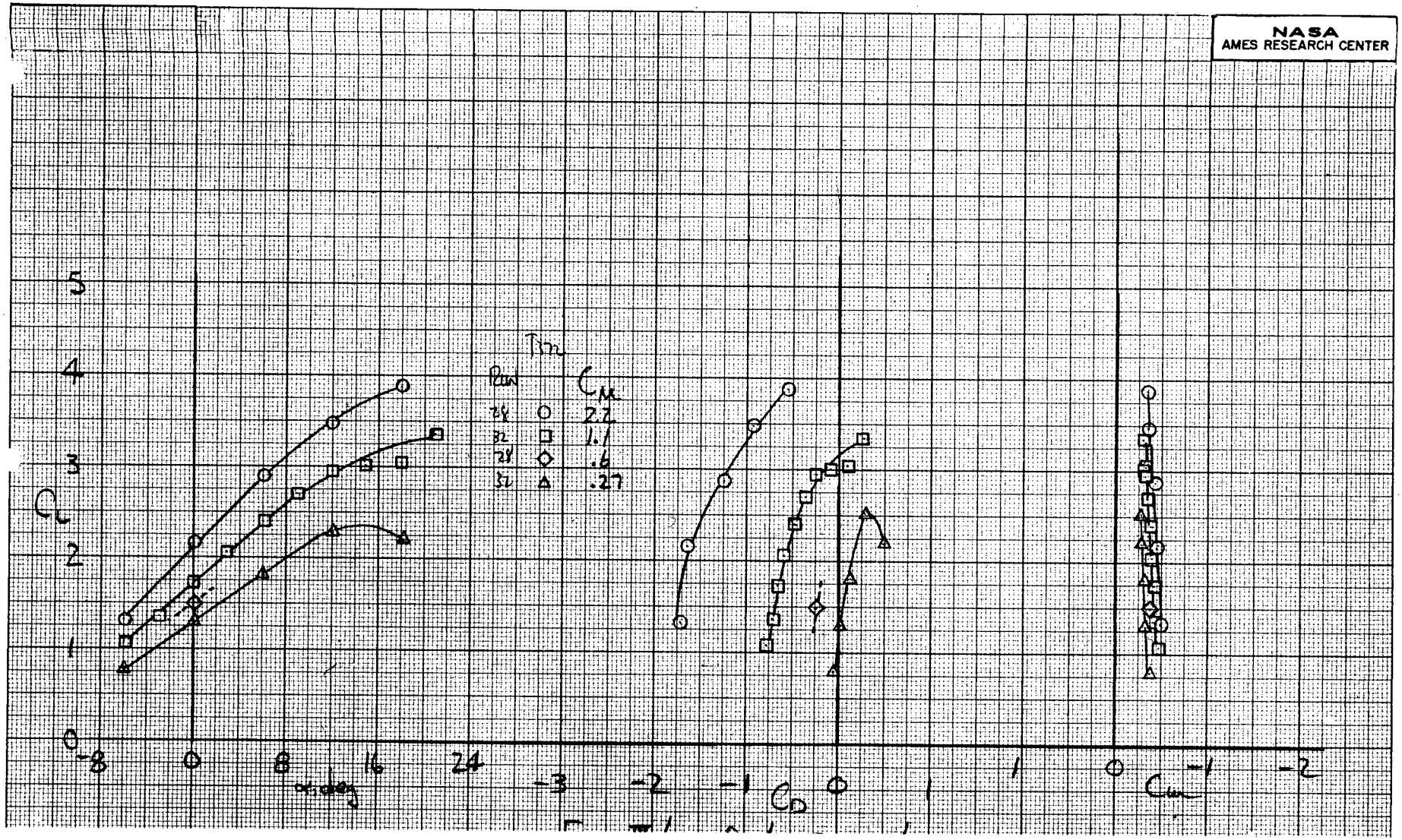

(c) $\delta_f = 30°$

Figure 15.- Continued.

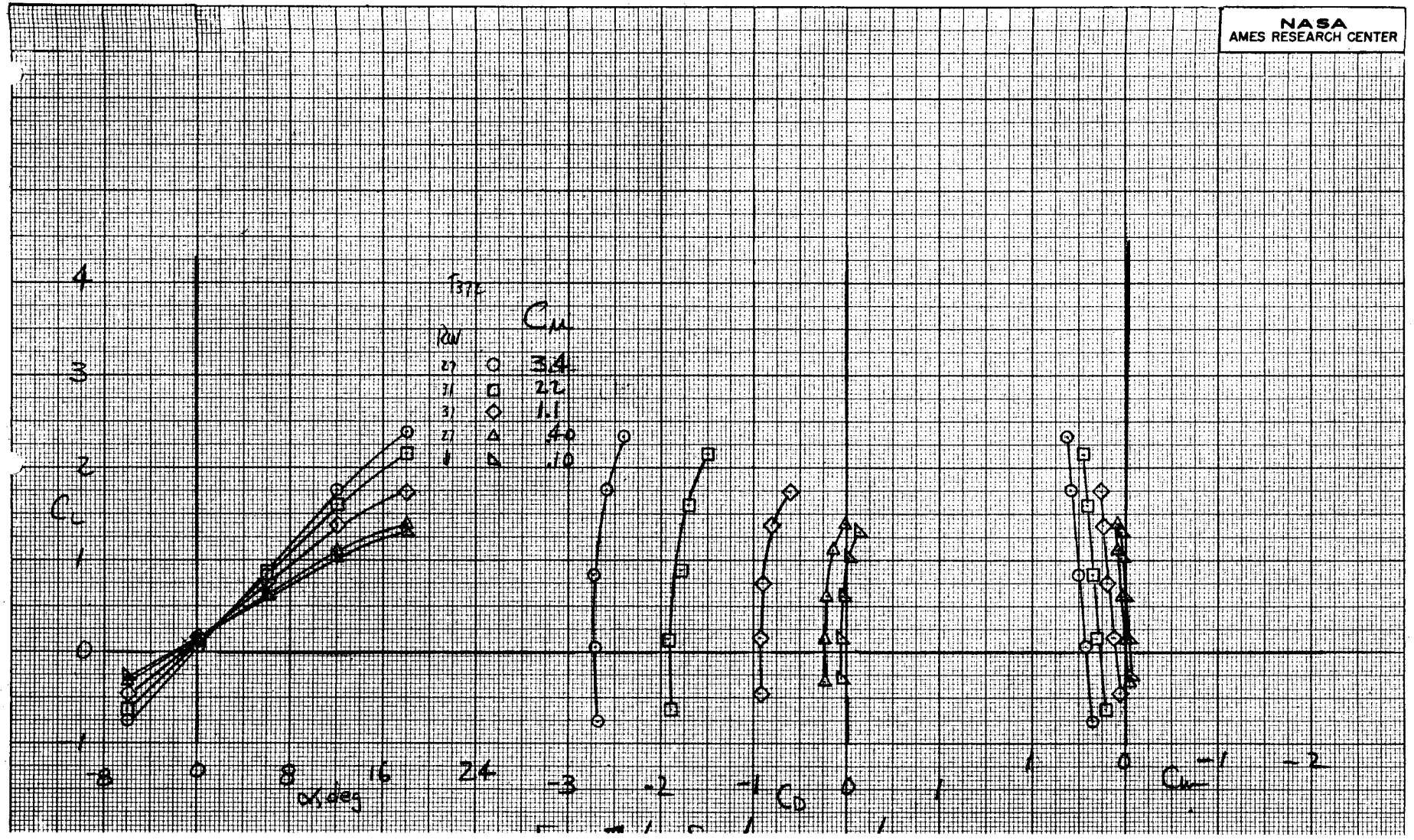

(d) $\delta_f = 0°$

Figure 15.- Continued.

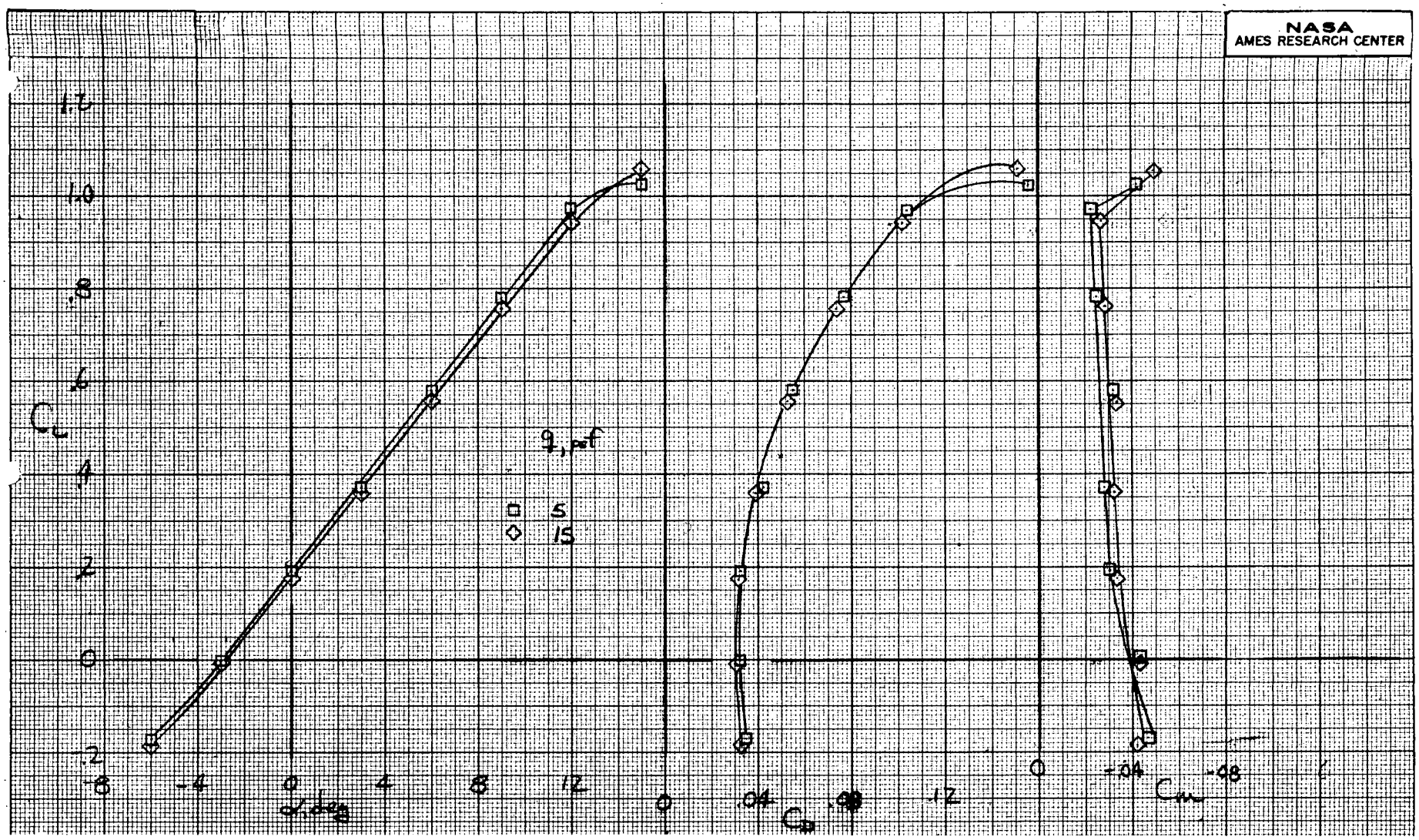

(e) $\delta_f = 0°$, nacelle removed

Figure 15.- Concluded.

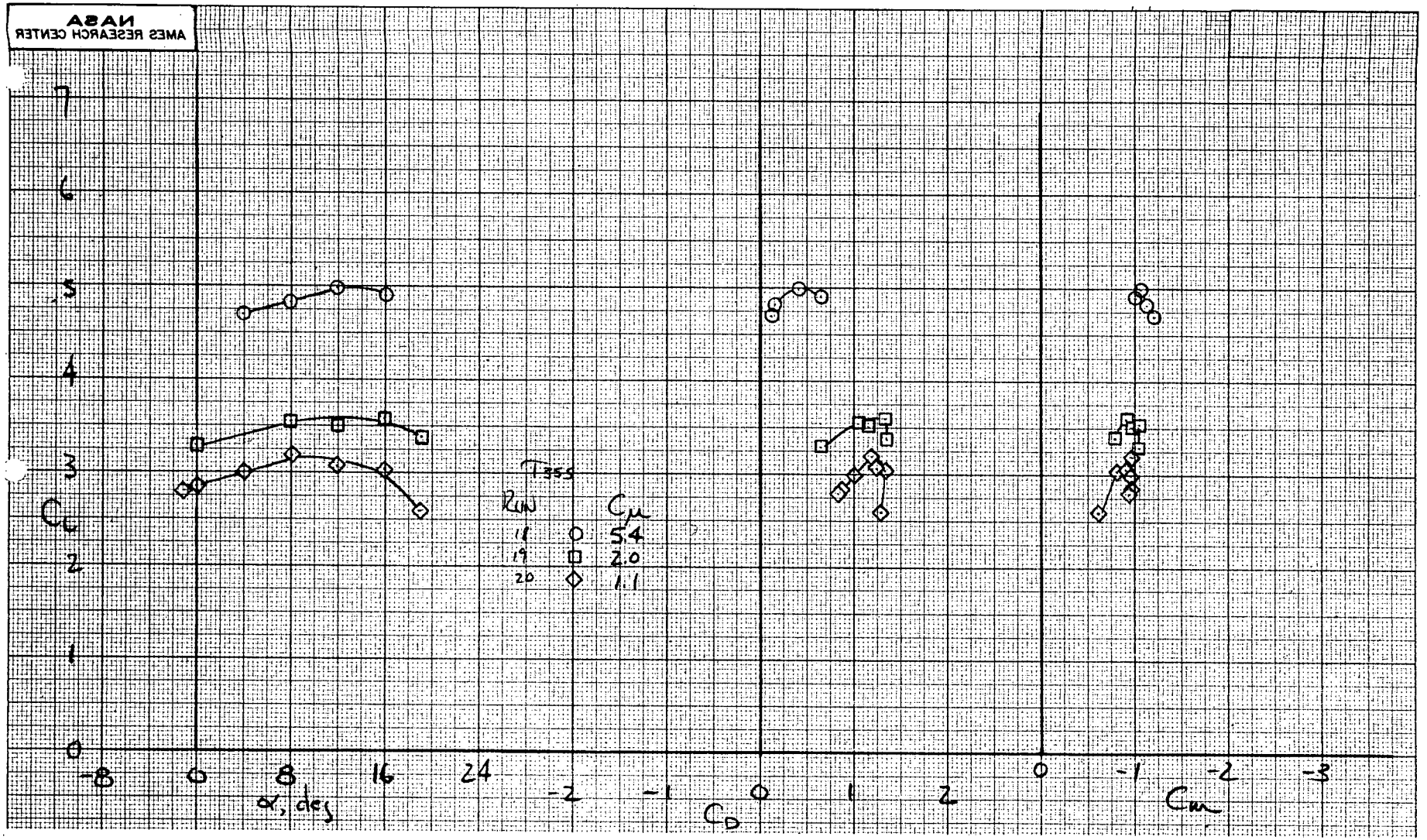

(a) $\delta_f = 90°$

Figure 16.- Longitudinal aerodynamic characteristics; $\Lambda = 30°$, long pylon, flap I.

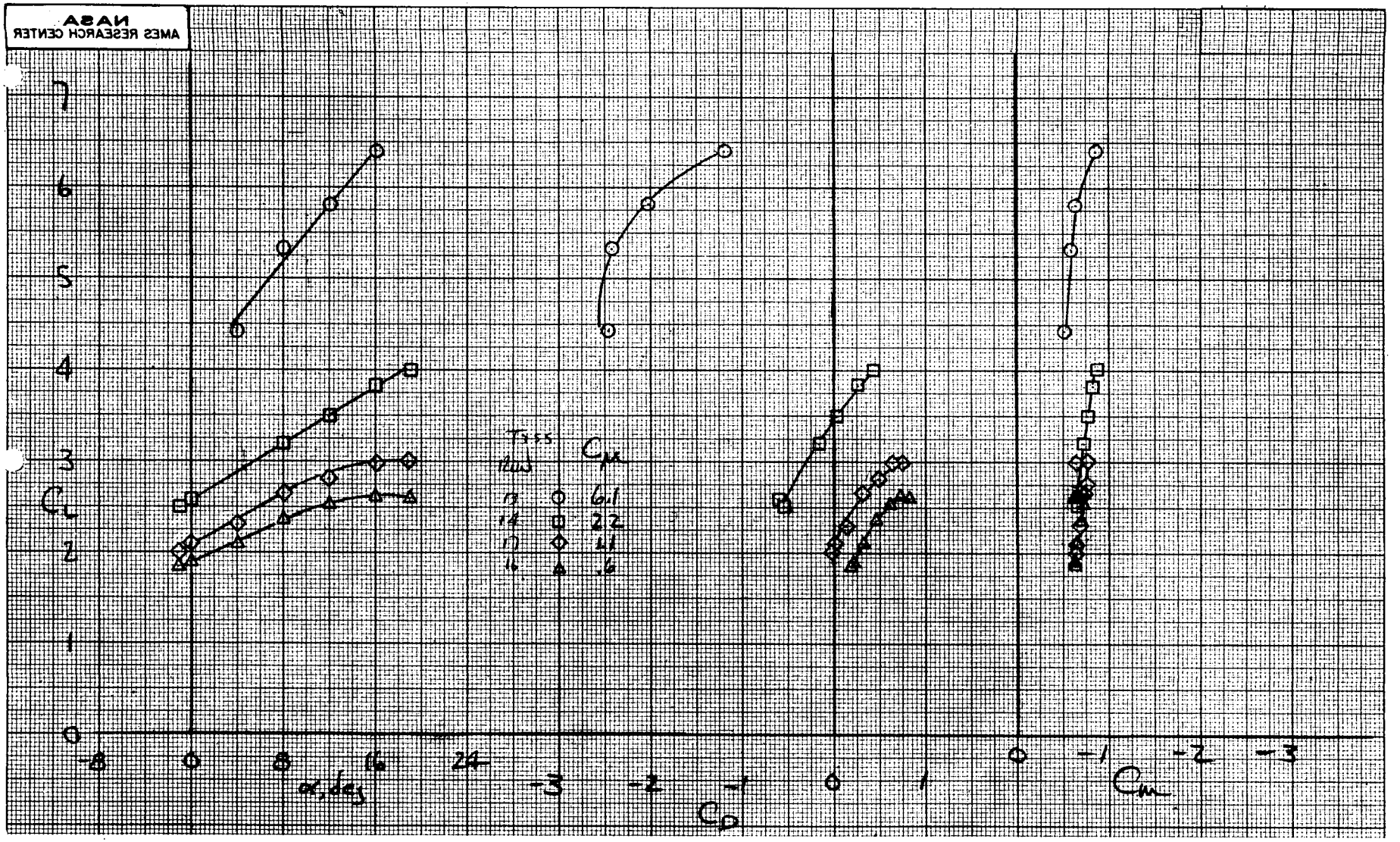

(b) $\delta_f = 60°$

Figure 16.- Continued.

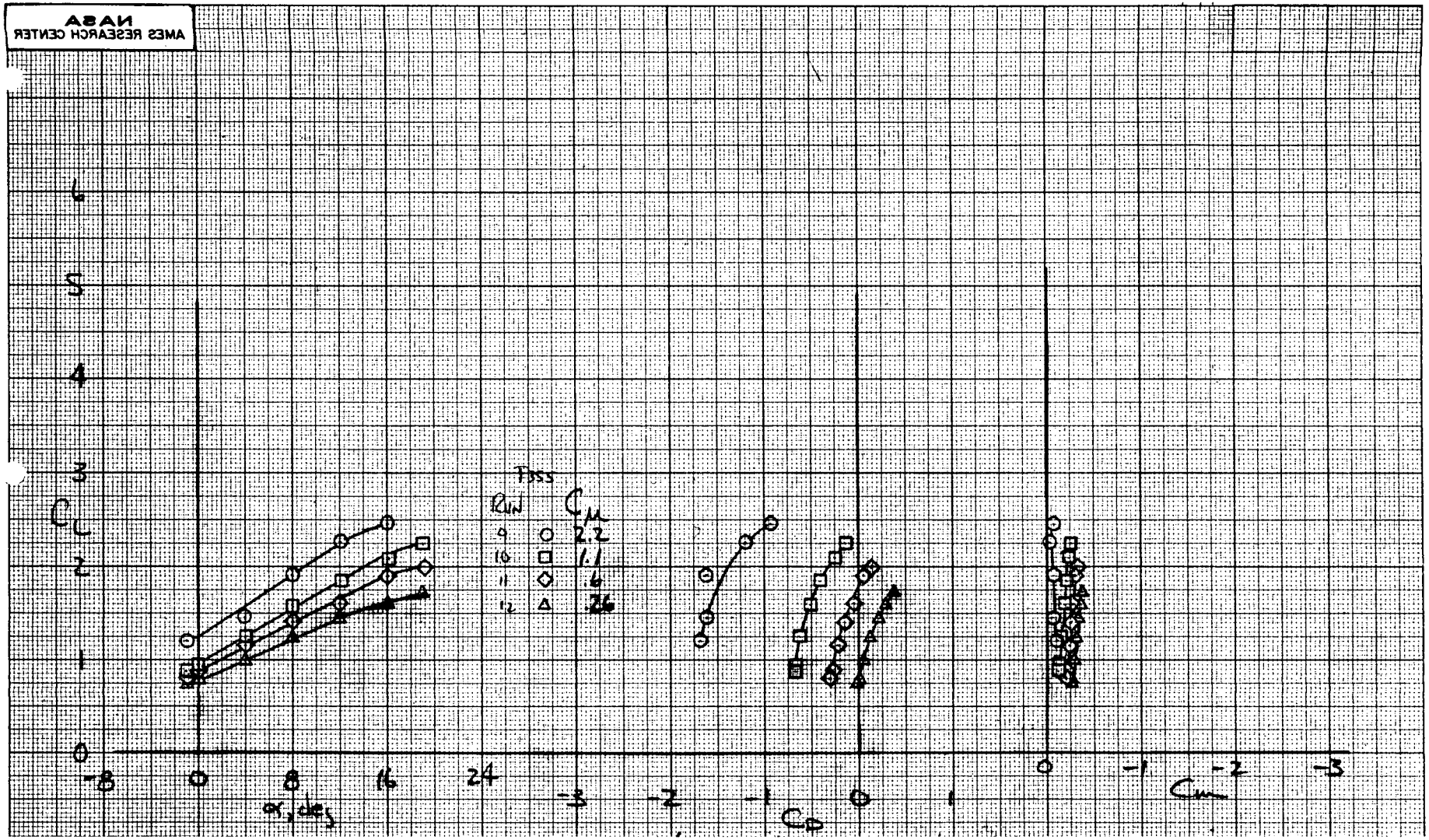

(c) $\delta_f = 30°$

Figure 16.- Continued.

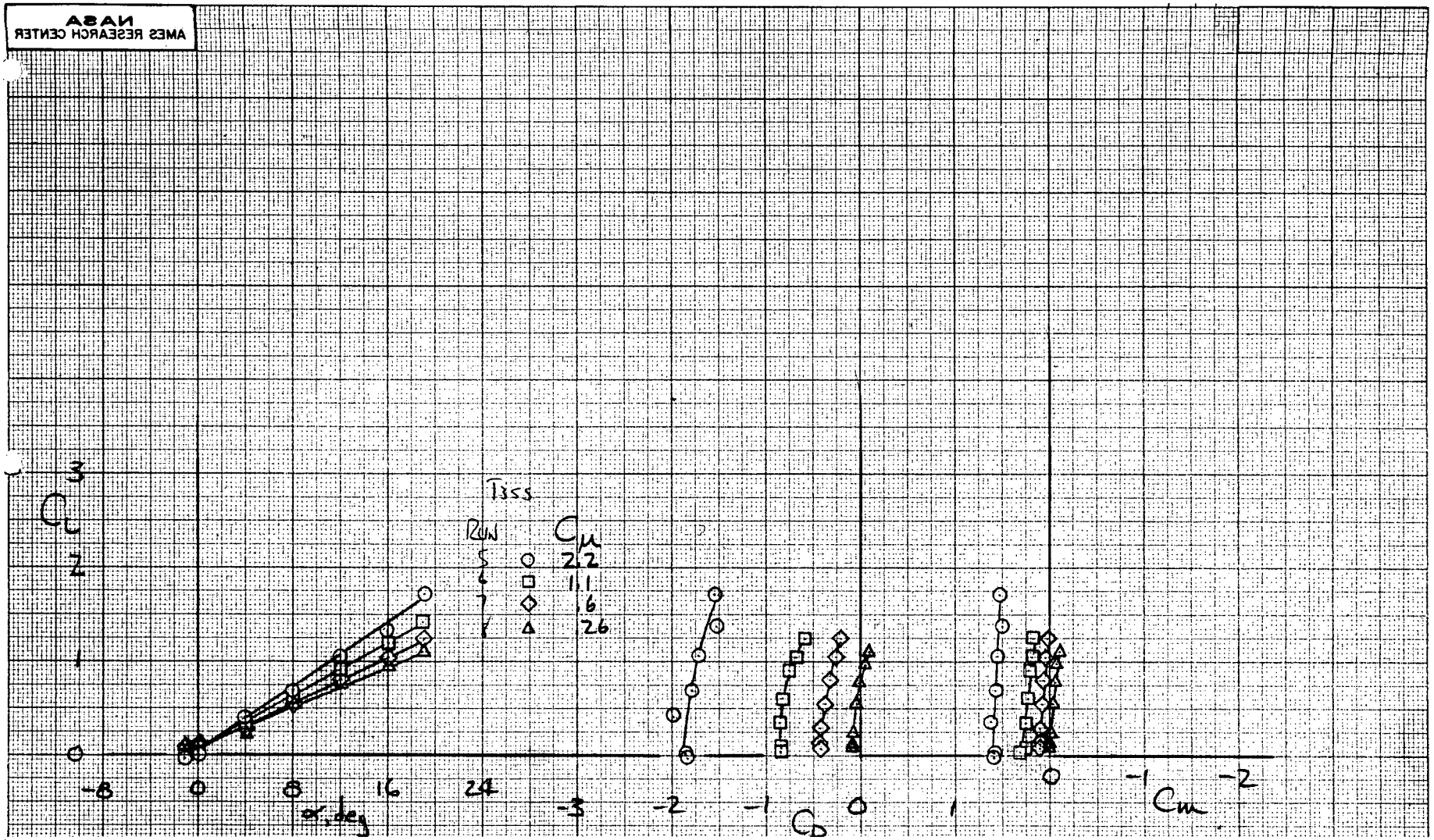

(d) $\delta_f = 0°$

Figure 16.- Concluded.

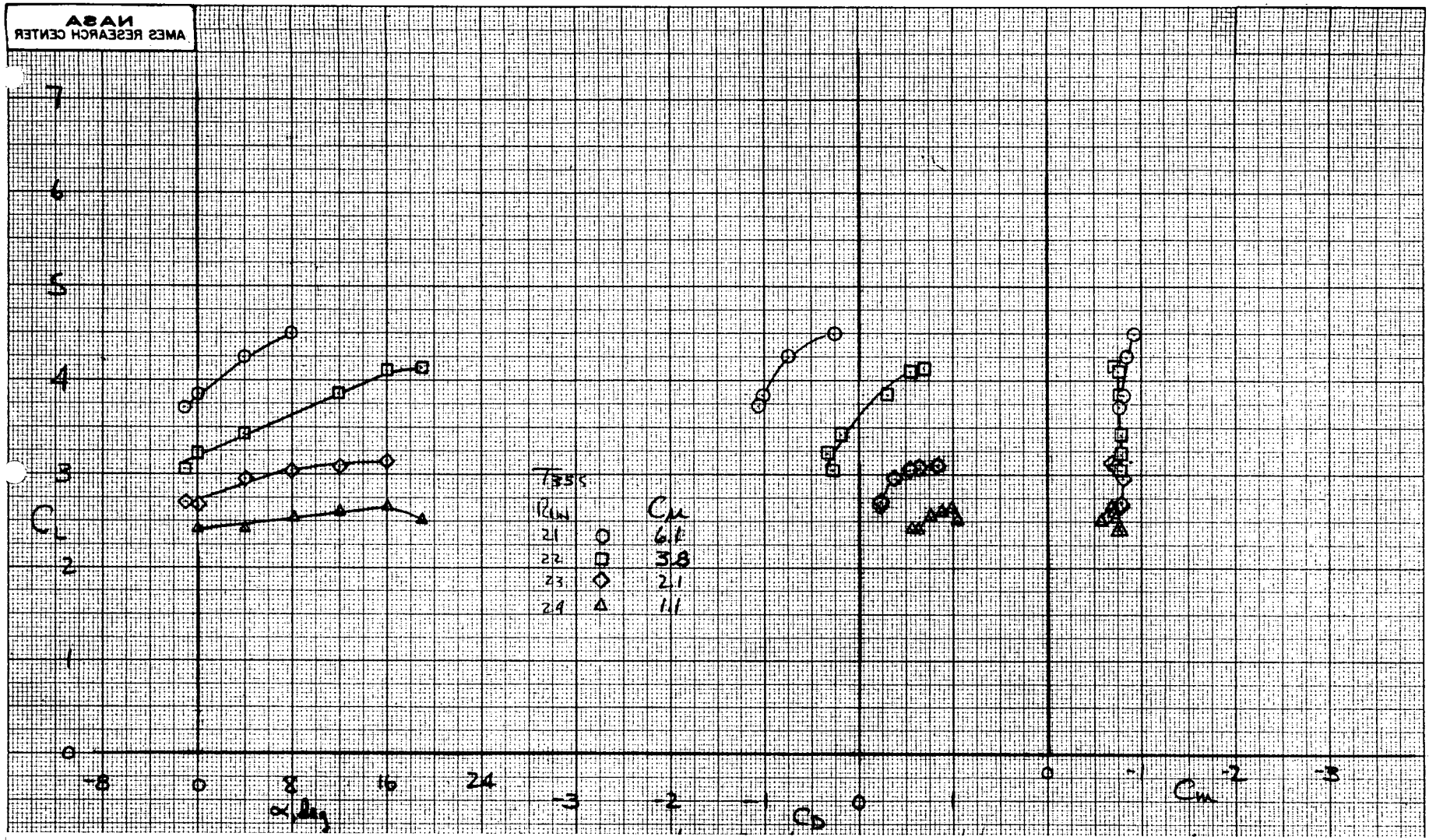

(a) $\delta_f = 90°$

Figure 17.- Longitudinal aerodynamic characteristics; $\Lambda = 30°$, long pylon, flap II.

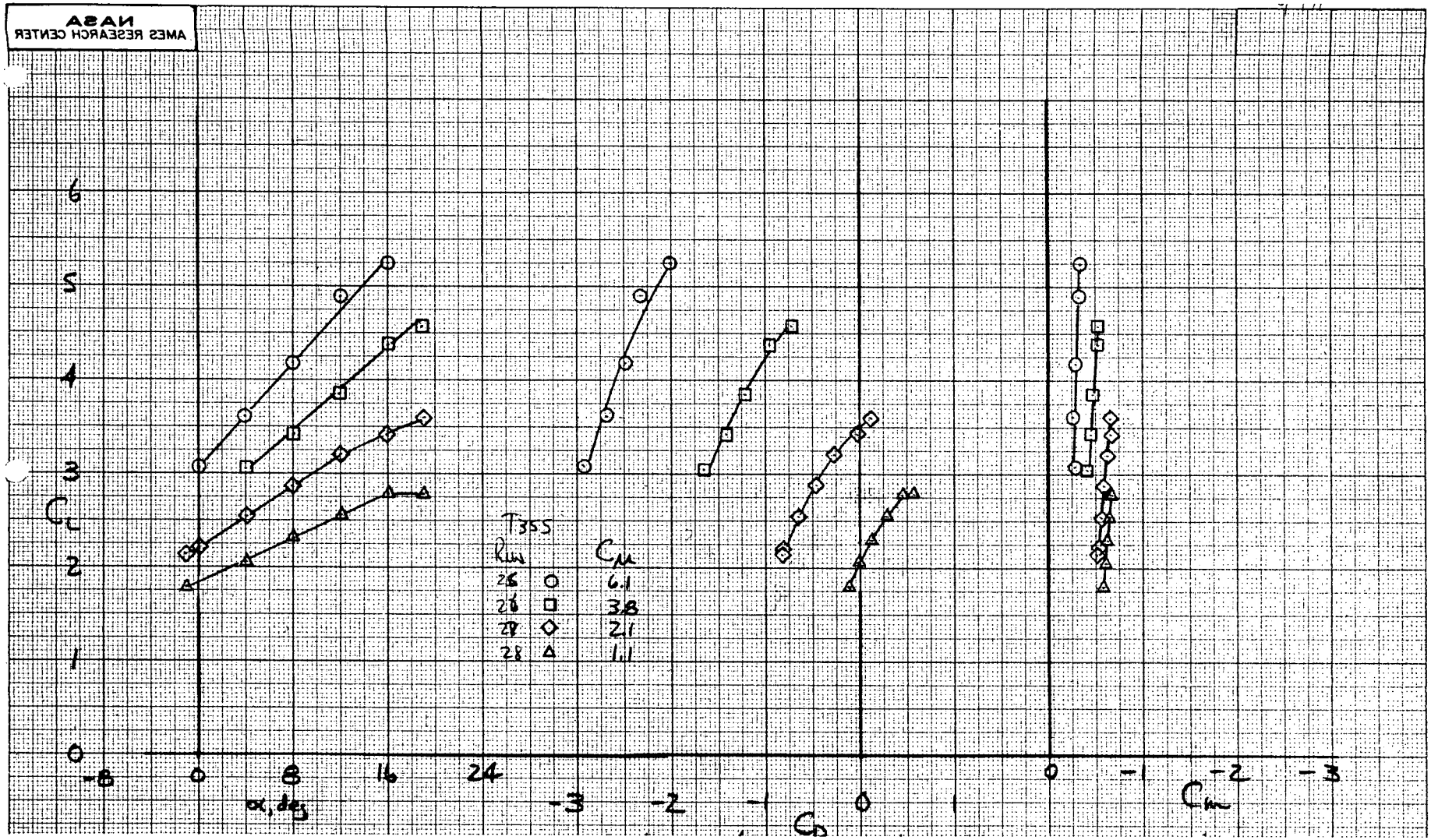

(b) $\delta_f = 60°$

Figure 17.- Continued.

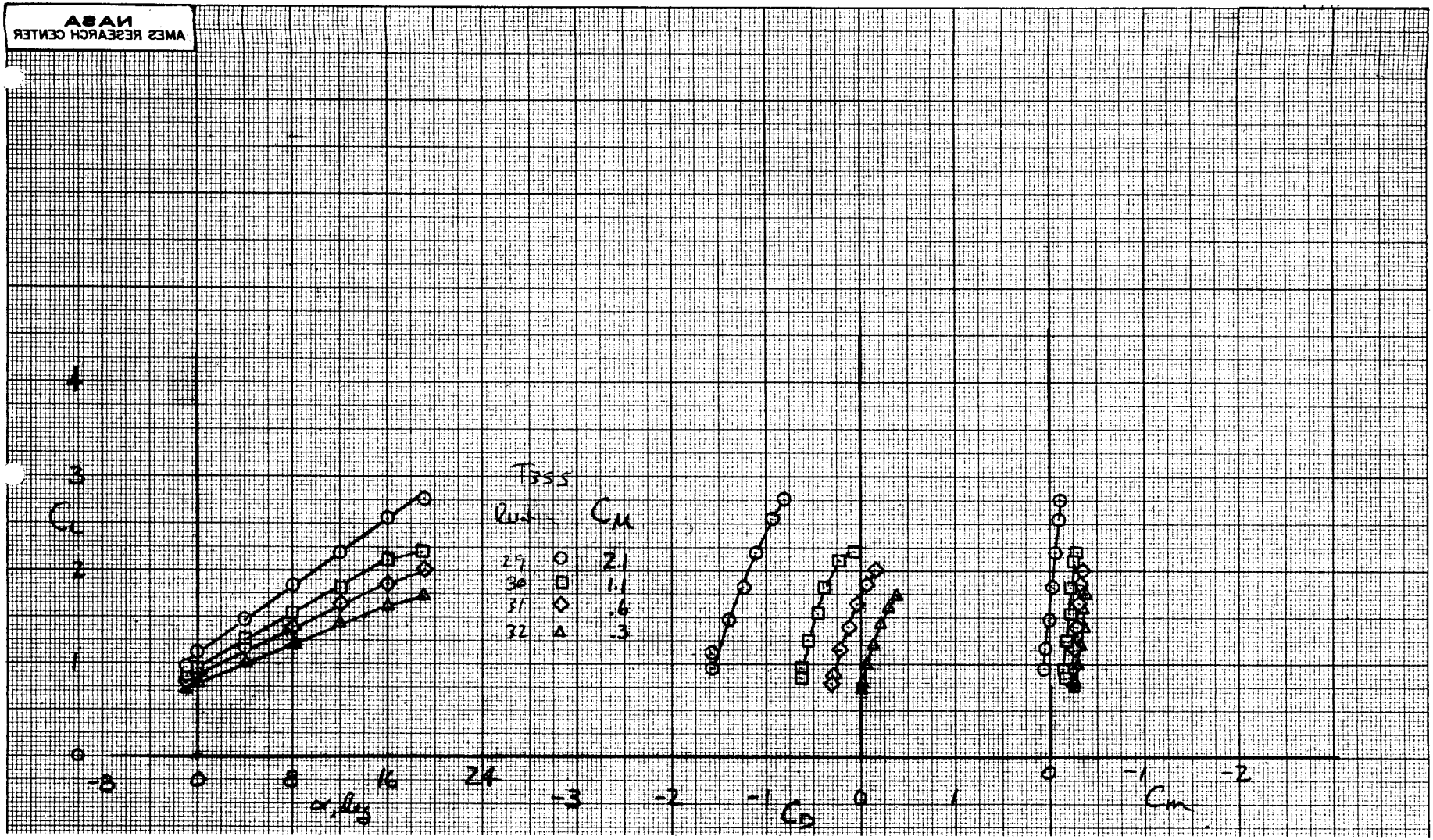

(c) $\delta_f = 30°$

Figure 17.- Continued.

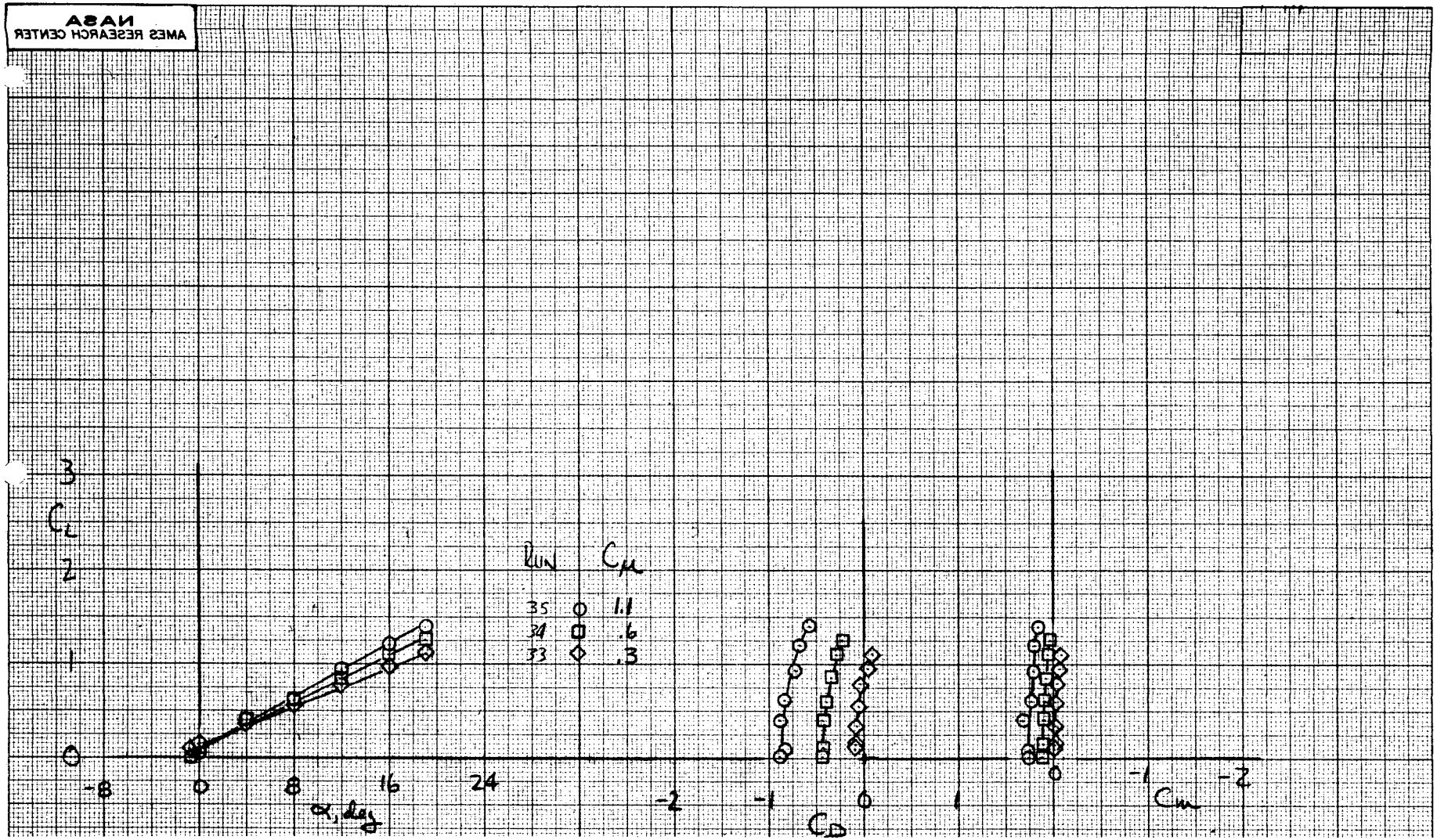

(d) $\delta_f = 0°$

Figure 17.- Concluded.

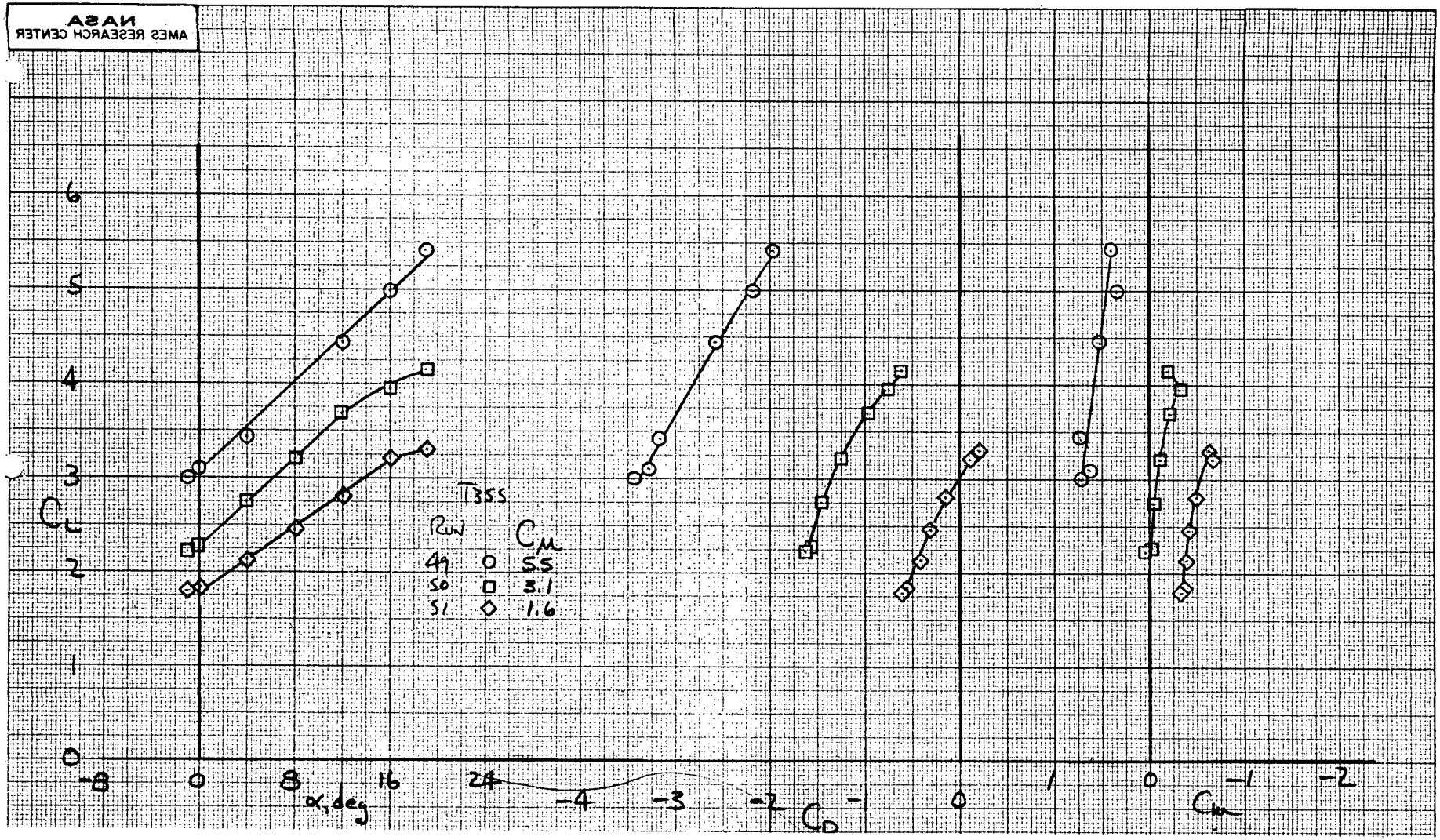

(a) $\delta_f = 90°$

Figure 18.- Longitudinal aerodynamic characteristics;

$\Lambda = 30°$, long pylon, flap III.

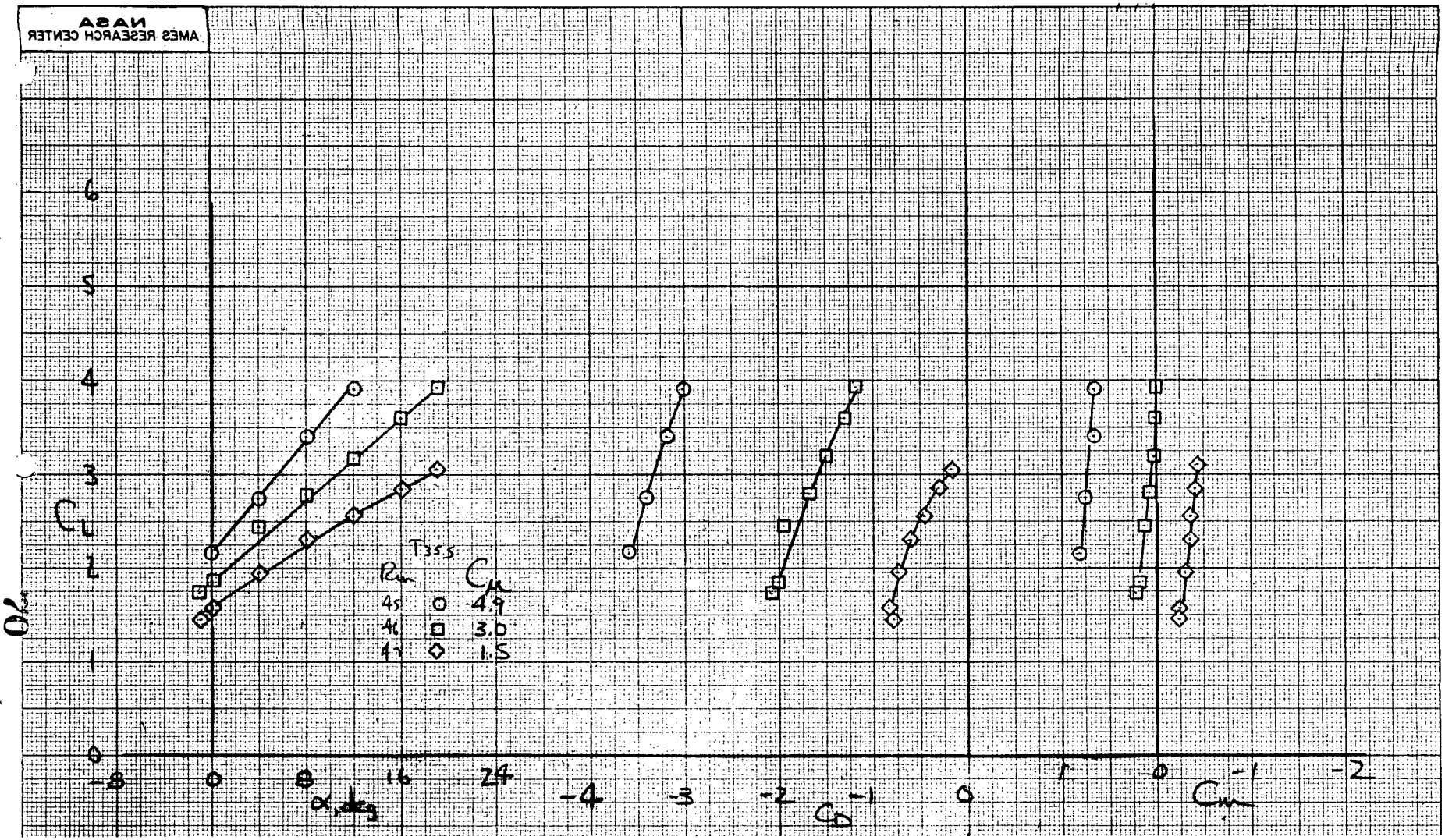

(b) $\delta_f = 60°$

Figure 18.- Continued.

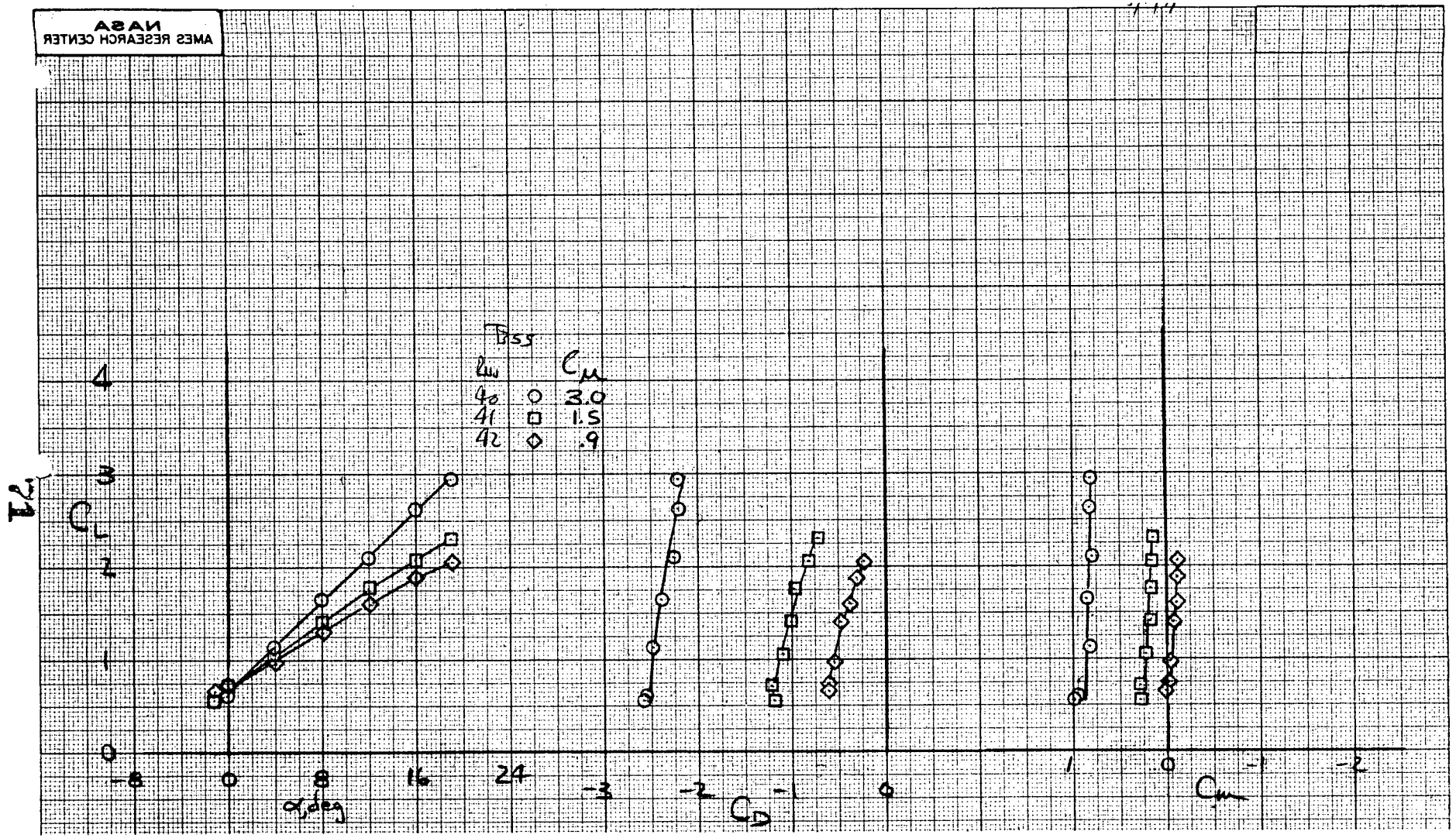

(c) $\delta_f = 30°$

Figure 18.- Continued.

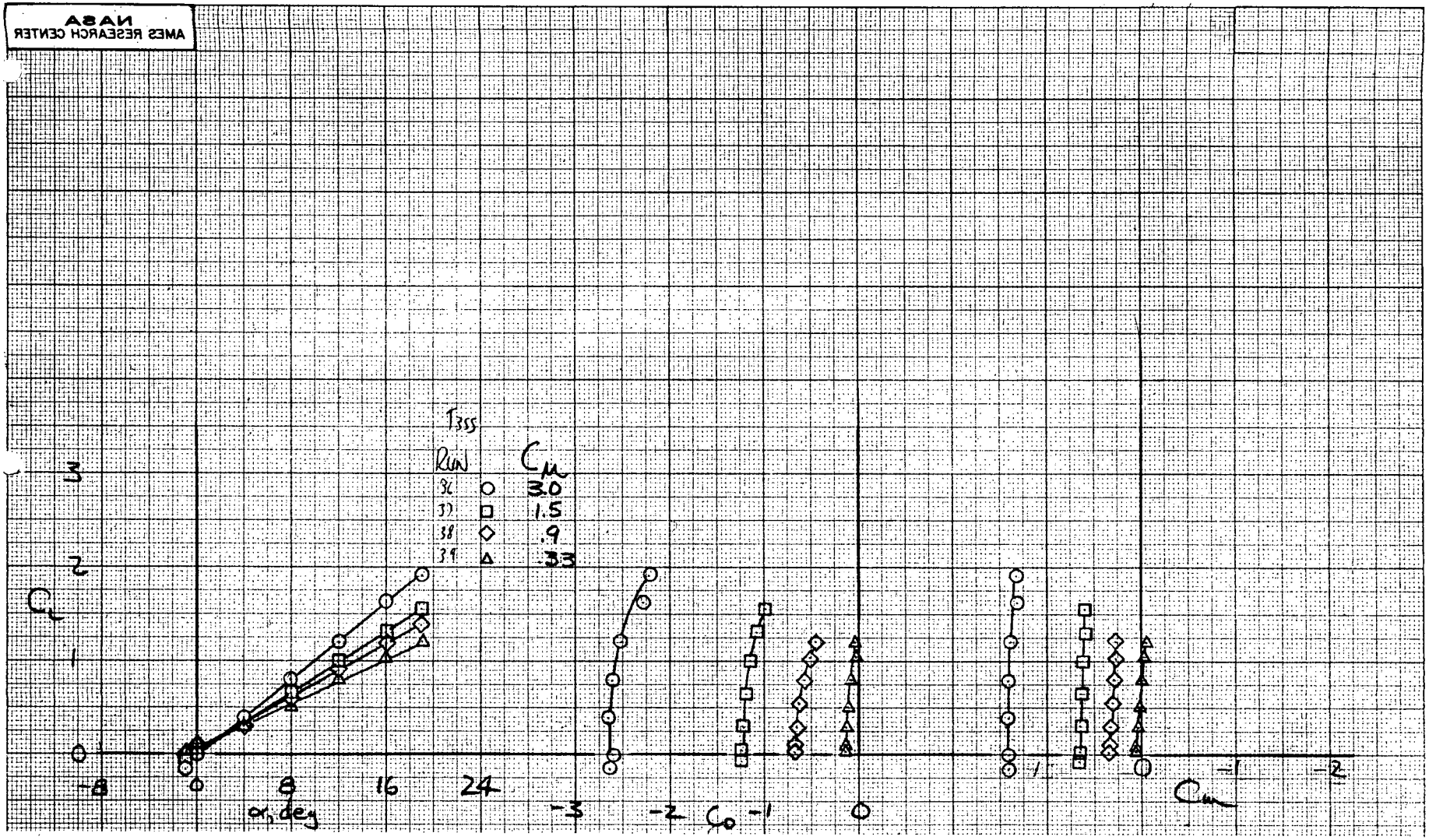

(d) $\delta_f = 0°$

Figure 18.- Concluded.

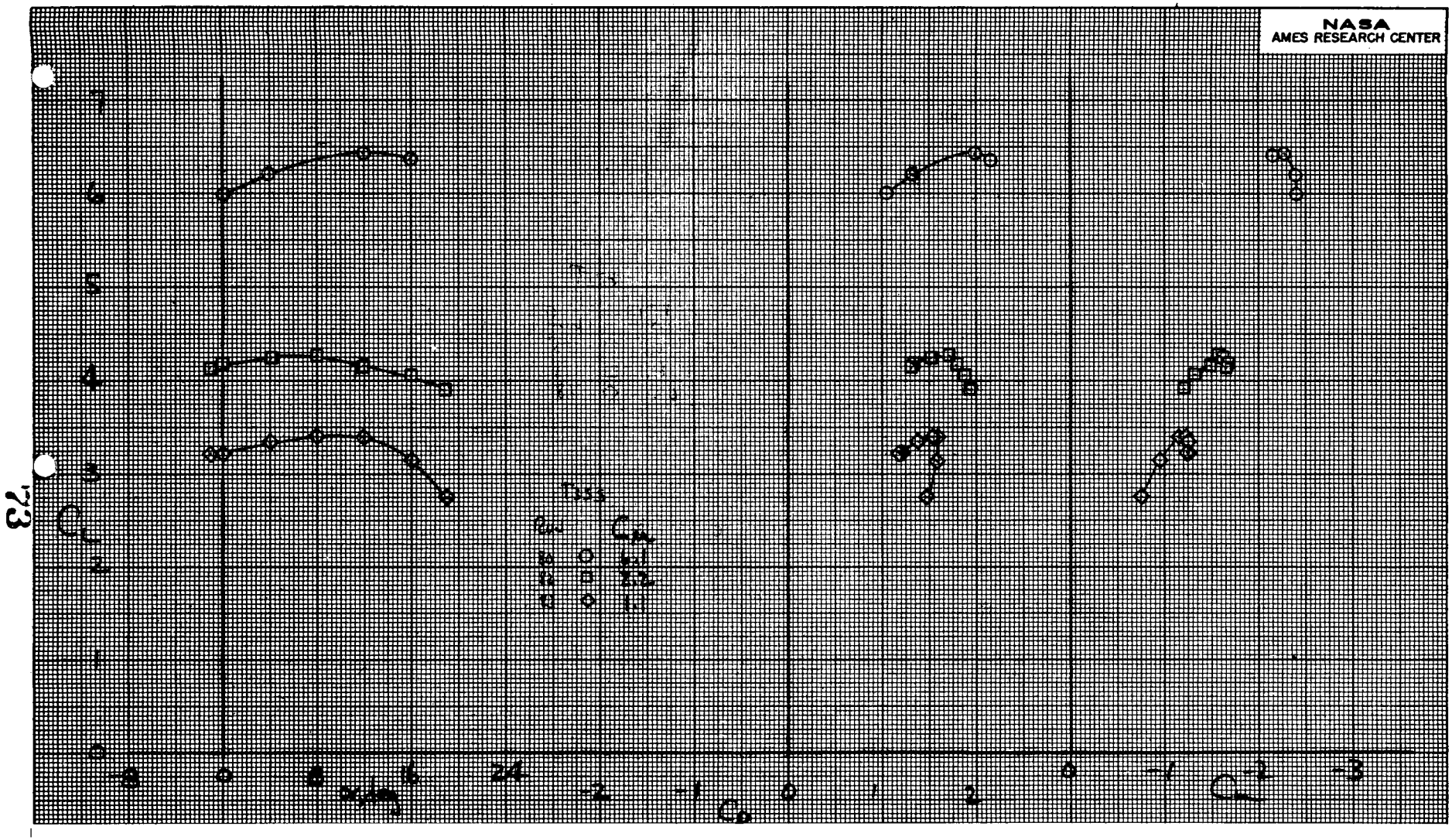

(a) $\delta_f = 90°$

Figure 19.- Longitudinal aerodynamic characteristics;

$\Lambda = 30°$, medium pylon, flap I.

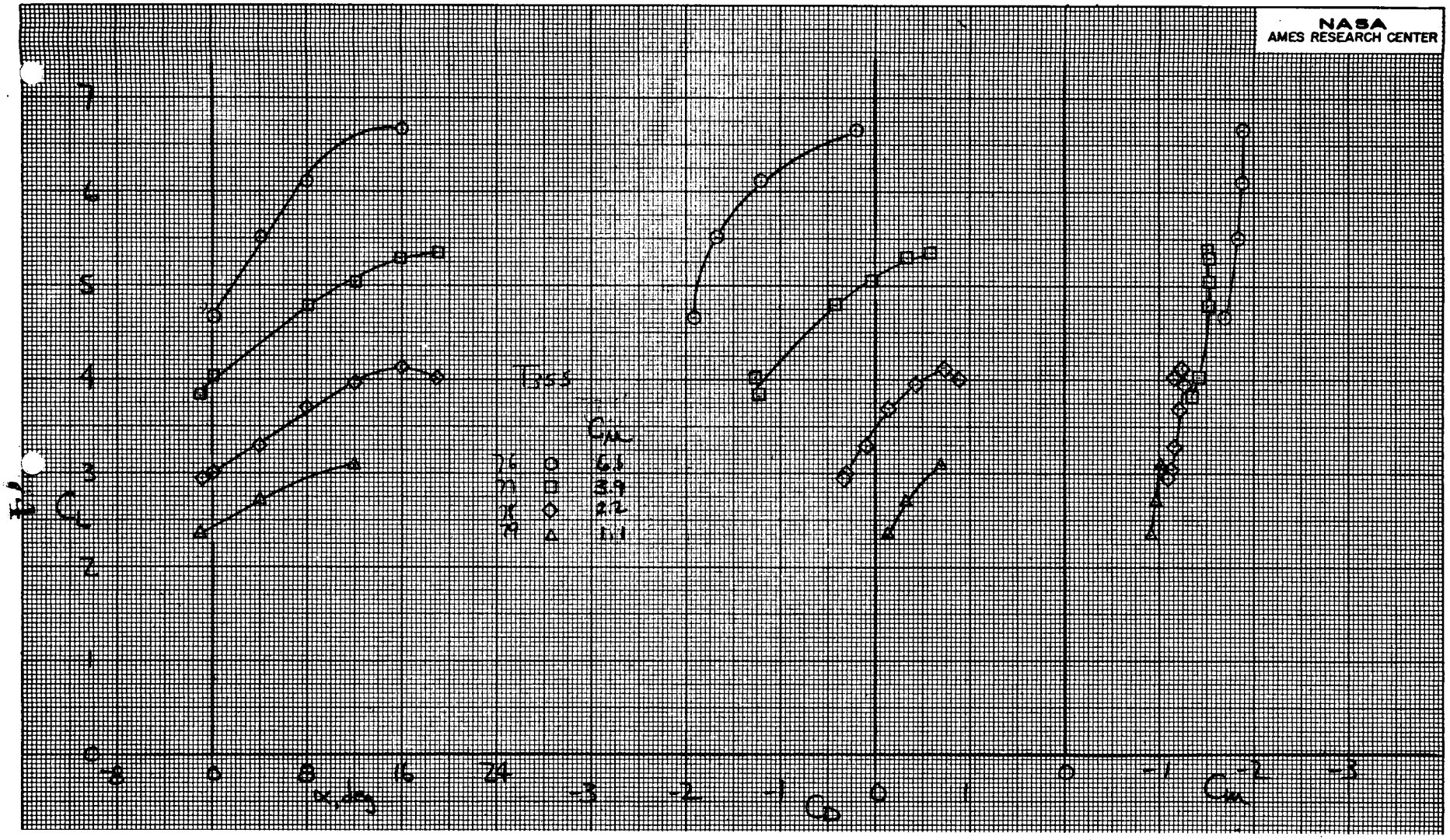

(b) $\delta_f = 60°$

Figure 19.- Continued.

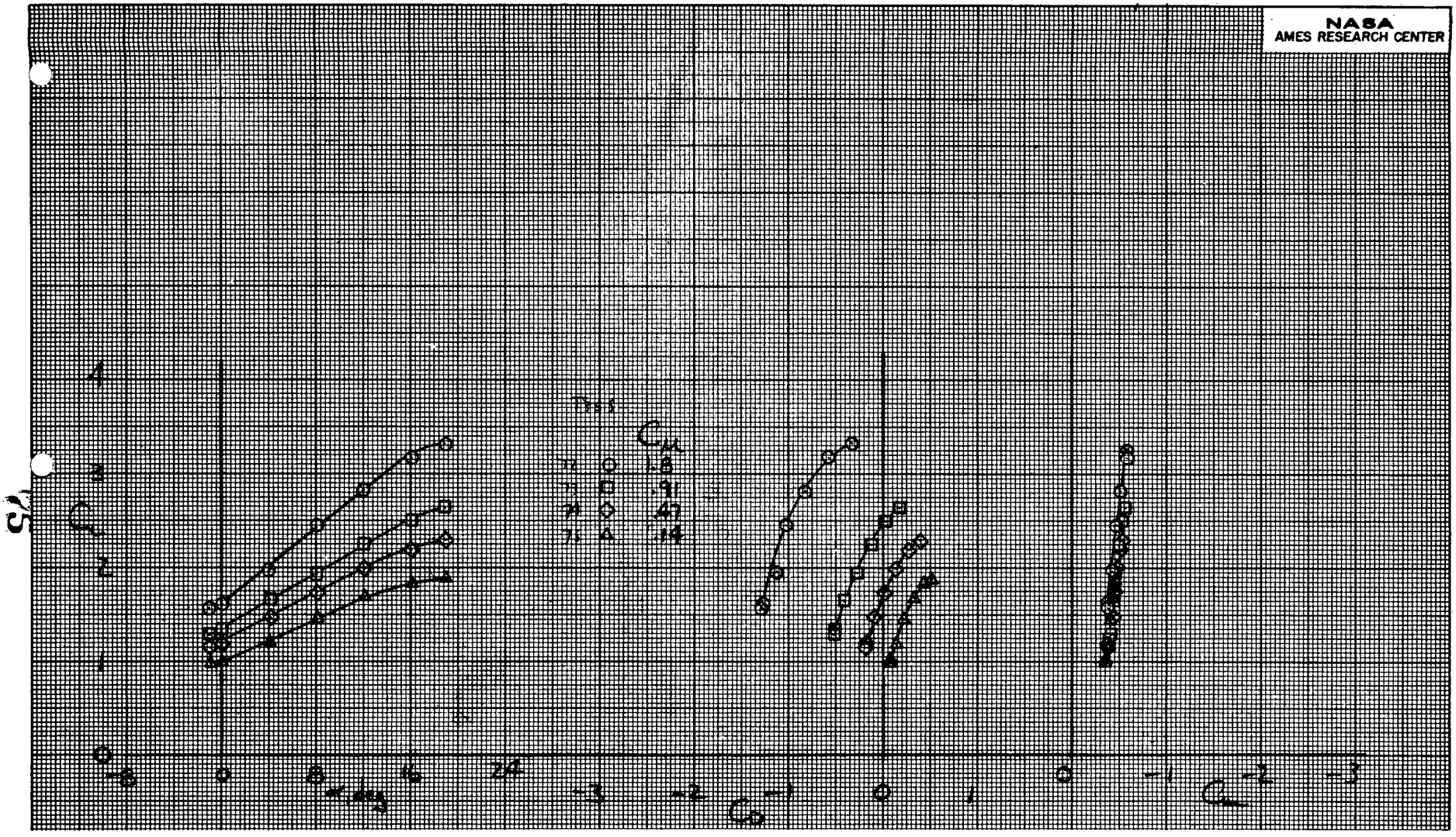

(c) $\delta_f = 30°$

Figure 19.- Continued.

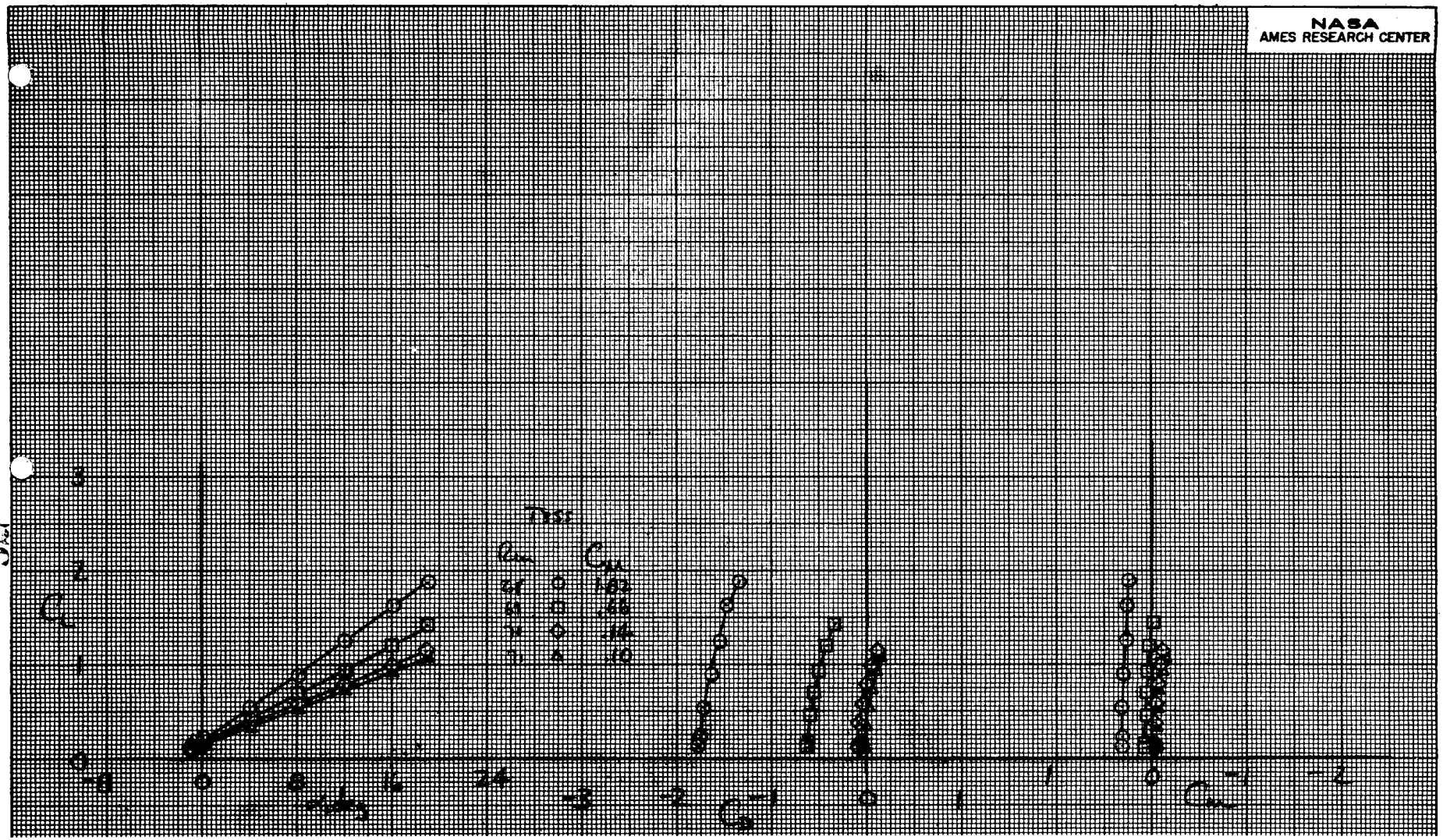

(d) $\delta_f = 0°$

Figure 19.- Concluded.

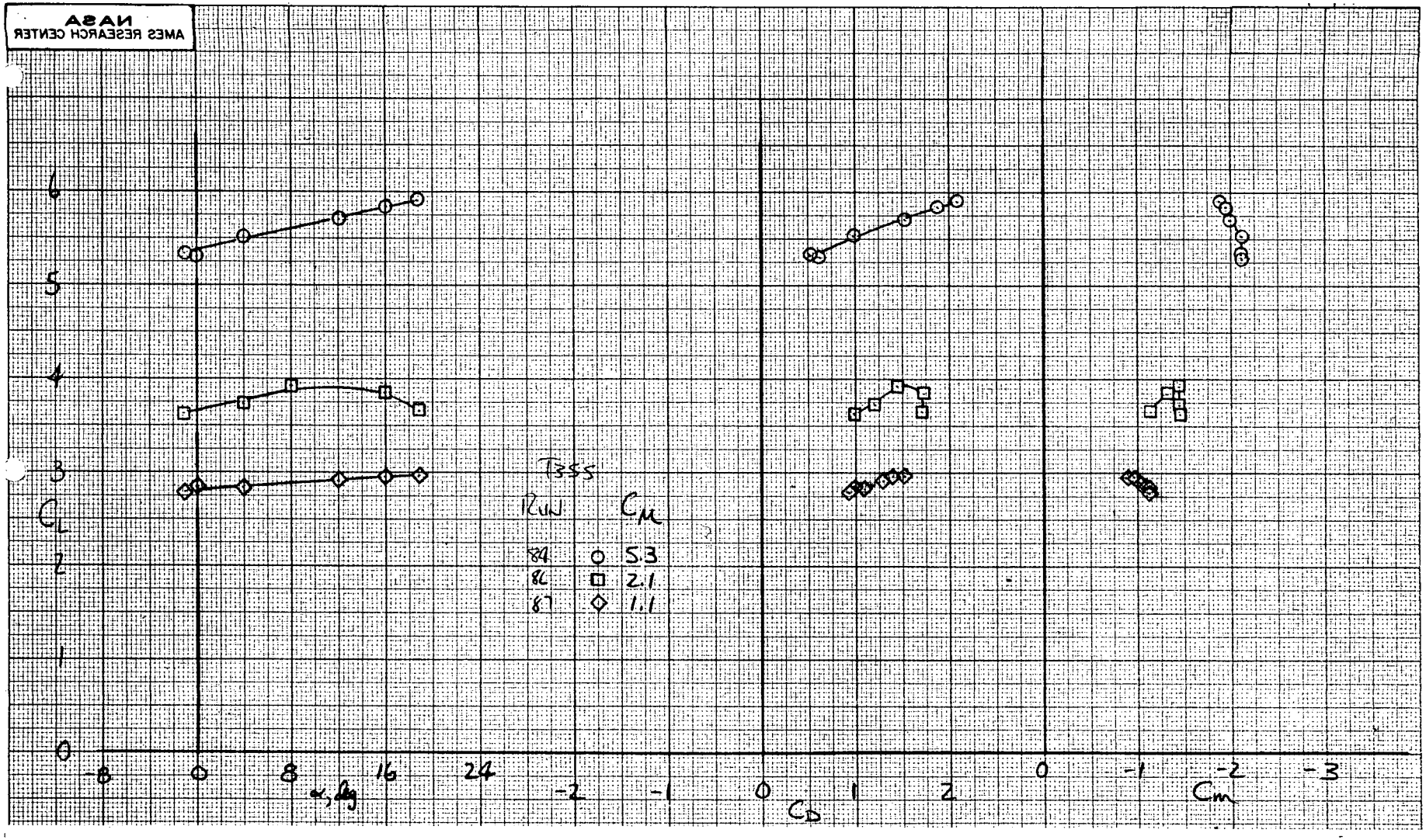

(a) $\delta_f = 90°$

Figure 20.- Longitudinal aerodynamic characteristics; $\Lambda = 30°$, medium pylon, flap II.

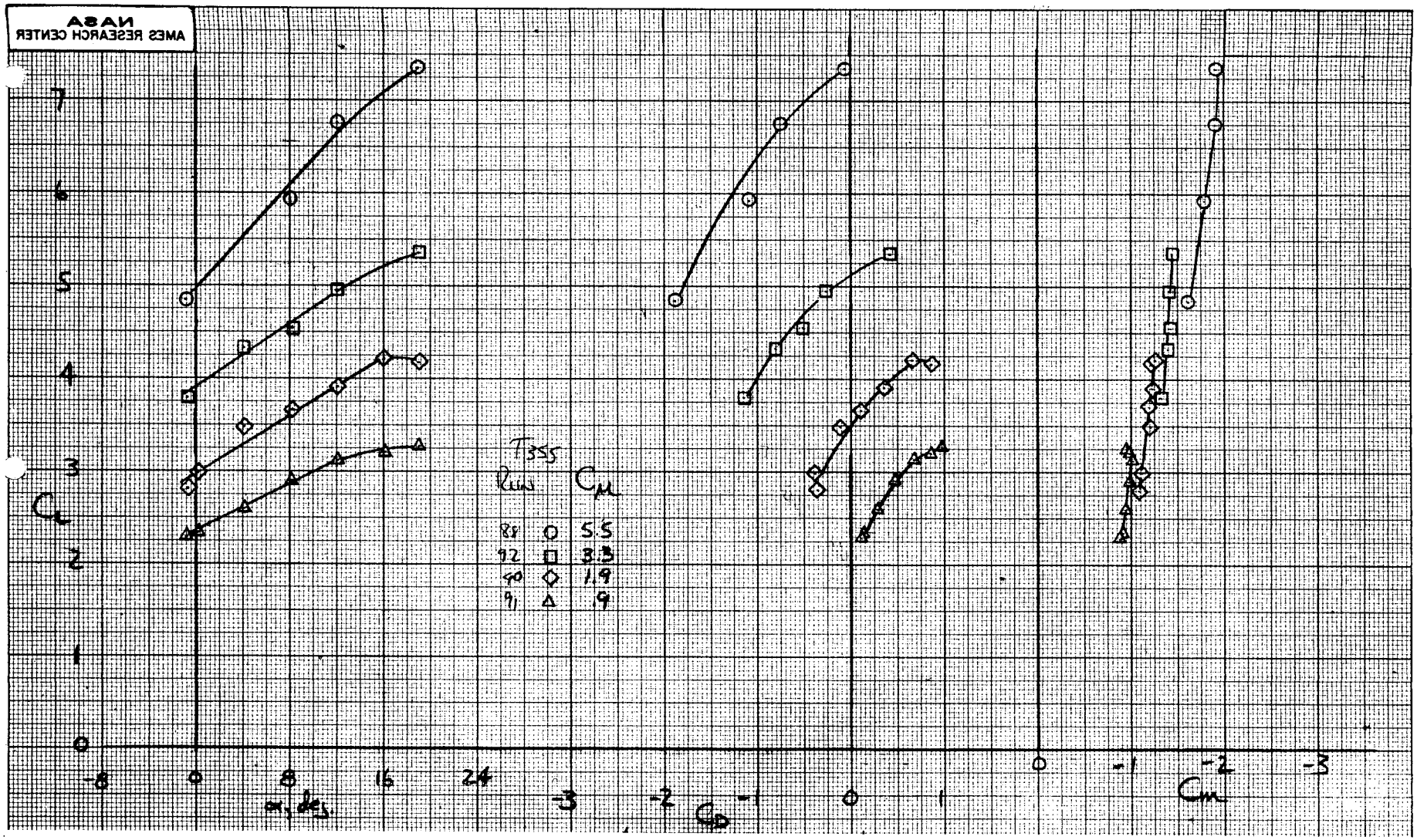

(b) $\delta_f = 60°$

Figure 20.- Continued.

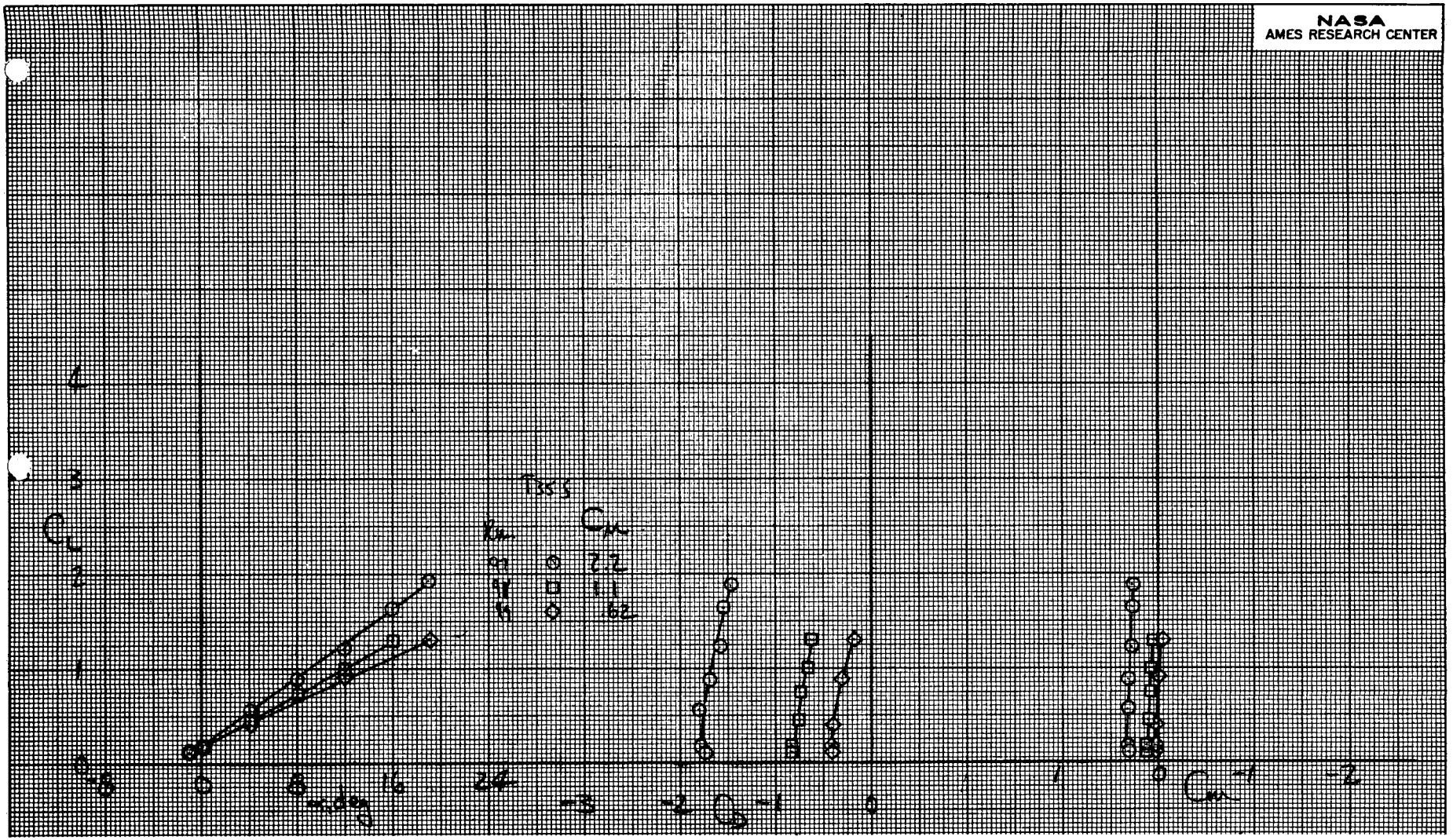

(c) $\delta_f = 0°$

Figure 20.- Concluded.

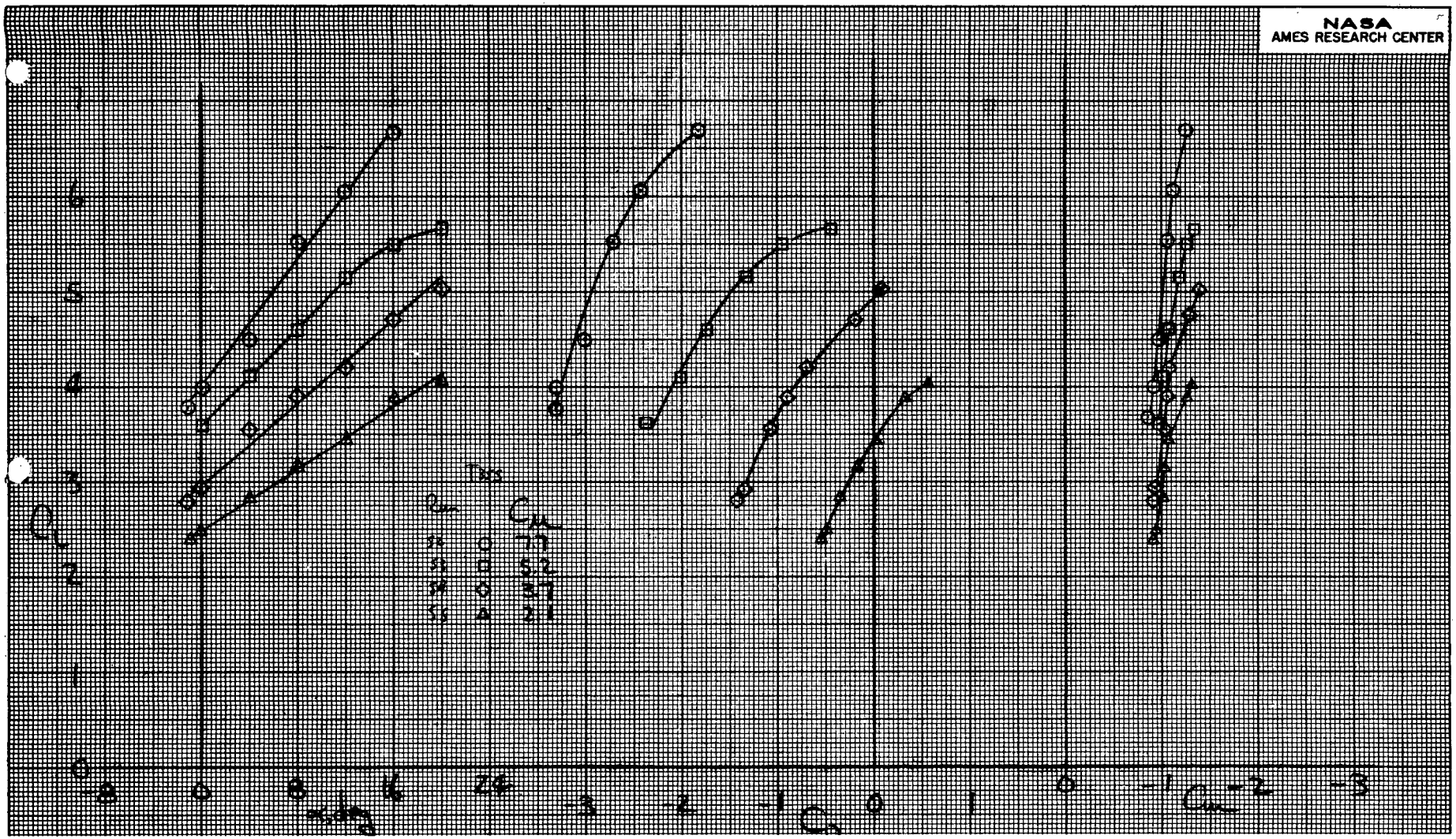

(a) $\delta_f = 90°$

Figure 21.- Longitudinal aerodynamic characteristics; $\Lambda = 30°$, medium pylon, flap III.

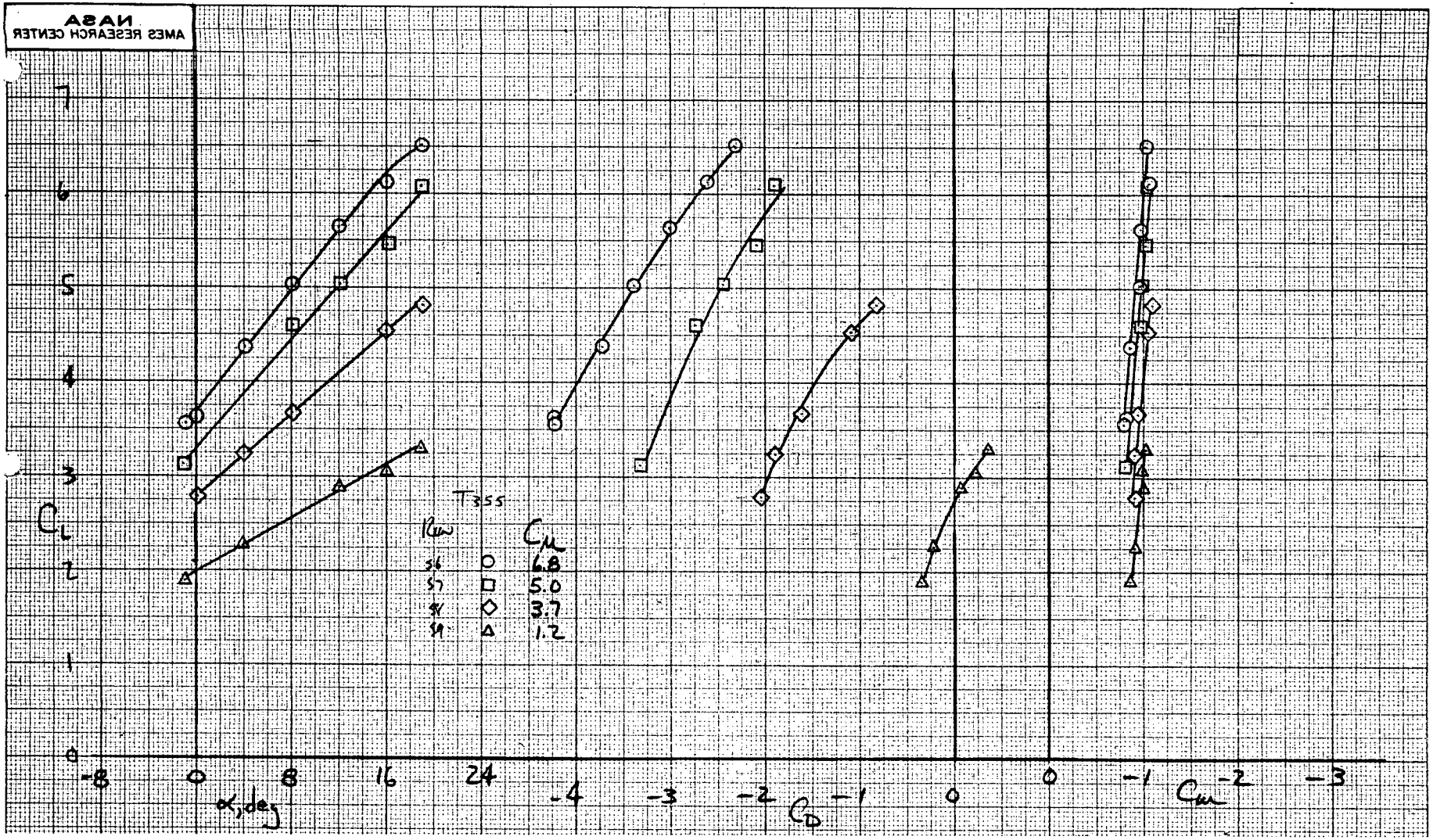

(b) $\delta_f = 60°$

Figure 21.- Continued.

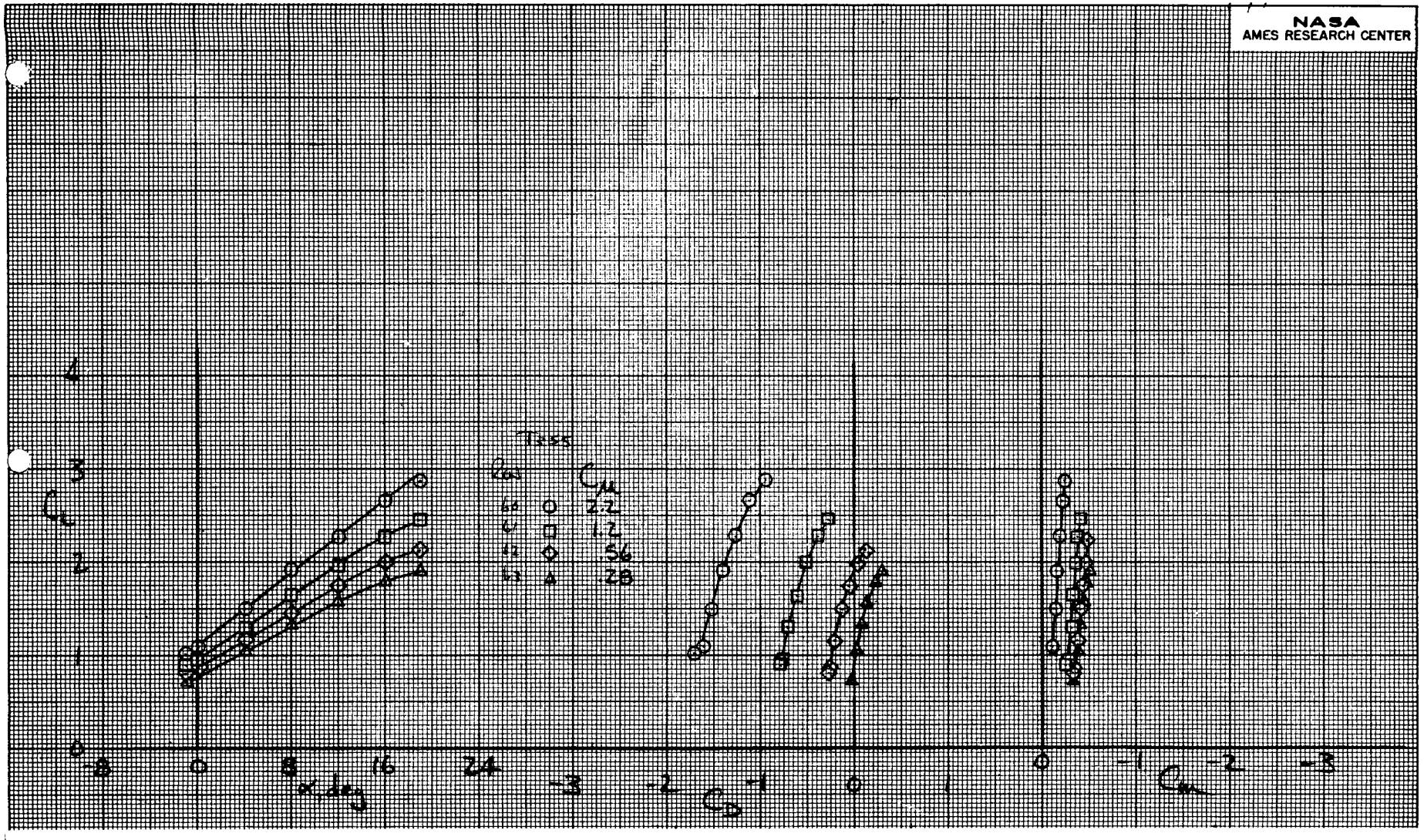

(c) $\delta_f = 30°$

Figure 21.- Continued.

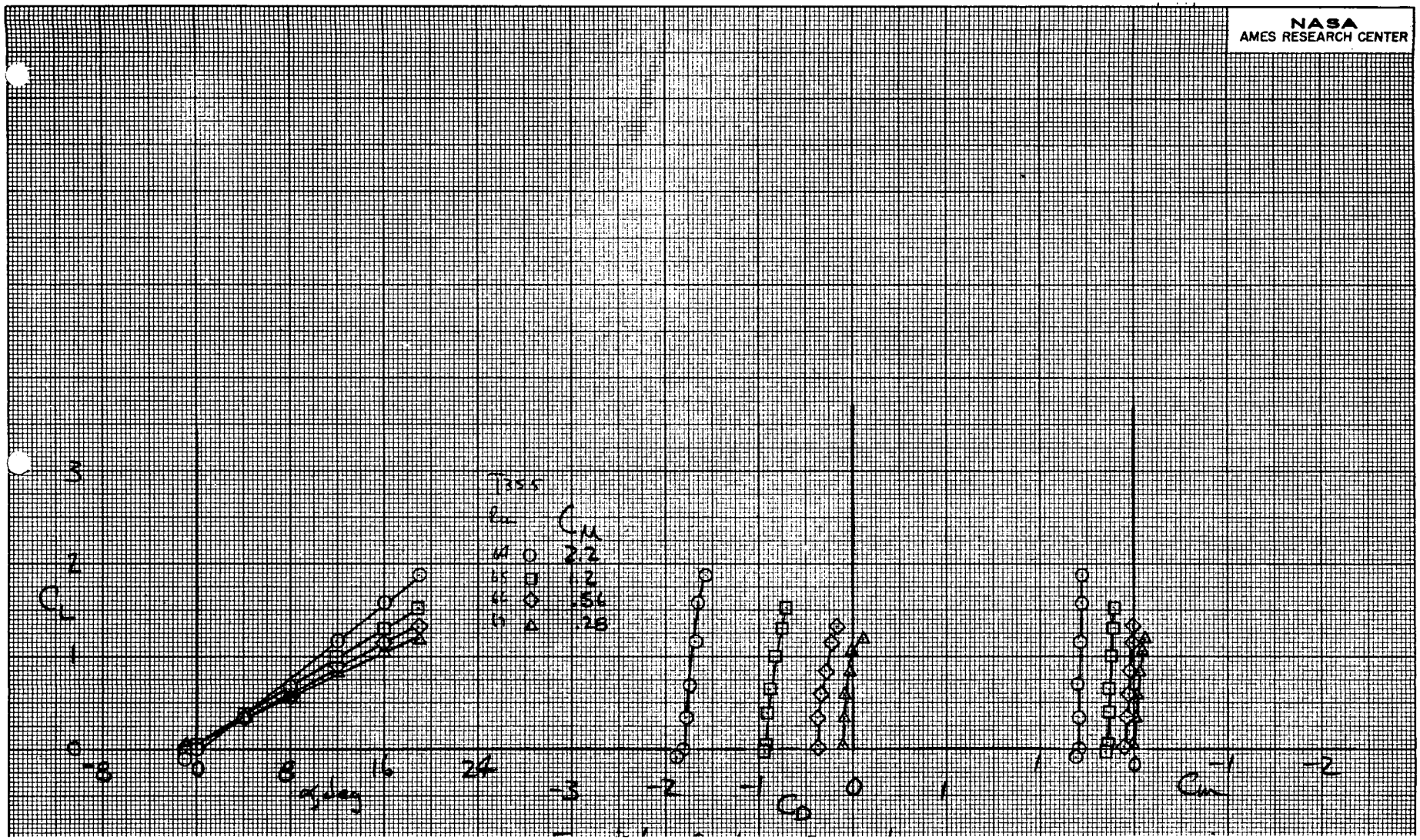

(d) $\delta_f = 0°$

Figure 21.- Concluded.

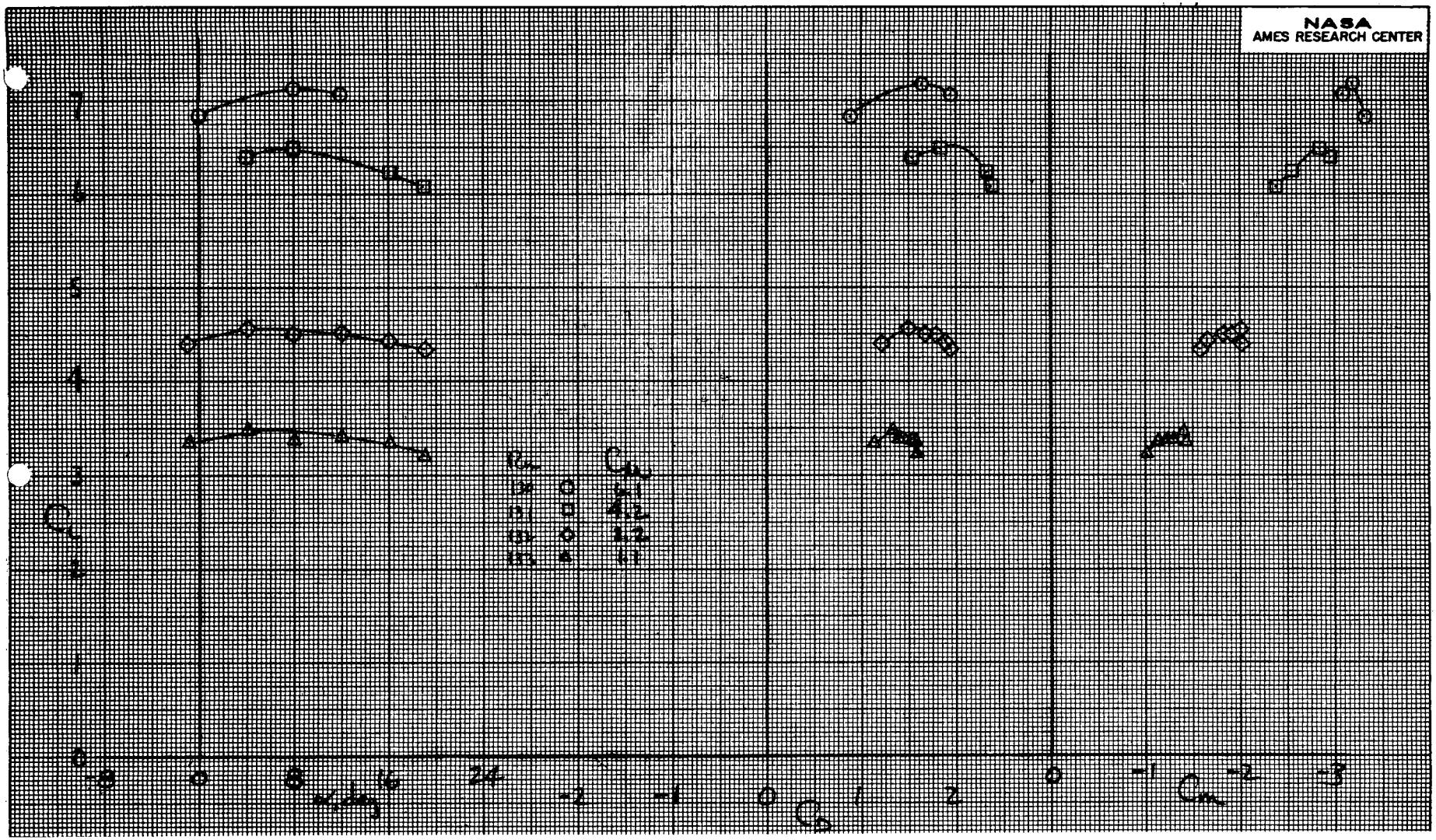

(a) $\delta_f = 90°$

Figure 22.- Longitudinal aerodynamic characteristics; $\Lambda = 30°$, no pylon, flap I.

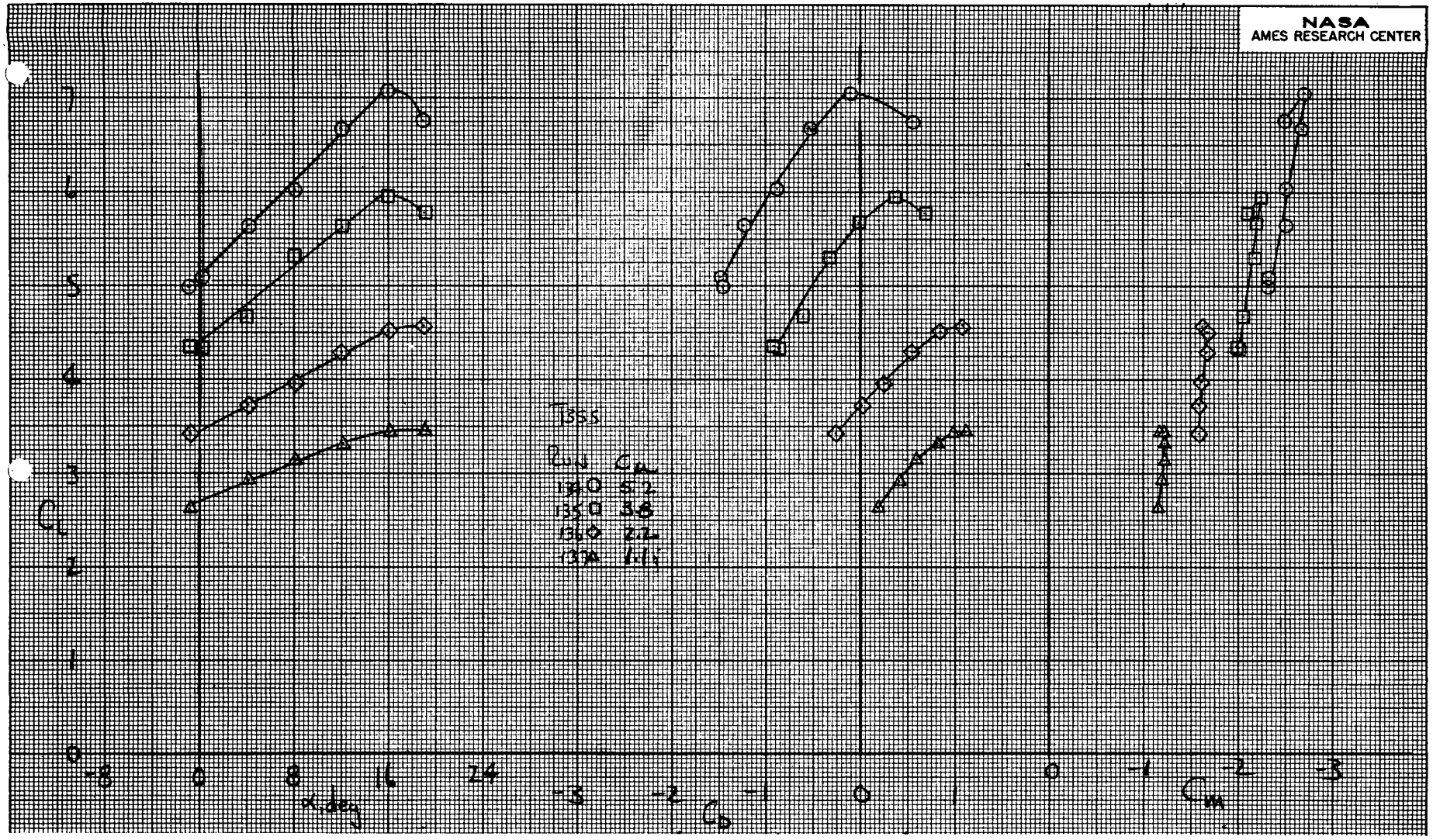

(b) $\delta_f = 60°$

Figure 22.- Continued.

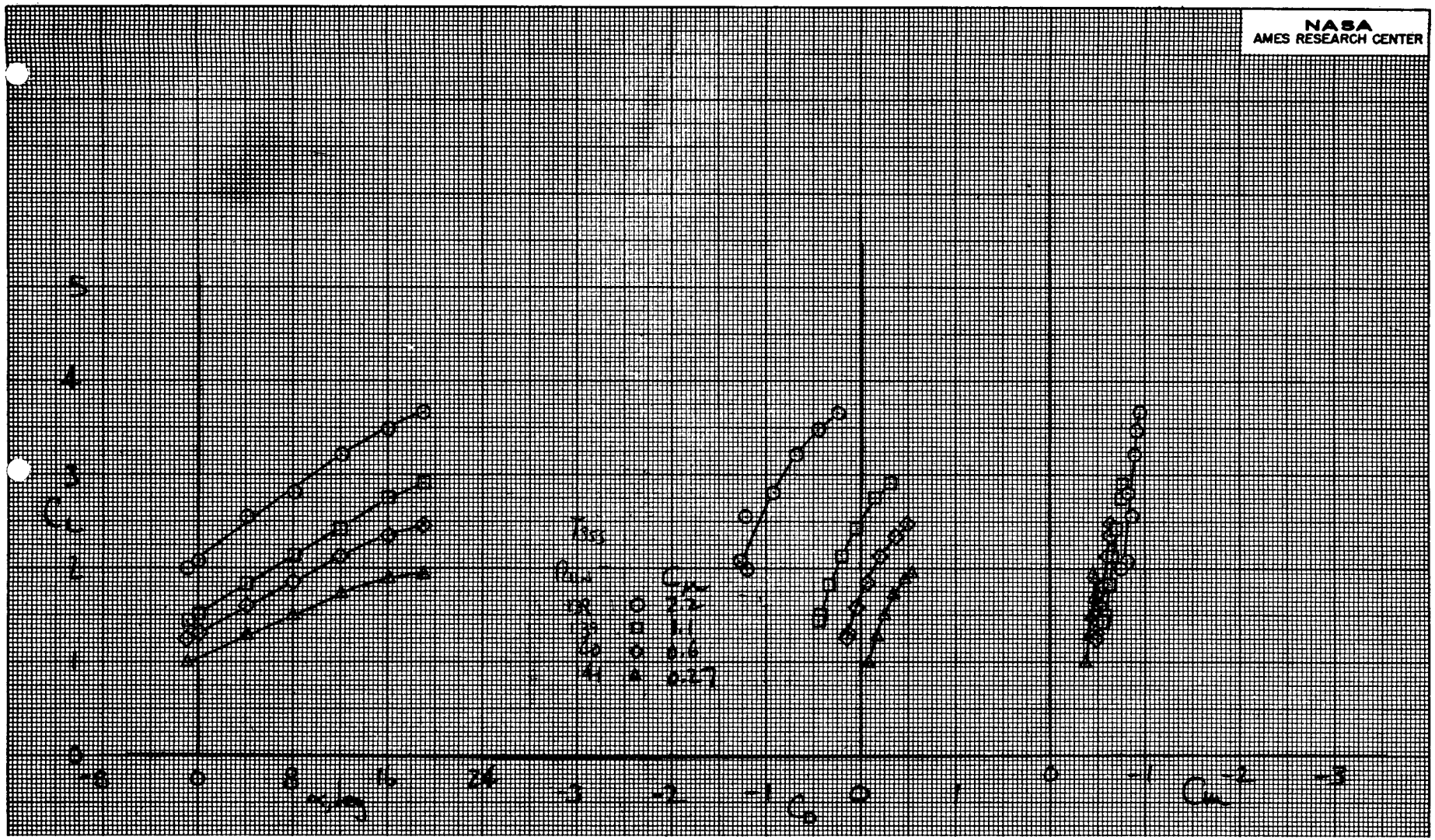

(c) $\delta_f = 30°$

Figure 22.- Concluded.

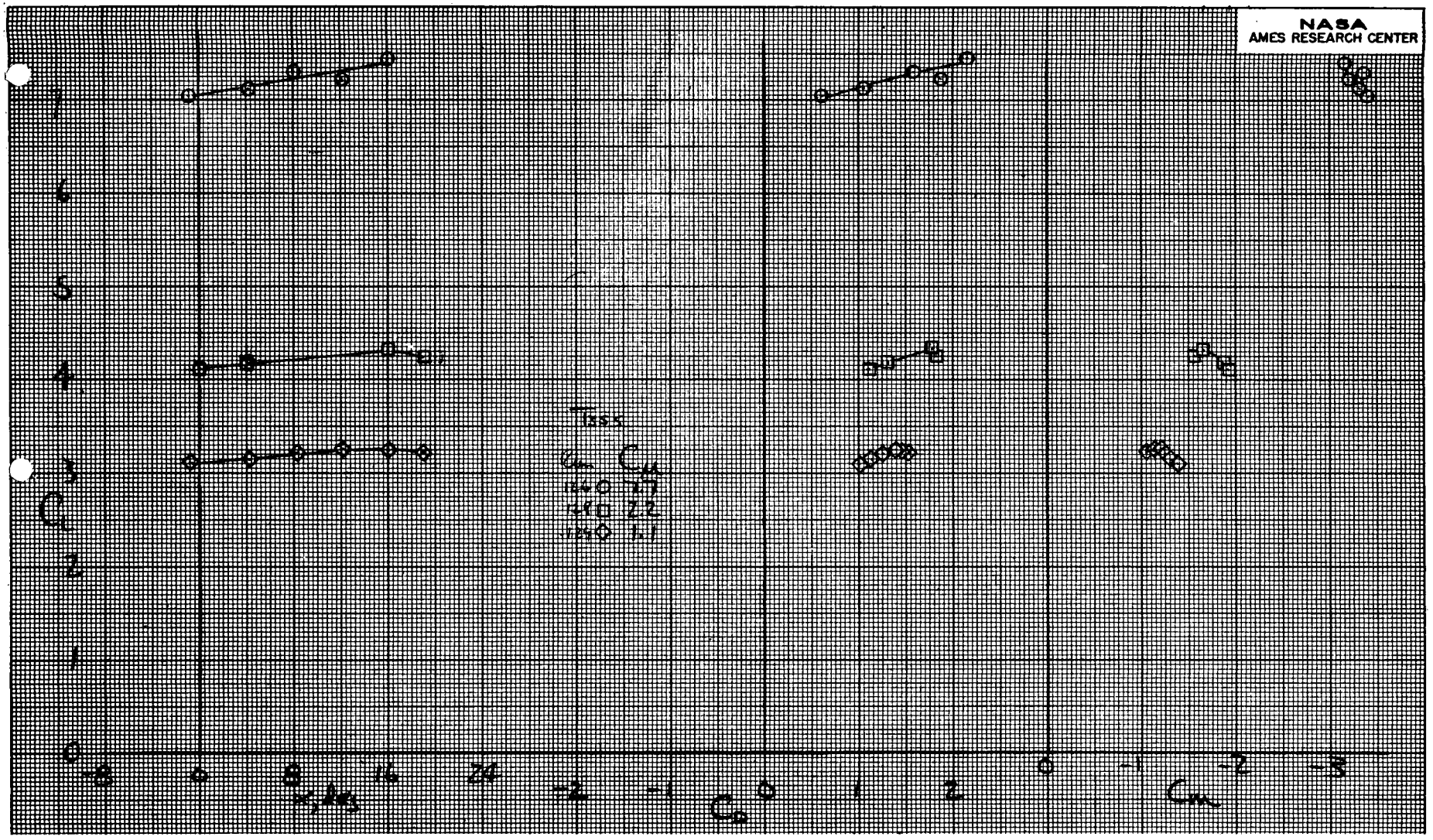

(a) $\delta_f = 90°$

Figure 23.- Longitudinal aerodynamic characteristics; $\Lambda = 30°$, no pylon, flap II.

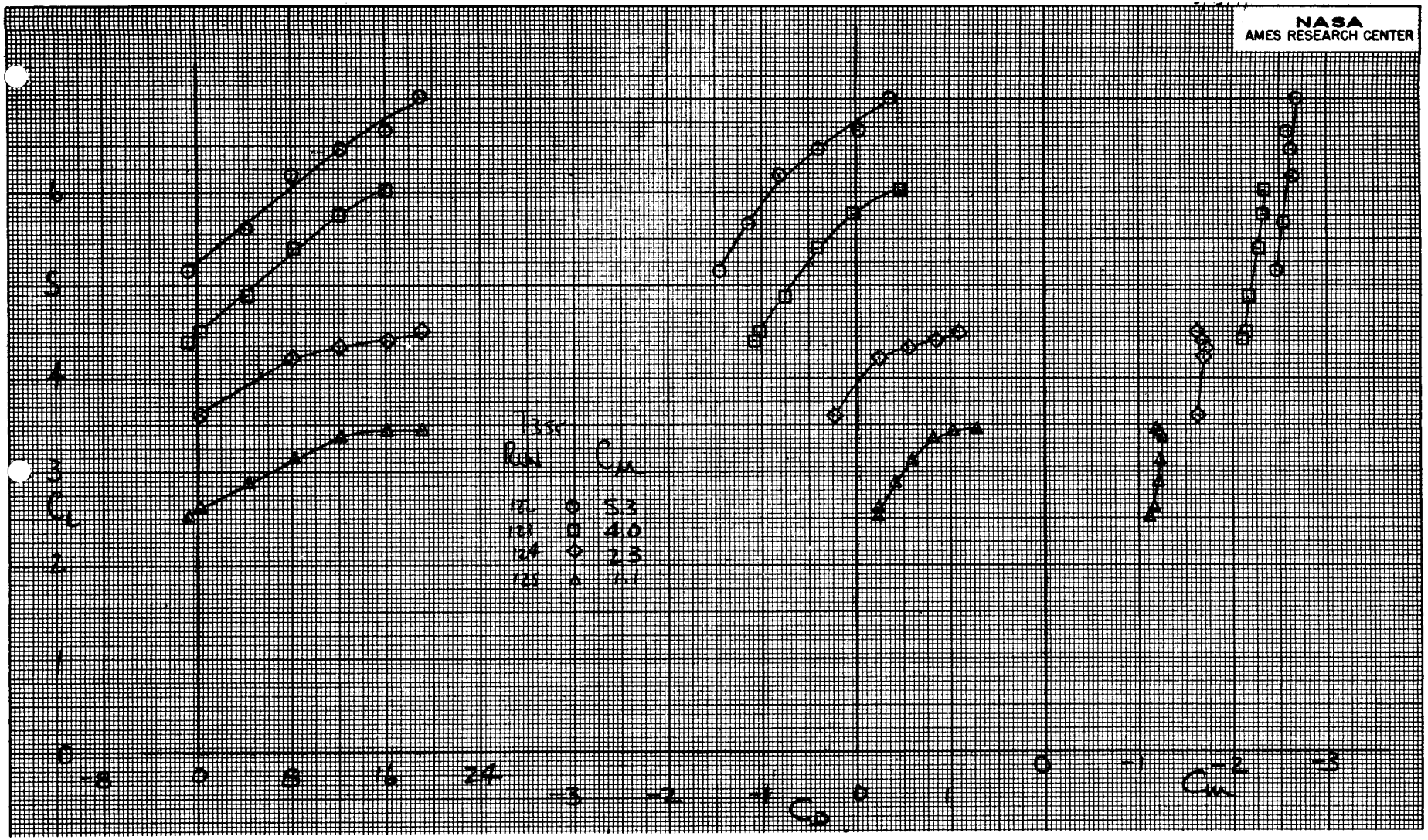

(b) $\delta_f = 60°$

Figure 23.- Continued.

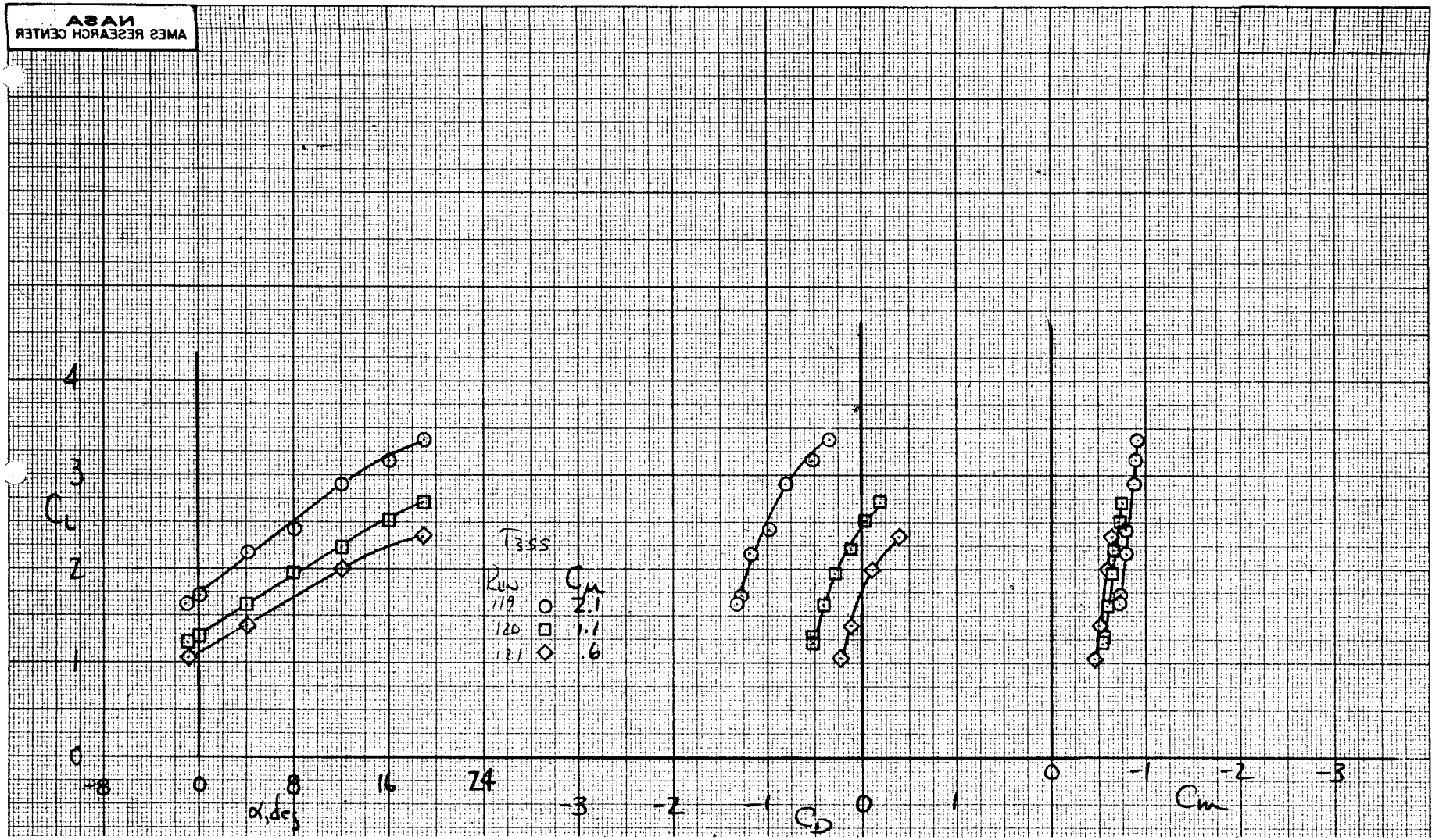

(c) $\delta_f = 30°$

Figure 23.- Continued.

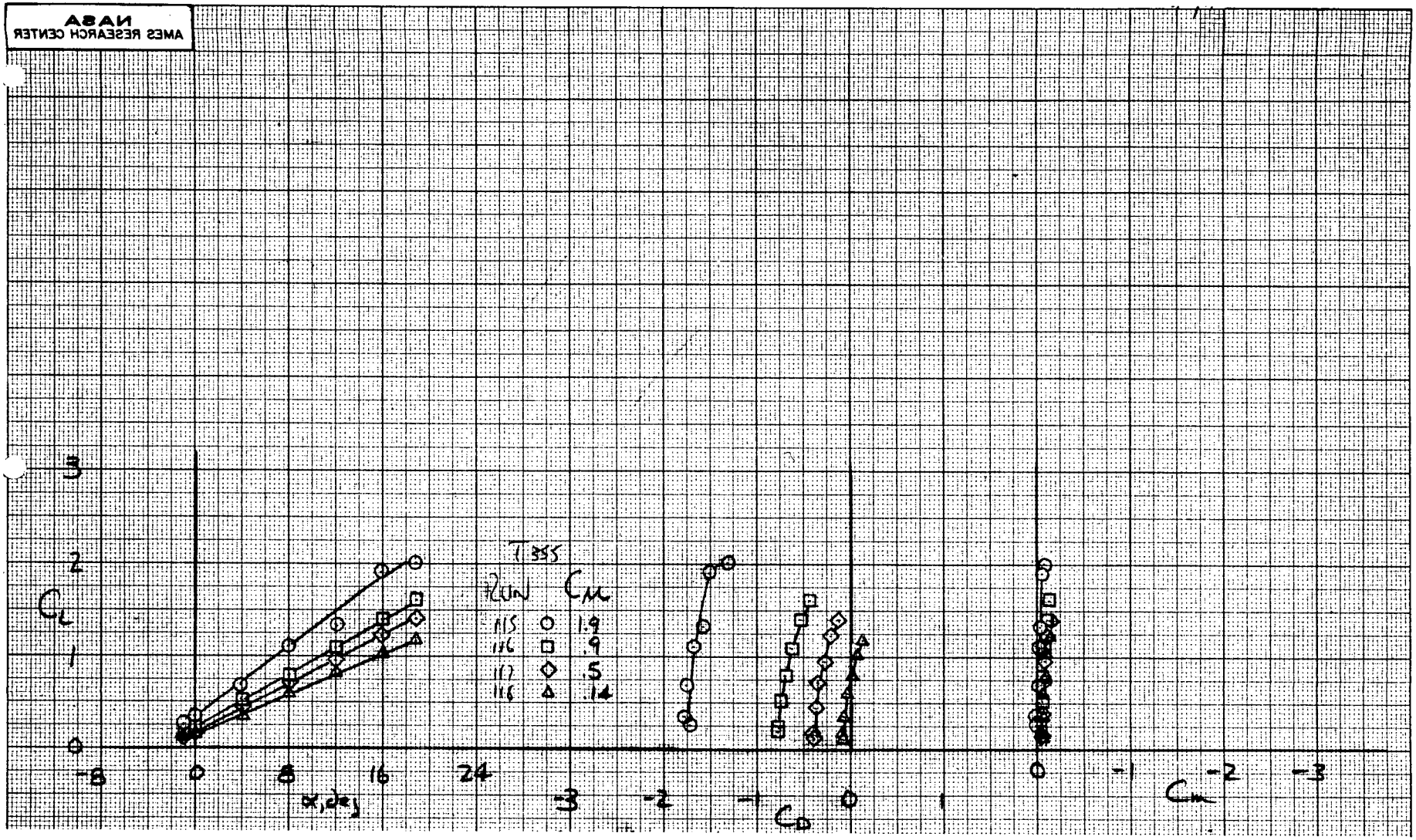

(d) $\delta_f = 0°$

Figure 23.- Concluded.

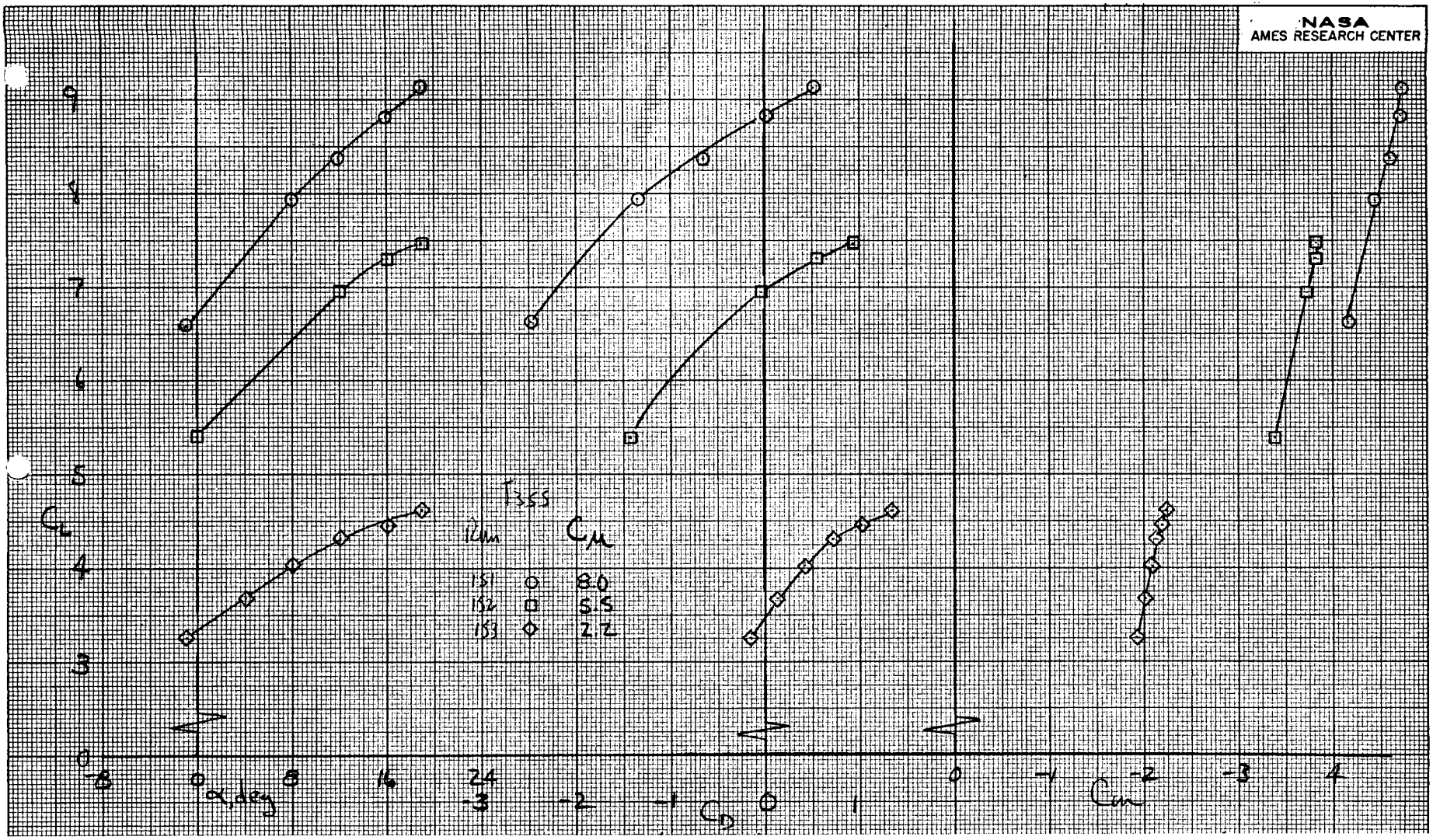

(a) $\delta_f = 90°$

Figure 24.- Longitudinal aerodynamic characteristics; $\Lambda = 30°$, no pylon, flap III.

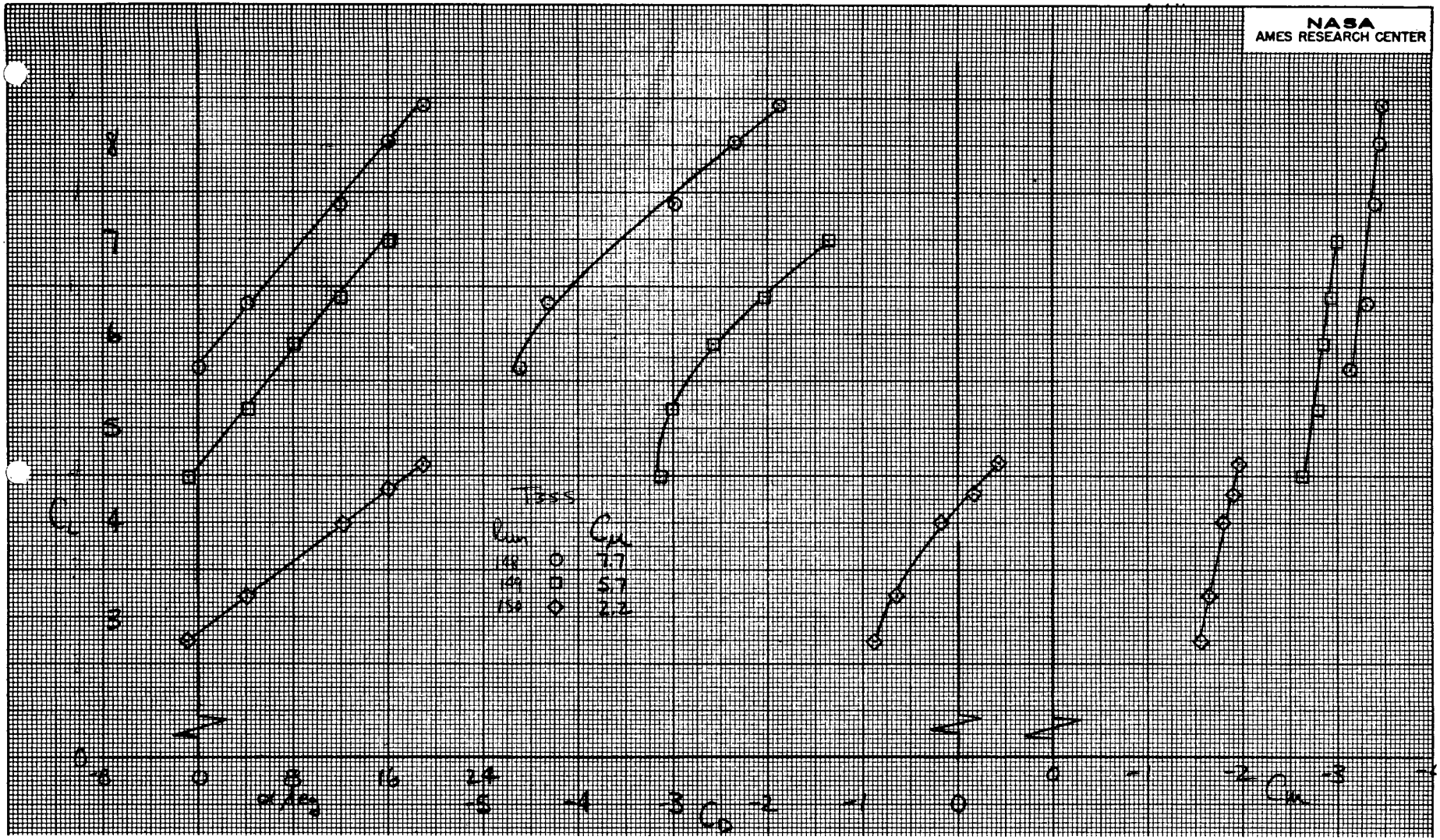

(b) $\delta_f = 60°$

Figure 24.- Continued.

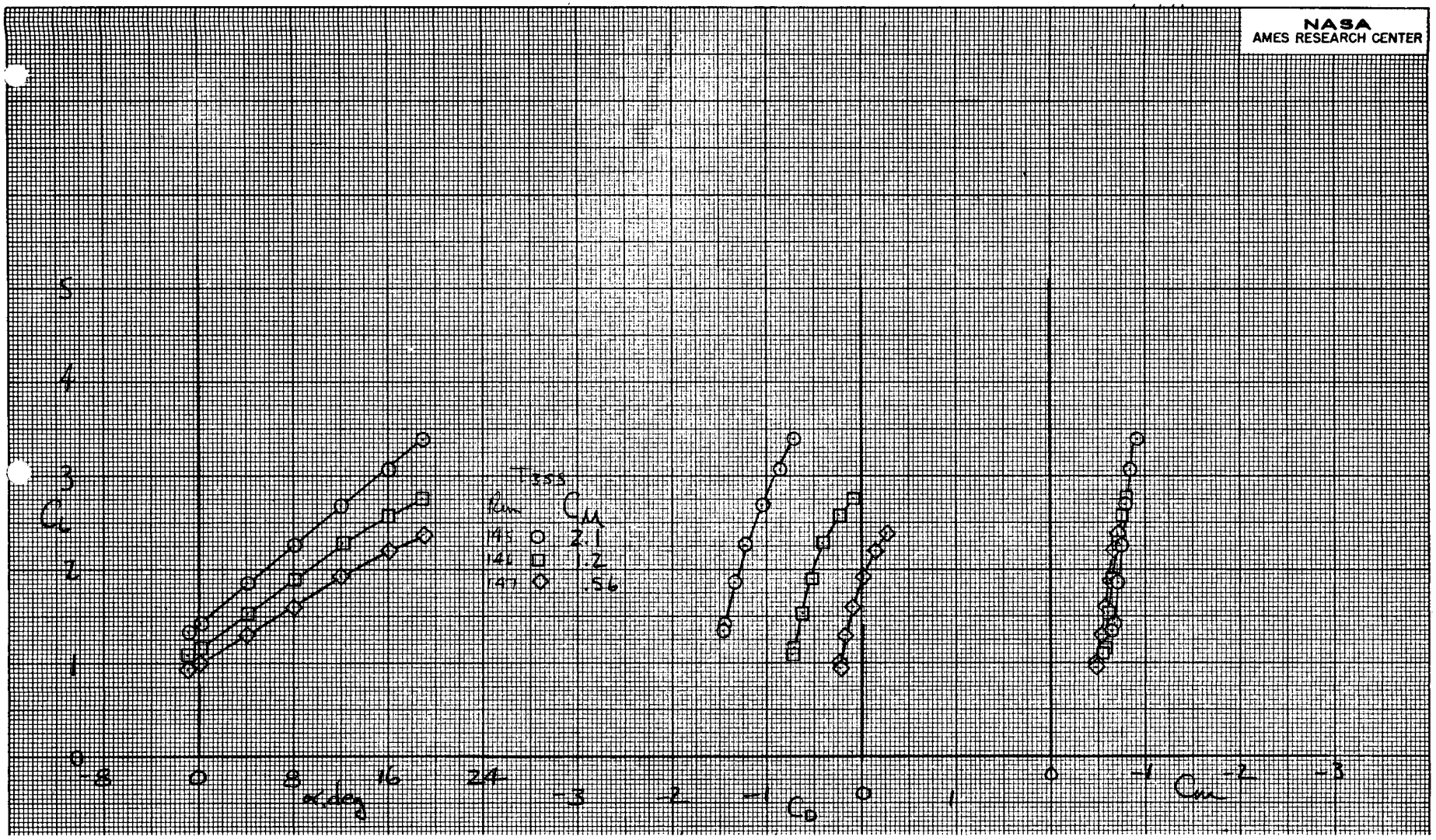

(c) $\delta_f = 30°$

Figure 24.- Continued.

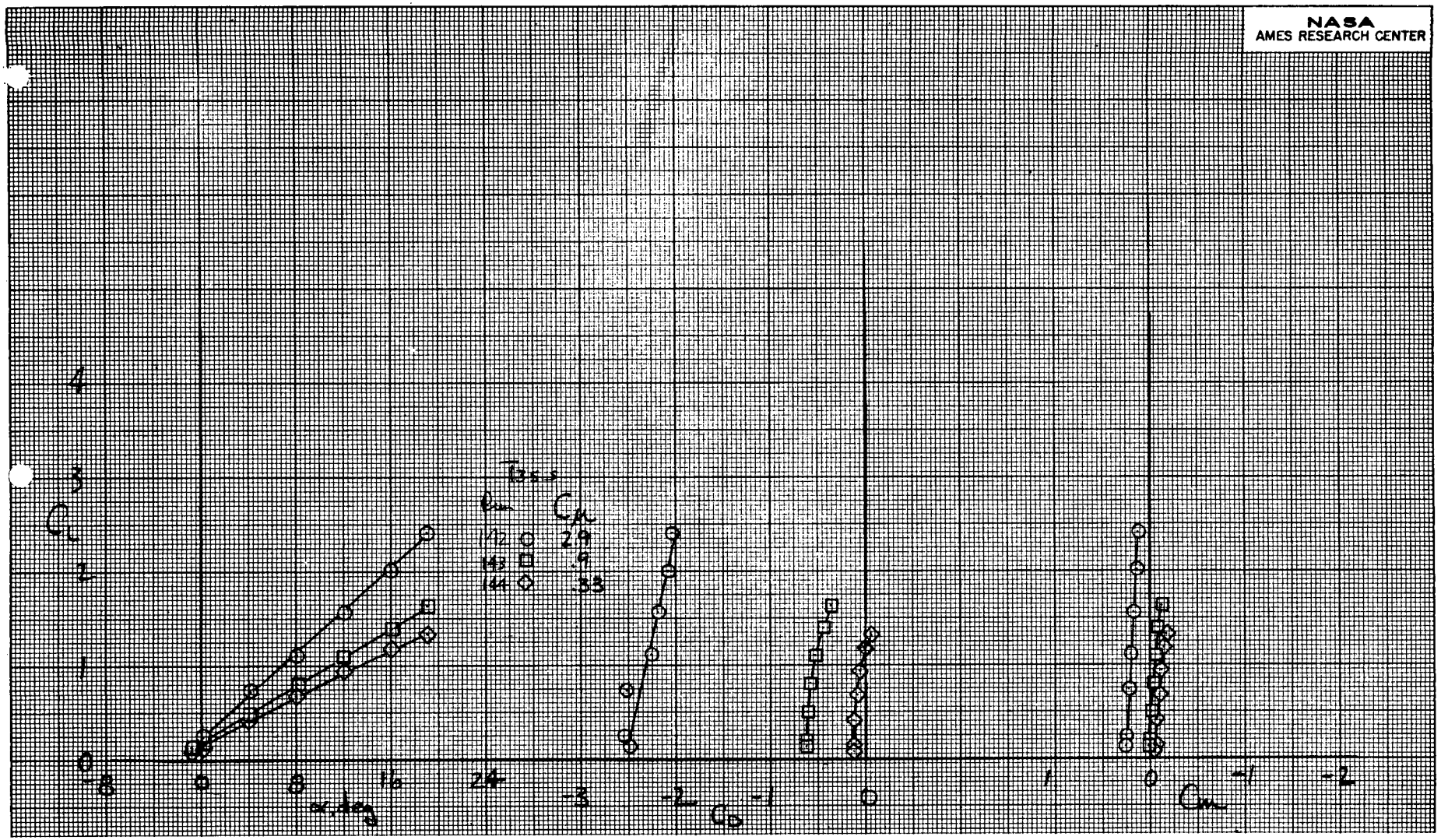

(d) $\delta_f = 0°$

Figure 24.- Concluded.

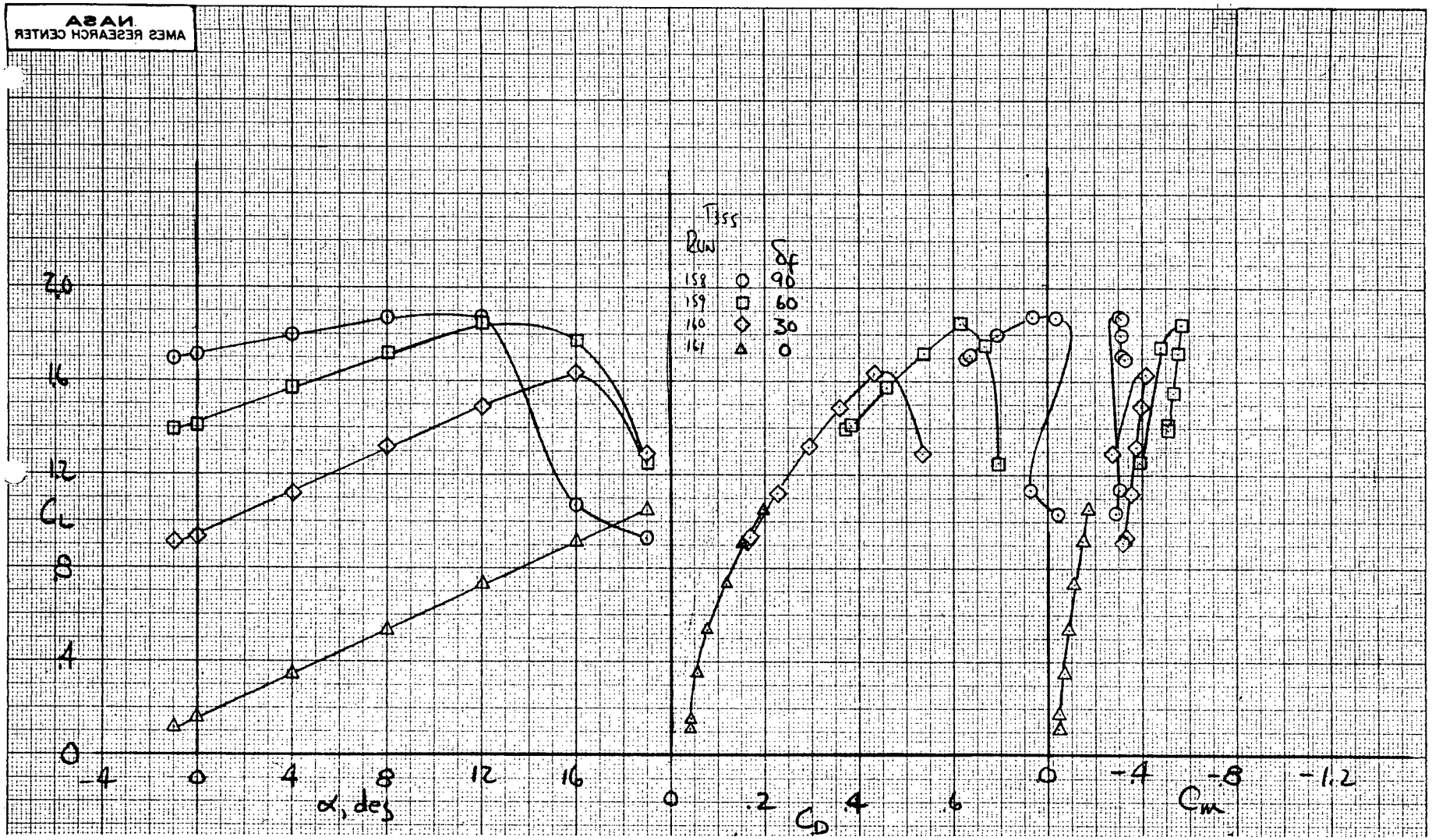

(a) Flap I

Figure 25.- Longitudinal aerodynamic characteristics; $\Lambda = 30°$, nacelle removed.

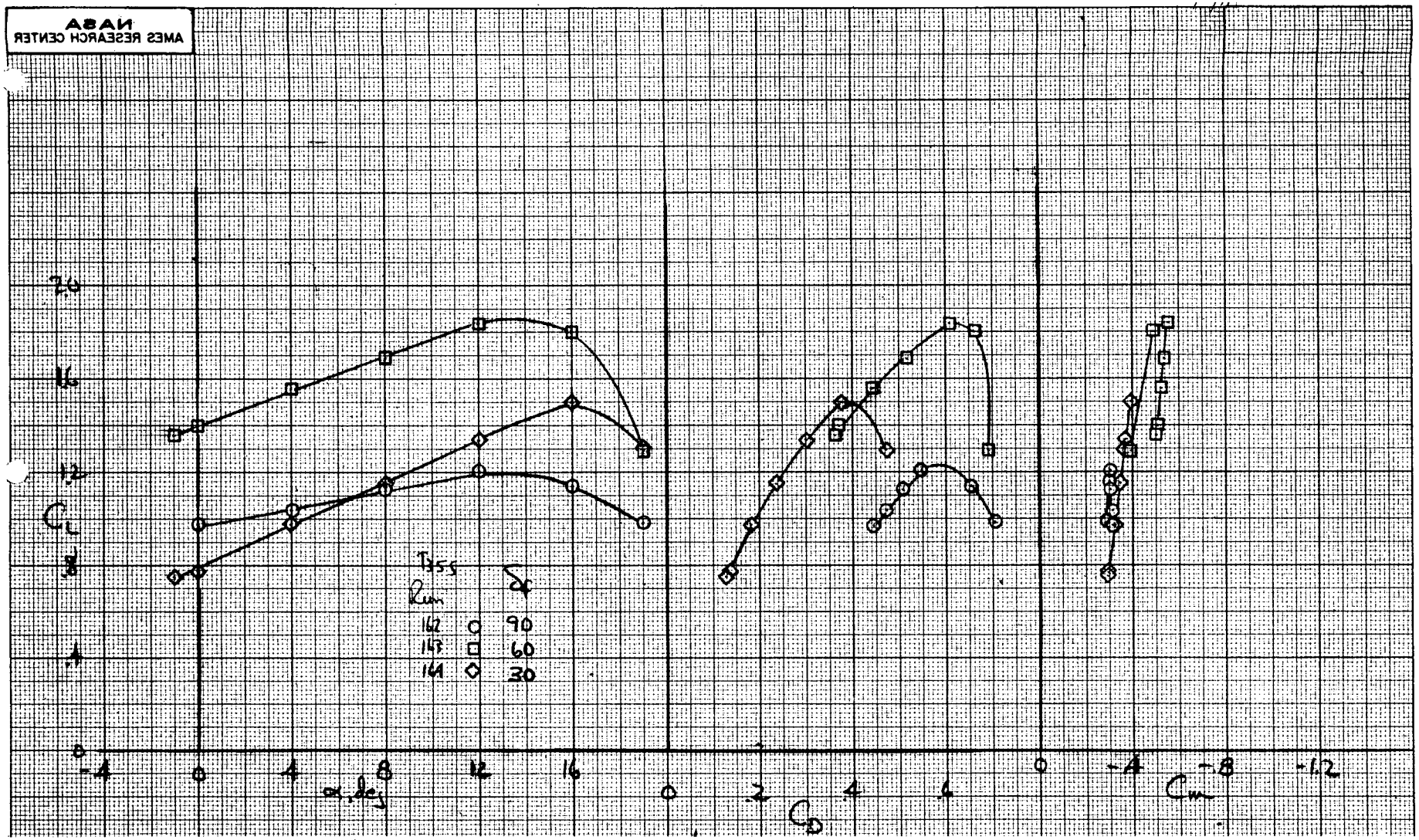

(b) Flap II

Figure 25.- Continued.

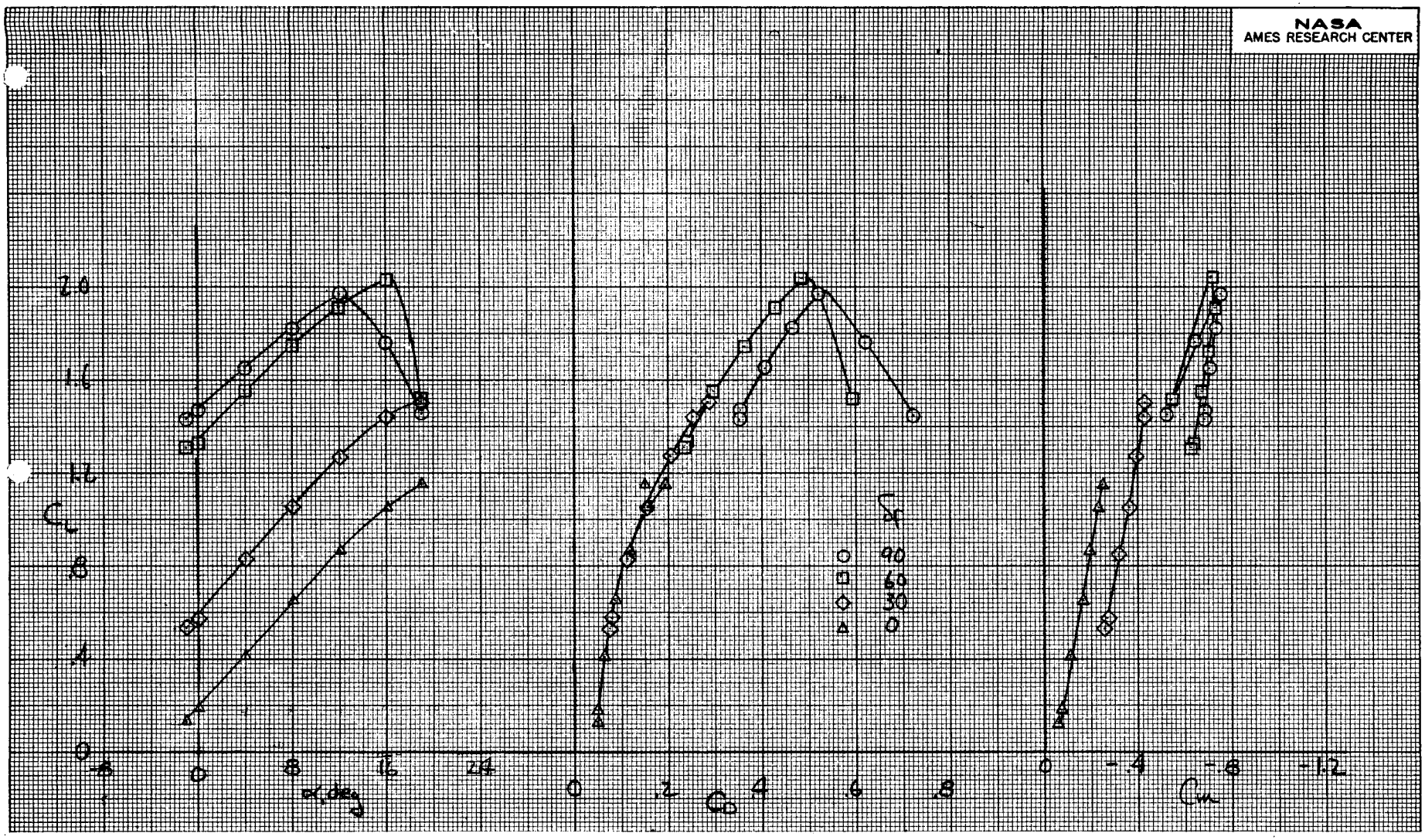

(c) Flap III

Figure 25.- Concluded.